

The copyright of this thesis vests in the author. No quotation from it or information derived from it is to be published without full acknowledgement of the source. The thesis is to be used for private study or non-commercial research purposes only.

Published by the University of Cape Town (UCT) in terms of the non-exclusive license granted to UCT by the author.



AN INTEGRATED APPROACH FOR THE MITIGATION OF ACID ROCK DRAINAGE (ARD) ASSOCIATED WITH PYRRHOTITE IN NICKEL DEPOSITS

Tapiwa Chimbganda

Thesis submitted for the Degree of Master of Science in Chemical Engineering

Aug 2012

Faculty of the Engineering and Built Environment

University of Cape Town

*Glory be to my Creator and my Heavenly Father without whom life in
itself would not be possible*

Declaration

I declare that this thesis has not been submitted prior to this for any degree at this university or any other institution.

Signed: _____

University of Cape Town

SYNOPSIS

Pyrrhotite is a non-stoichiometric sulfide mineral that occurs in a number of ore deposits such as Ni-Cu, Pb-Zn and platinum group elements (PGE). The focus of this project was on nickel deposits. Pyrrhotite is considered to be one of the most reactive sulfide minerals due to its vacancy layers which facilitate electron transfer. Pyrrhotite occurs in different crystallographic forms more commonly known as magnetic and non-magnetic pyrrhotite. These forms exhibit varying physico-chemical properties, of which the magnetic phase has been shown to be more reactive. The principal nickel mineral, pentlandite ($(\text{FeNi})_9\text{S}_8$), occurs almost ubiquitously inter-grown with pyrrhotite.

Currently in nickel processing circuits, pyrrhotite is rejected during flotation to the tailings to control SO_x emissions in smelting. A number of rejection mechanisms have been explored but chemical depressants like polyethylene polyamines are the more favoured rejection methods. Improved pyrrhotite rejection improves pentlandite grade which results in reduced total energy requirements and harmful gaseous emissions.

Pyrrhotite rich tailings are sent to tailings dams, where they are susceptible to oxidation by oxidising agents such as oxygen, water or bacteria that catalyse the oxidation process. Oxidation of sulfide minerals leads to the generation of acid rock drainage (ARD), also referred to as acid mine drainage (AMD). Current ARD management focuses on end-of-pipe level techniques such as lime addition and mine backfill. In line with the sustainable development goals, which aim to minimise waste by mitigating environmental impacts at the source, there arises a need to incorporate into the mineral processing flow sheet a measure of dealing with the sulfide mineral tailings before they are disposed.

This project identified the possibility of manipulating rejection mechanisms in flotation to produce passivated pyrrhotite tailings. Passivation enables surface coating of the sulfide thus inhibiting attack by oxidising agents. Promotion of passivation of pyrrhotite during flotation to produce un-reactive tailings has not been explored to date. Polyethylene polyamines (DETA/TETA), which are already used as depressants in flotation, have been proved to be effective coating agents, significantly reducing the oxidation of pyrrhotite and

pyrite in both abiotic and biotic systems. However, passivation by polyethylene polyamines (DETA and TETA) has only been explored on waste rock and pristine pyrrhotite. Furthermore, studies of the mechanism of oxidation of pyrrhotite have observed the formation of a hydrophilic ferric oxyhydroxide layer which enables depression of pyrrhotite during flotation. This layer has been reported in literature to inhibit the further oxidation of the pyrrhotite surface. Thus passivation can also take advantage of the formation of the ferric oxyhydroxide layer to inhibit further oxidation of the mineral.

This project is limited to investigating two methods of depression and passivation, namely TETA and O₂ sparging (artificial oxidation). TETA is currently used in conjunction with SO₂ derivatives (e.g. sodium metabisulfite i.e. SMBS) as a depressant in several operations. Depression by oxidation has been explored on laboratory scale but has not been implemented. Thus these two methods were selected due to their application in the rejection and passivation of pyrrhotite. Based on previous research which showed the magnetic phase is more reactive, experiments were conducted on a magnetic pyrrhotite bearing nickel ore. The ore selected in this study is a low grade disseminated nickel ore containing (10.9 wt %) pyrrhotite, with minor to trace amounts of pyrite (2.9 wt %), pentlandite (1.5 wt %) and chalcopyrite (0.95 wt %).

The mineralogical composition of the feed and tails samples of the ore was measured by QEMSCAN. The reactivity of the sample was obtained by conducting oxygen uptake tests prior to flotation. The TETA dosages and oxidation times were varied to determine their effect on pyrrhotite rejection and passivation. Prior to collection, the tailings were further treated either by further oxidation or dosing them with TETA to promote further formation of passivation layers. The passivation efficiency was quantified by measuring the acid producing potential using static and biokinetic ARD prediction tests.

Depression by oxygen during flotation proved to be a potentially viable rejection method for this particular ore. Pre-oxidation achieved an 85 % pyrrhotite rejection was achieved, while maintaining pentlandite recovery above 50 %. The use of TETA and SMBS achieved 92 % rejection of pyrrhotite and a pentlandite recovery of 50 %.

Treatment of the pyrrhotite tailings initially showed a decrease in the acid producing potential of the samples indicating possible passivation of the mineral surface. Further treatment by TETA resulted in a larger decrease in the initial net acid producing potential of the samples. However, sequential NAG tests showed that the initial reduction in NAG was insignificant and the samples remained acid forming. Biokinetic tests further confirmed that treated tailings remained acid producing.

This study also showed the importance of mineralogical analysis during ARD characterisation. ARD reaction rates are very dependent on the mineralogy of the sample, therefore ARD prediction based on theoretical mineralogical calculations are very important in understanding chemical tests. Previous test protocol has been largely focused on pyrite bearing samples. Mineralogical ARD prediction used in this study showed that a different approach is required when pyrrhotite and pyrite are both present in a sample. Chemical ARD tests may overestimate or underestimate ARD potential, therefore mineralogical calculations and analysis can provide understanding to chemical tests and provide better characterisation of samples.

Overall this study showed that passivation during flotation may not be feasible, seeing that the acid producing potential of the tailings was not significantly reduced. However passivation has been shown by other authors to be effective on dry pyrrhotite samples. Thus the processing stage at which passivation may be used would need to be evaluated. From reviewing the two rejection methods, this project however did bring to light that rejection by pre-oxidation needs to be reviewed for its potential application in the depression of pyrrhotite bearing nickel sulfide ores. Using oxygen as a depressant would be a 'green solution' and may minimize reagent costs.

LIST OF PUBLICATIONS AND PRESENTATIONS

Chimbganda, T., Becker, M., Broadhurst, J.L., Franzidis, J., Harrison, S.T.L. Pyrrhotite depression in Nickel ores and its potential environmental implications. Submitted for presentation at *The 5th International Minerals Engineering International (MEI) Flotation Conference (Flotation '11)*, Cape Town

Chimbganda, T., Becker, M., Broadhurst, J.L., Franzidis, J., Harrison, S.T.L. 2011. A comparison of pyrrhotite rejection and passivation in two Nickel ores. Submitted for review in *Minerals Engineering Journal*.

Chimbganda, T., Becker, M., Broadhurst, J.L., Franzidis, J., Harrison, S.T.L. Characterization and mitigation of acid rock drainage associated with pyrrhotite in Nickel deposits. Submitted for the *Southern African Institute of Mining and Metallurgy (SAIMM) Mineral Processing Annual Conference (2009)*, Cape Town

ACKNOWLEDGEMENTS

First and foremost I would like to thank my primary supervisor, Dr Megan Becker, my shepherd and support. I would like to thank you for all your guidance, knowledge and motivation through my masters; I could have not done it without your kind words and patience. Secondly I would like to thank Dr Jenny Broadhurst for all her support and motivation.

I would also like to extend my gratitude to the following people;

- Prof J-P Franzidis for the support of the project through the Minerals to Metals initiative.
- To the CMR team, Monde Bekahpi, Moegsien SouthGate, Rubin Van Schalkwyk, Kenneth Maseko and Jenny Wiese, thank you for all your support
- Prof Sue Harrison for your support through CeBER. As well as others from CeBER Dr Chris Bryan, Dr Rob Van Hille, Emmanuel Ngoma
- Helen Divey and the analytical lab team
- Kerry Gray and Lorraine Kemba for their assistance with QEMSCAN
- Miranda Waldron for her assistance with SEM analysis

I would also like to thank the National Research Foundation, Department of Science and Technology Institute (Research Development Grant) and Vale Inco for the funding which made this project possible.

A special thanks to my friends and family for their prayers and support.

Last but not least I would like to thank my loving parents Ambrose and Reah Chimbanga, who have held my hand, stood beside and behind me, through my journey in life thus far. There are no words to describe my gratitude to you both. I love you Mummy and Daddy.

TABLE OF CONTENTS

SYNOPSIS	iv
LIST OF PUBLICATIONS AND PRESENTATIONS	vii
ACKNOWLEDGEMENTS	viii
LIST OF FIGURES	xiii
LIST OF TABLES	xv
GLOSSARY	xvi
1 Introduction.....	1
1.1 Background to the study	1
1.2 Problem statement.....	4
1.3 Research objectives.....	4
1.4 Thesis scope and structure	5
2 Literature review	7
2.1 Overview of nickel ore deposits.....	7
2.2 Mineralogy of pyrrhotite	8
2.2.1 Pyrrhotite crystallographic forms	8
2.2.2 Pentlandite and pyrrhotite association	8
2.3 Pyrrhotite oxidation	10
2.3.1 Oxidation reactions	10
2.3.2 Mechanism of pyrrhotite oxidation.....	12
2.3.3 Factors affecting oxidation	13
2.4 Flotation of pyrrhotite bearing ores.....	16
2.4.1 Principles of flotation.....	16
2.4.2 Pyrrhotite rejection.....	17
2.5 Acid rock drainage generation	23
2.5.1 ARD generation mechanisms	24
2.5.2 Factors affecting ARD generation	26
2.5.3 Environmental impacts of ARD	30
2.6 ARD mitigation.....	32

2.6.1	Current disposal techniques.....	32
2.6.2	Current ARD treatment technologies	32
2.6.3	ARD mitigation by passivation or “surface coating”	35
2.7	ARD potential prediction	38
2.7.1	Acid base accounting (ABA)	39
2.7.2	Net generating potential (NAG).....	42
2.7.3	ARD potential classification.....	42
2.7.4	Biokinetic prediction test	44
2.8	Summary and objective of the study	45
2.9	Thesis Approach.....	47
3	Experimental methods and materials.....	50
3.1	Sample selection and preparation.....	50
3.2	Mineralogical characterisation.....	51
3.2.1	Optical microscopy.....	51
3.2.2	QEMSCAN	52
3.2.3	Chemical assays.....	53
3.2.4	Scanning electron microscopy (SEM)	53
3.3	Flotation experiments.....	54
3.3.1	Pyrrhotite reactivity	54
3.3.2	Pyrrhotite rejection.....	55
3.3.3	Tailings passivation treatment.....	57
3.4	ARD prediction tests	59
3.4.1	ABA (Acid base accounting)	59
3.4.2	NAG (Net acid generation) tests	60
3.4.3	Biokinetic test.....	61
4	Pyrrhotite characterisation and rejection.....	63
4.1	Introduction	63
4.2	Ore characterisation.....	64
4.2.1	Discrimination between magnetic and non-magnetic pyrrhotite.....	64

4.2.2	Mineral composition and Liberation.....	65
4.3	Pyrrhotite reactivity	67
4.3.1	No depressant	67
4.3.2	Oxidation as a depressant	68
4.3.3	TETA + SMBS as a depressant	69
4.3.4	Summary of reactivity numbers.....	71
4.4	Flotation test work.....	72
4.4.1	Oxygen as a depressant	72
4.4.2	TETA + SMBS as a depressant	73
4.4.3	Summary of pentlandite and pyrrhotite recovery	74
5	ARD characterisation.....	76
5.1	Introduction	76
5.2	Tailings mineralogy	77
5.3	Acid base accounting (ABA) results	78
5.3.1	MPA.....	78
5.3.2	ANC	79
5.3.3	NAPP	81
5.3.4	Net acid generation (NAG) results	82
5.3.5	NAG of the tailings after treatment by oxidation	82
5.3.6	NAG of the tailings after treatment by TETA	83
5.4	Biokinetic test results	85
5.4.1	Time course results.....	85
5.4.2	SEM image analysis	88
6	Discussion.....	90
6.1	Introduction	90
6.2	Pyrrhotite rejection	91
6.2.1	Rejection by oxygen.....	91
6.2.2	Rejection by TETA and SMBS	92
6.2.3	Comparison of the two rejection methods	93

6.3	ARD characterisation	94
6.3.1	Acid base accounting	94
6.3.2	Evaluation Net acid generation potential prediction	95
6.3.3	Interpretation of Biokinetic test results	96
6.4	Pyrrhotite passivation	97
6.4.1	Passivation by the ferric oxyhydroxide layer	97
6.4.2	Passivation by TETA	98
6.5	Implications of this study	99
7	Conclusions and recommendations	101
7.1	Research outcomes	101
7.2	Integrated approach to ARD characterisation	102
7.2.1	Concluding remarks	104
7.3	Recommendations	105
	Bibliography	107
	Appendix	116

LIST OF FIGURES

Figure 1: A schematic presentation of the thesis structure.	6
Figure 2: Photomicrographs of a typical pyrrhotite bearing nickel ore showing (a) Granular and (b) Flame pentlandite (Becker, 2009).	9
Figure 3: Pyrrhotite reaction zones (Mycroft et al., 1995).	12
Figure 4: Schematic of a flotation cell (http://sic.ici.ro/sic2002_1/art09.htm).	16
Figure 5: INCO Clarabelle circuit flow sheet (Lawson et al., 2005).	19
Figure 6: Typical mining and beneficiation flow sheet (Broadhurst, 2007).	23
Figure 7: Acid rock drainage formation evolution trend (Smart et al, 2004).	26
Figure 8: Factors affecting the rate ARD generation (Akci, 2006).	27
Figure 9: Cross section of a typical tailings dam (Lottermoser, 2010).	28
Figure 10: Schematic of pyrrhotite oxidation by acidophilic bacteria, adapted from Bryan (2006) FOB ferrous oxidising bacteria, SOB: Sulfur oxidising bacteria.	29
Figure 11: Conceptual model of Sources, Pathways and Sinks (adapted from INAP, 2009).	30
Figure 12: Examples of ARD remediation options (adapted from Johnson and Hallberg, 2005).	33
Figure 13: Polyethylene polyamine structure (Kirk-Othmer, 1984).	35
Figure 14: Schematic showing the steps of Fe oxyhydroxide coating formation on pyrite (Huminicki and Rimstidt, 2009).	37
Figure 15: ARD classification plot showing the boundary regions (Stewart et al., 2006).	43
Figure 16: Thesis approach by integrating cross disciplinary knowledge.	47
Figure 17: Flow sheet summary of test methodology approach.	49
Figure 18: Photographs of the ore (a) rock samples (b) crushed sample	51
Figure 19: Image showing SMS analysis of various particles grains. Each colour represents a different mineral.	52
Figure 20: Image showing a section of BMA analysis. Each colour represents a different mineral.	52
Figure 21: Graph showing the correlation between ICP-OES chemical assay and QEMSCAN data for the major elements present in the feed sample. The x=y shows 1:1 relation.	53
Figure 22: Schematic of the experimental set up.	54
Figure 23: 3 L LEEDS Flotation cell at the CMR research lab at UCT.	55
Figure 24: Milling curve obtained at a milling speed of 90 rpm at different milling times	55
Figure 25: Particle size distribution (PSD) of the sample.	56
Figure 26: Reflected light photomicrographs of the ore; (a) Magnetic colloid adheres to magnetic pyrrhotite (b) Pentlandite inter-grown with pyrrhotite.	64

Figure 27: Reflected light photomicrographs of the ore; (a) photomicrograph showing the different sulfide minerals present in the ore (b) Granular pentlandite.....	65
Figure 28: Summary of the feed mineral composition (wt %) as determined by QEMSCAN.....	65
Figure 29: Comparison of the reactivity number (RN_{norm}) of different nickel sulfide ores (Becker et al. 2010a) with the ore used in this case study.....	67
Figure 30: Reactivity number (RN) with oxygen as a depressant. Standard error is shown.....	68
Figure 31: Summary of reactivity numbers (RN) obtained when TETA was used as a depressant. Standard error is shown.....	69
Figure 32: Comparison of the reactivity number (RN) with TETA and SMBS as a depressant. Standard error is shown.....	70
Figure 33: Pentlandite and pyrrhotite recovery with oxygen as a depressant. Standard error is shown.....	72
Figure 34: Pentlandite and pyrrhotite recovery using TETA only and TETA/SMBS as a pyrrhotite depressant. Standard error is shown.....	73
Figure 35: Mineral composition for the feed, oxygen as a depressant tails (5 minutes oxidation), TETA (125 g/t) only tails, TETA + SMBS (125 g/t : 500g/t) tails.....	77
Figure 36: ANC values from chemical tests and mineralogical calculations. Standard error is shown.....	80
Figure 37: The NAPP (net acid producing potential) values obtained from chemical tests and mineralogical calculations. Standard error is shown.....	81
Figure 38: Net acid generation profile of tailings after they were further treated by oxidation. Standard error is shown.....	82
Figure 39: Net acid generation profile of tailings as they were further treated further addition of TETA. Standard error is shown.....	84
Figure 40: Change in pH with time for the biokinetic test for feed sample and tailings sample	86
Figure 41: Change in Ferric iron concentration with time for biokinetic tests for the feed samples and tailings samples	86
Figure 42: Change in Redox potential with time for the for biokinetic tests for the feed samples and tailings samples (reference electrode +199 mV vs. SHE).....	87
Figure 43: SEM images of tailings treated with further oxidation before biokinetic tests [(a), (b)] and during biokinetic tests (after 35 days) [(c),(d)].	88
Figure 44: SEM images of tailings treated with TETA before biokinetic tests [(a), (b)] and during biokinetic tests (after 35 days) [(c), (d)].....	89
Figure 45: Classification plot comparing acid base accounting (NAPP) results with NAG pH	95
Figure 46: An integrated approach to ARD characterisation.....	102

LIST OF TABLES

Table 1: The relative resistance to oxidation of different sulfide minerals (Moncur et al., 2009).	10
Table 2: The silicate mineral neutralisation reactions, assuming complete dissolution (Paktunc, 1999a).....	25
Table 3: Weathering rates of typical minerals found in gangue (Kwong, 1993; Lawrence and Scheske, 1997).....	25
Table 4: Main characteristics of ARD water and environmental impacts (Lottermoser, 2007; Ritchie, 1994).....	31
Table 5: Commonly used ANC tests.	40
Table 6: The ARD classification guidelines (Stewart, Miller and Smart, 2006).....	43
Table 7: A summary of the reagent dosages and the conditioning times.	57
Table 8: The concentration of the ions present in the synthetic plant water used in the batch flotation tests (Wiese et al, 2005).	57
Table 9: Tailings passivation experimental matrix.	58
Table 10: Further treatment dosages.	58
Table 11: The percentage liberation and association of the minerals in feed sample.	66
Table 12: Summary of the reactivity numbers and the associated R^2 values obtained to calculate the reactivity numbers.	71
Table 13: A summary of the cumulative recovery to the concentrate of pentlandite and pyrrhotite.....	74
Table 14: Selectivity ratio of Pentlandite (Pn) : Pyrrhotite (Po)	75
Table 15: The base metal sulfide (BMS) wt% composition of the tailings from the selected flotation tests.....	78
Table 16: The maximum potential acidity (MPA) of the tailings samples.	79
Table 17: Mineralogical composition (wt %) of the acid neutralising minerals contained in the feed and tailings samples.....	80
Table 18: The NAG pH of the tailings samples (T_n = Tailings at time n minutes of oxidation).	83
Table 19: The NAG pH and cumulative NAG of selected samples treated by further oxidation, after 2 stage sequential NAG test.	83
Table 20: The NAG pH of the tailings samples (TT_n = Tailings at n dosage (g/t) of TETA). .	84
Table 21: The NAG pH and cumulative NAG of selected samples treated with TETA after 2 stage sequential NAG test.	85

GLOSSARY

ABA	Acid base accounting
AMD	Acid mine drainage
ARD	Acid rock drainage (also known as acid mine drainage)
ARDI	Acid rock drainage index
ANC	Acid neutralizing capacity
ANC _{MN}	Acid neutralizing capacity based on mineralogy (MN)
DETA	Di-ethylene triamine
DO	Dissolved oxygen
MPA	Maximum potential acidity
MPA _{MN}	Maximum potential acidity based on mineralogy (MN)
NAF	Non-acid forming
NAG	Net acid generating potential
NAPP	Net acid producing potential
NAPP _{MN}	Net acid producing potential based on mineralogy(MN)
NMD	Neutral mine drainage
MPA	Maximum potential acidity
PAF	Potentially acid forming
PAX	Potassium amyl xanthate
PGE	Platinum group element
Pn	Pentlandite
Po	Pyrrhotite
Py	Pyrite

RN	Reactivity number
RN _{norm}	Reactivity number normalised based on pyrrhotite content
ROM	Run of mine
SD	Saline drainage
SEM	Scanning electron microscope
SHE	Standard Hydrogen Electrode
SIBX	Sodium Isobutyl Xanthate
SMBS	Sodium metabisulfite
SO _x	Sulphur oxide gases
TDS	Total dissolved solids
TEM	Transmission electron microscopy
TETA	Tri-ethylene tetramine
XRD	X-ray Diffraction
XRF	X-ray fluorescence spectrometry
QEMSCAN	Quantitative Evaluation of Minerals by Scanning electron microscopy
UC	Uncertain

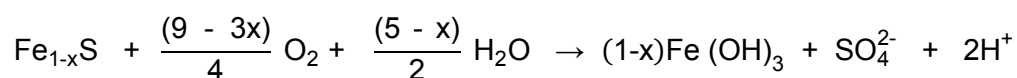
1 INTRODUCTION

1.1 Background to the study

The non-stoichiometric sulfide mineral pyrrhotite ($\text{Fe}_{n-1}\text{S}_n$ where $n \geq 8$) occurs in a number of ore deposits such as Ni-Cu, Pb-Zn and platinum group elements (PGE); but the focus in this project will be on nickel deposits. In Ni ores, the principal nickel mineral, pentlandite ($(\text{FeNi})_9\text{S}_8$), occurs almost ubiquitously inter-grown with pyrrhotite. Pyrrhotite occurs in different crystallographic forms more commonly known as magnetic and non-magnetic pyrrhotite, which exhibit varying physico-chemical properties, of which the magnetic phase has been shown to be more reactive (Becker et al., 2010b).

In most magmatic nickel sulfide deposits, pyrrhotite is more abundant than pentlandite, thus in Nickel processing pyrrhotite is rejected to the tailings to control the concentrate grade and reduce SO_2 emissions (Wells et al., 1997; Kerr, 2002). Optimising pyrrhotite rejection (also known as depression) produces a better pentlandite grade which in turn reduces the total energy requirements across the concentrator smelter process chain (Evans et al., 2011). A number of pyrrhotite rejection methods have been explored over the years such as magnetic separation, the use of chemical reagents such as polyamines and polymeric depressants, and using nitrogen or oxygen as the flotation gas (see for example Kelebek, 1993, 1995, 2007; Senior et al., 1995; Wells, 1997; Kim, 1998; Kerr, 2002; Lawson, 2005). The different methods exploit different physico-chemical properties to optimise the rejection of pyrrhotite to tailings.

The pyrrhotite rich tailings are then sent to a tailings dam where they are susceptible to oxidation in the presence of oxygen, water, and bacteria which catalyse the oxidation process. The oxidation of pyrrhotite can be represented by the following equation;



Oxidation of sulfide minerals such as pyrite and pyrrhotite, leads to the generation of acid rock drainage (ARD), also referred to as acid mine drainage (AMD). Although this process

occurs naturally, mining and anthropogenic activity increase the amount of sulfides exposed, making the minerals more susceptible to water and air which are key oxidizing agents (INAP, 2009).

ARD is characterized by low pH, high heavy metal and sulphate concentrations which can degrade the quality of the water to a point where it is unfit for human and animal consumption or crop irrigation. Mining activity greatly accelerates the weathering of reactive sulfides by exposing large volumes of material and increasing the surface area of the reactive component. The increased acidic environment gives rise to the opportunity for colonization by microorganisms that catalyse the oxidation processes (Johnson and Hallberg, 2003).

The generation and mobility of ARD is a complex process governed by physical, chemical and biological factors (Ackil, 2006). ARD is one of the major environmental issues facing the world's water resources and it has various consequences and multigenerational ramifications. South Africa is currently facing a number of critical environmental challenges, but ARD maybe one of the biggest problems in terms of its ramifications for the country. In 2010, 36 million cubic meters of ARD were estimated to be imploding into the Witwatersrand basin from nearby closed mining operations (Azarch, 2011). The poor management of ARD can have detrimental effects on the communities surrounding the mining area, now and for generations to come. Sustainable development requires an integrated, balanced and responsible approach that accounts for short-term and long-term environmental, social and economic considerations long after mining operations have stopped (MMSD, 2002).

Different ARD management techniques have been explored which include treatment and prevention methods. Treatment methods include an end-of-pipe level approach, which focuses on pH adjustment of the resulting drainage and the removal of dissolved metal ions by precipitation, while prevention methods involve mitigating ARD at the source. ARD management techniques can be classified into chemical (abiotic) and biological methods (biotic). Both systems include methods which can be described as "active" (require a continuous input to sustain the process) and "passive" (input once in operation) (Johnson and Hallberg, 2005). Mitigation is site specific as factors such as physical, biological and climatic conditions will differ from site to site (Ackil, 2006); and preventing ARD at the source

is considered to be a more cost effective management approach (Johnson and Hallberg, 2005). ARD prediction tests are important in characterising the acid producing potential of waste. However previous test protocols have been largely focused on pyrite bearing samples (Smart et al., 2002, Lei and Watkins, 2005).

Surface coating of the sulfide minerals, which is classified as a preventative passive method, has been identified as a possible means of mitigating ARD associated with pyrite and pyrrhotite (Johnson and Hallberg, 2005; Cai et al., 2005; Chen et al., 2006). Oxygen is one of the key factors affecting the generation of acid rock drainage, and the inhibition of oxidation of the mineral surface can possibly mitigate the formation of acid. Mycroft et al. (1995) and Pratt et al. (1994) observed that after the formation of a thin hydrophilic ferric oxyhydroxide layer (5 Å), further oxidation of the pyrrhotite is inhibited and the surface seems to be passivated. Huminicki and Rimstidt (2009) studied the possibility of using iron oxyhydroxide coating for acid rock drainage control of pyrite. It was found that when pyrite is oxidized at alkaline pH, as the oxyhydroxide layer thickens, it is possible to reduce the oxidant's diffusion coefficient by more than five times. The formation of this hydrophilic layer has been observed to promote the depression of pyrrhotite during flotation (Kelebek, 1993; Legrand et al., 2005a, 2005b). Depression of pyrrhotite by oxidation has been explored on laboratory scale, but it has never been implemented (Wells et al., 1997).

A number of surface coating agents have been tested on pyrite and were found to reduce the oxidation rate significantly (Belzile et al., 1997; Lan et al., 2002). Lan et al. (2002) showed that the oxidation of pyrite can be significantly reduced by using a strong insoluble chelating agent, 8-hydroxyquinoline, as a coating agent. Kim (1998), Cai et al. (2005) and Chen et al. (2006), by using polyethylene polyamines (diethylenetriamine (DETA) or triethylenetetramine (TETA)) as coating agents on pristine pyrrhotite samples showed that both chemical and biotic oxidation of pyrrhotite could be limited. Polyethylene polyamines are basic substances which neutralise protons during oxidation processes. Currently DETA and TETA are used as pyrrhotite depressants in conjunction with SO₂ derivatives (e.g. sodium metabisulfite i.e. SMBS) in nickel processing circuits such as Sudbury operations (Lawson et al., 2005). Use of these reagents for passivation is advantageous as they are already used as depressants in flotation. Thus this opens the possibility of manipulating flotation conditions to promote surface coating of pyrrhotite by DETA/TETA.

1.2 Problem statement

ARD is a major environmental issue and its effects can last for years affecting water quality. Current ARD management technologies focus on end-of-pipe level methods. Passivation using mineral surface coating has been recognised as a viable preventative method. Previous studies on surface coating have been done on laboratory scale on waste rock and pristine pyrrhotite. Limited work has been done to attempt to integrate passivation techniques into current process design. Furthermore current ARD characterisation prediction tests have previously been focused on pyrite. Limited work has been done in characterisation of the acid producing potential of pyrrhotite bearing ores.

1.3 Research objectives

It is hypothesised that it is possible to simultaneously reject and promote the passivation of pyrrhotite during flotation using either polyethylene polyamines or artificial oxidation. The objective of this project is to investigate the feasibility of mitigating the ARD generating potential of pyrrhotite tailings through the formation of passivation layers on the pyrrhotite surface in nickel ores during flotation. Particularly, this project aims to address the following key questions;

- i. Is it plausible to simultaneously depress and passivate pyrrhotite during flotation?
- ii. Which depressant mechanism is more effective at pyrrhotite depression?
 - (a) TETA or TETA/SMBS
 - (b) Artificial oxidation
- iii. Which depressant is more effective at pyrrhotite passivation?
 - (a) TETA or TETA/SMBS
 - (b) Artificial oxidation

1.4 Thesis scope and structure

The project is part of the Minerals to Metals Initiative at the University of Cape Town which aims to facilitate the sustainable development and utilisation of natural resources within the minerals industry by integrating knowledge across various disciplines. This project explores the concept of cleaner production which aims to identify options within a mineral beneficiation process flow sheet to minimise waste and/or its impacts. In this study knowledge from mineralogy and mineral processing is combined with current ARD mitigation and characterisation techniques to provide an integrated approach to mitigating ARD pyrrhotite in nickel ores.

This project is limited to investigating two methods of depression and passivation, namely TETA (triethylenetetramine) and O₂ sparging (artificial oxidation). TETA and DETA are currently used as a depressant in some operations (Lawson et al., 2005). Whilst depression by oxidation has been explored on laboratory scale but has not been implemented (Wells et al., 1997). These two methods have also been shown to be capable of inhibiting pyrrhotite oxidation through the formation of passivation layers. Previous studies have shown the two crystallographic phases (magnetic and non-magnetic) show different oxidation rates and the magnetic phase is more reactive (Becker et al., 2010a). Thus experiments will be conducted on a predominantly magnetic pyrrhotite bearing Nickel ore.

The thesis is organised into 7 chapters: Chapter 1 gives the background to the study, introduces the problem statement and outlines the research objectives. Chapter 2 gives a review of the literature on pyrrhotite mineralogy and processing, ARD mitigation and potential prediction. The experimental methods are presented in Chapter 3. The results are divided into two chapters, i.e., Chapters 4 and 5. Chapter 4 gives the results from the reactivity measurements and flotation tests. Chapter 5 gives the results obtained from the ARD characterisation tests. Chapter 6 discusses the results obtained and compares the rejection and passivation efficiencies. Finally, Chapter 7 draws conclusions from the study as well as discusses the research outcomes and recommendations. A schematic flow chart of the thesis structure is given in Figure 1.

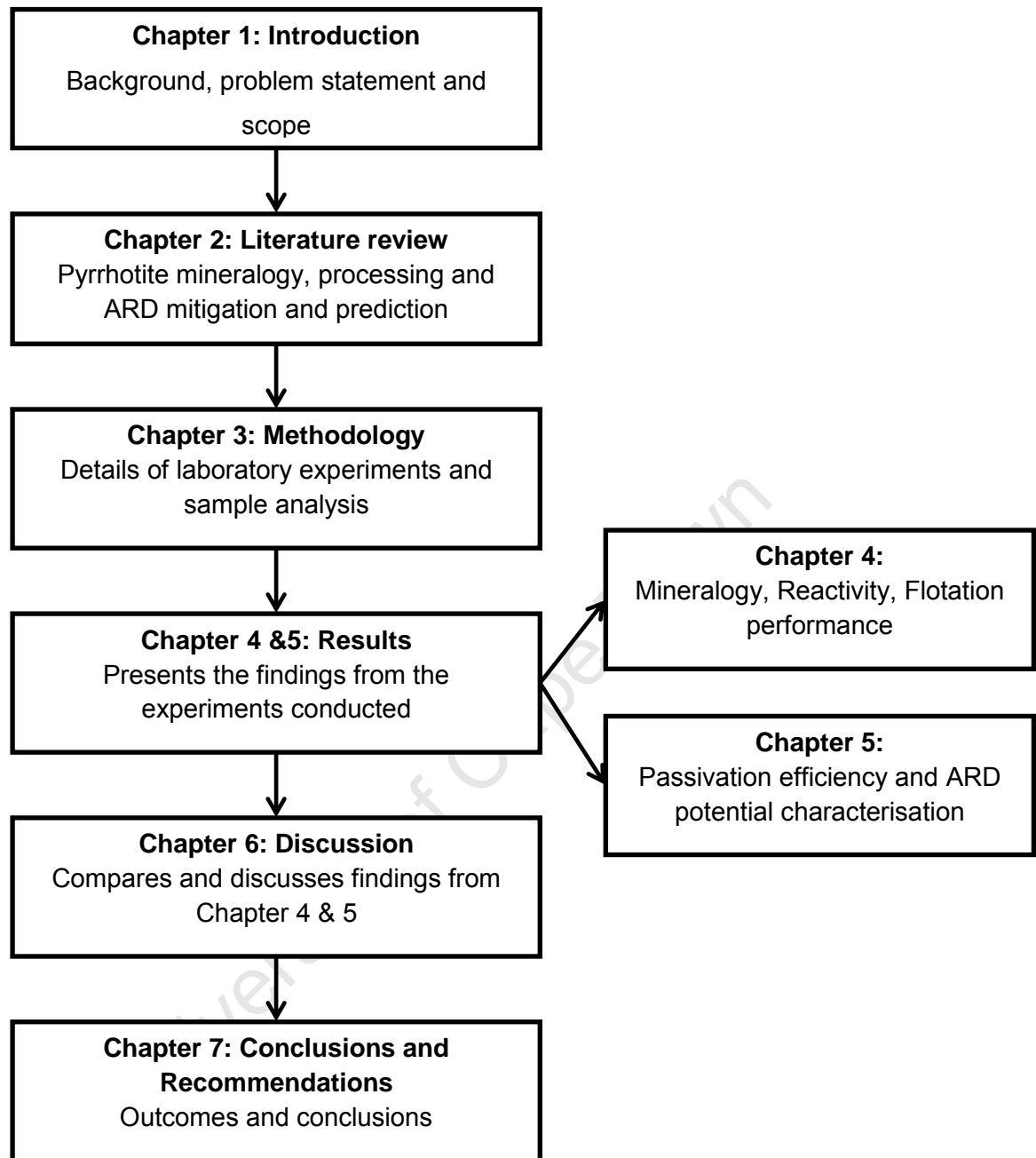


Figure 1: A schematic presentation of the thesis structure.

2 LITERATURE REVIEW

This chapter gives a detailed background to the study and develops the problem statement and objectives. The chapter starts with an overview and background of pyrrhotite ore deposits and pyrrhotite mineralogy (section 2.1 and 2.2 respectively). Section 2.3 then describes the oxidation of pyrrhotite and the factors that affect pyrrhotite oxidation. Section 2.4 then gives a background of pyrrhotite rejection and flotation of pyrrhotite bearing nickel ores. Sections 2.5, 2.6 then discuss ARD generation and mitigation. Section 2.7 describes current ARD prediction and characterisation methods. A summary of the literature is then given in section 2.8 and the objectives of the study are presented. The chapter then concludes with a description of the thesis approach and the key questions.

2.1 Overview of nickel ore deposits

Pyrrhotite is a common sulfide mineral found in a number of ore deposits; lead-zinc, nickel-copper and platinum group elements (PGE); however the focus of this study is on Nickel sulfide ore deposits. Nickel ore deposits are classified into magmatic i.e. sulfide deposits and laterite i.e. oxide and silicate deposits. Lateritic deposits are generally found in equatorial and paleoequatorial locations with the principal ore minerals being nickeliferous limonite and garnierite. Magmatic deposits are nickel-copper and PGE sulfide deposits which have formed through segregation and concentration of ultramafic magma (Naldrett, 2004). The principal nickel mineral that occurs in sulfidic deposits is pentlandite. The deposit selected for this study is a magmatic sulfide deposit related to stratiform deposits occurring as intrusions in cratonic areas e.g. Bushveld Igneous Complex, Utikomst Complex and Sudbury Igneous Complex. The dominant sulfides found in these deposits are pyrrhotite (Po), pentlandite (Pn), chalcopyrite (Cp) and pyrite (Py). Mining has previously been focused on the massive sulfide body however this resource has run out and mining is currently focused on the more disseminated ore.

2.2 Mineralogy of pyrrhotite

2.2.1 Pyrrhotite crystallographic forms

Pyrrhotite has a non-stoichiometric composition, Fe_{1-x}S where x varies from 0 (FeS) to 0.125 (Fe_7S_8); the chemical formula can also be expressed as $\text{Fe}_{n-1}\text{S}_n$ with $n \geq 8$ (Morimoto et al., 1970). Pyrrhotite has a disordered NiAs structure which results from having a non-stoichiometric composition. Pyrrhotite is a metallic conductor making it very reactive and prone to oxidation (Belzile et al., 2004; Ekmecki et al., 2010). Pyrrhotite occurs in two crystallographic forms commonly known as magnetic and non-magnetic pyrrhotite (Becker et al., 2010b). They can exist alone, or occur as inter grown mixtures of the two crystallographic forms (Becker et al., 2010b).

Magnetic pyrrhotite is ferromagnetic and is characterised by ordered vacancy layers, with each layer being separated by completely filled metal cation layers (Tokonami et al., 1972). The ideal composition of magnetic pyrrhotite is Fe_7S_8 with 46.6 – 46.9 % atomic iron (Carpenter and Desborough, 1964) and has monoclinic crystallography. Non-magnetic pyrrhotite is also known as intermediate pyrrhotite comprising Fe_8S_9 , Fe_9S_{10} and $\text{Fe}_{11}\text{S}_{12}$ (Morimoto et al., 1975a; Morimoto et al., 1975b). Although non-magnetic is commonly known as hexagonal pyrrhotite, recent studies have shown it to be orthorhombic (de Villiers et al., 2009). The iron content of non-magnetic pyrrhotite at ambient conditions is found to vary between 47- 48 % atomic iron (Carpenter and Desborough, 1964; Becker et al., 2010b). Magnetic and non-magnetic pyrrhotite, occur in various inter-grown textures such as lamellar intergrowths and fissure controlled irregular intergrowths (Lianxing and Vokes, 1996).

2.2.2 Pentlandite and pyrrhotite association

The dominant nickel mineral in sulfidic deposits is pentlandite, $(\text{FeNi})_9\text{S}_8$, it almost occurs ubiquitously inter-grown with pyrrhotite. Pyrrhotite is usually more abundant in nickel sulfide deposits than pentlandite; ratios of pyrrhotite to pentlandite can vary from 1:1 to 10:1 (Kerr, 2002). Pentlandite is classified as a metal sulfide with an excess of metal to sulfur ratio (Becker et al., 2010b). Nickel ores typically comprise of bands of pyrrhotite and pentlandite with trace amounts of chalcopyrite, pyrite, violarite, gersdorffite and chromite. Pentlandite forms as discrete grains or flames in the pyrrhotite structure (Kelly and Vaughan, 1983).

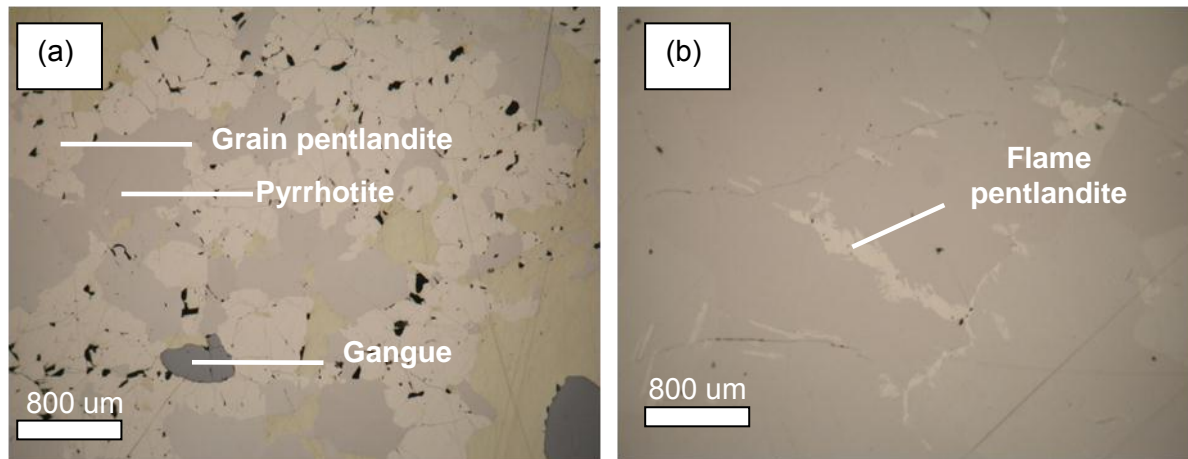



Figure 2: Photomicrographs of a typical pyrrhotite bearing nickel ore showing (a) Granular and (b) Flame pentlandite (Becker, 2009).

2.3 Pyrrhotite oxidation

Pyrrhotite is considered to be one of the most reactive sulfide minerals due to its vacancy layers which facilitate electron transfer, thus it is very susceptible to oxidation (Pratt et al., 1994; Mycroft et al., 1995; Mikhlin et al., 2002). Of the two crystallographic forms of pyrrhotite, magnetic pyrrhotite has been shown to be more prone to oxidation than non-magnetic pyrrhotite (Becker et al., 2010a). Table 1 shows the relative resistance to oxidation of different sulfide minerals (Moncur et al., 2009). The resistance of sulfide minerals to oxidation varies, and it depends on factors such as crystallinity, trace element content and mineral assemblage.

Table 1: The relative resistance to oxidation of different sulfide minerals (Moncur et al., 2009).

Sulfide	Formula	Resistance to oxidation
Pyrrhotite	Fe_{1-x}S	Low resistance
Galena	PbS	
Sphalerite	$(\text{Zn},\text{Fe})\text{S}$	
Bornite	Cu_5FeS_4	
Pentlandite	$(\text{Fe},\text{Ni})_9\text{S}_8$	
Arsenopyrite	FeAsS	
Marcasite	FeS_2	
Pyrite	FeS_2	
Chalcopyrite	CuFeS_2	
Molybdenite	MoS_2	High resistance

Understanding the mechanism of pyrrhotite oxidation and factors that affect oxidation is important in interpreting flotation behaviour and its acid producing potential. The oxidation reactions and the mechanism of oxidation will be subsequently discussed.

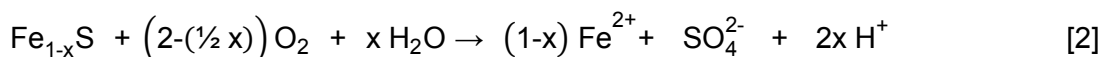
2.3.1 Oxidation reactions

Due to its sulfidic nature, pyrrhotite undergoes both oxidative and non-oxidative dissolution (Thomas et al., 2000). In acidic conditions, pyrrhotite will undergo non-oxidative dissolution.

Pyrrhotite is dissolved consuming acid via reaction [1] producing Fe^{2+} and H_2S . (Where x varies from 0 to 0.125 for pyrrhotite, Fe_{1-x}S)



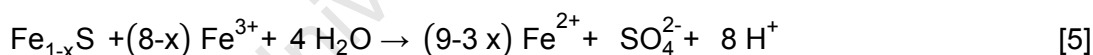
Non-oxidative dissolution is acid consuming whereas oxidative dissolution is acid forming. In oxidative dissolution oxygen is the primary oxidant, the oxidation reaction proceeds as follows;



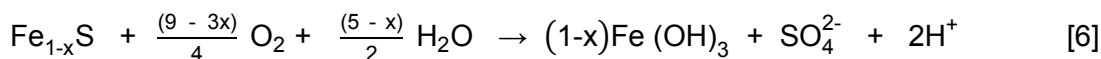
However, at low pH non-oxidative dissolution competes with oxidative dissolution (Belzile et al., 2004). At pH >4, oxygen is the primary oxidant of ferrous iron to ferric iron. Ferrous iron produced in [2] is further oxidised to produce ferric ions that can precipitate out of solution as ferric hydroxide [3-4].



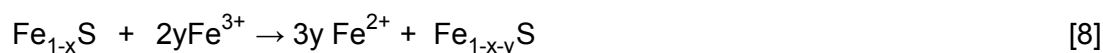
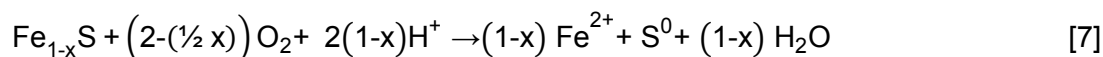
Ferric iron can further oxidise pyrrhotite:



The overall oxidation reaction for pyrrhotite [equation 6];



In acid conditions reaction [3] will continue to produce ferric irons and maintain a cyclic reaction with reaction [5]. Evidence from previous studies done has shown that oxidation may not proceed to completion as shown by equations [2] to [5] (Janzen et al., 2000). Incomplete oxidation of pyrrhotite may produce either elemental sulfur [7] or sulfur rich pyrrhotite [8].



It is further suggested that partial oxidation of pyrrhotite may proceed via a series of iron deficient sulfides and possibly polysulfides through to elemental sulfur, with the steps being acid consuming. Metastable intermediates of sulphate including thiosulphate, polythionate have been reported as being some of the intermediates (Mikhlin et al., 2002). Partial oxidation of pyrrhotite may produce either elemental sulfur via reaction [7] or sulfur rich pyrrhotite via reaction [8]. Acidophilic bacteria found in mine waste environments are capable of oxidising sulfide minerals (Sampson et al., 2000). The bacteria accepts electrons from the oxidation of ferrous iron (Fe^{2+}) acting as a catalyst for reaction [3]. The electrons provide the bacteria with the necessary energy for metabolic functions, growth and reproduction (Sampson et al., 2000). As the bacteria reproduce they become an electron sink and further increase the oxidation of Fe^{2+} .

2.3.2 Mechanism of pyrrhotite oxidation

Oxidation of pyrrhotite by air causes Fe to diffuse from the interior to the gas-solid interface, where it reacts with oxygen to form a thin layer of iron oxyhydroxide (Figure 3 - zone A). Depletion of Fe from the region immediately below zone A results in the formation of a sulfur rich region (zone B). Sulfur enrichment in zone B promotes the formation of disulfide and poly-sulfides. The Fe to S ratio decreases with increasing depth. Beneath zone B is unreacted pyrrhotite (zone C). (Pratt et al., 1994; Mycroft et al., 1995; Legrand et al., 2005b).

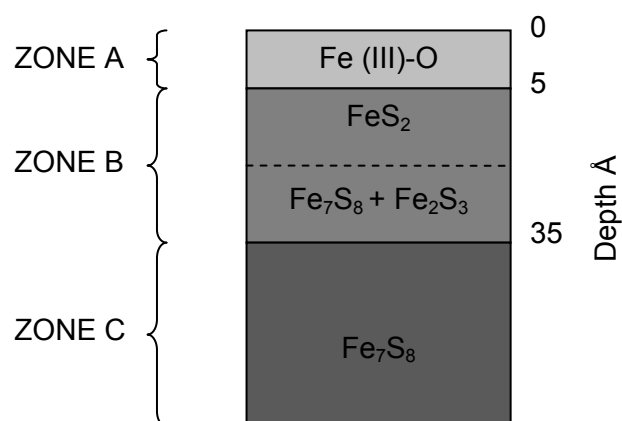


Figure 3: Pyrrhotite reaction zones (Mycroft et al., 1995).

Auger depth profiles conducted by Mycroft et al. (1995) showed that the outer ferric oxyhydroxide layer (zone A) is approximately 5 Å thick. The sulfur rich layer (zone B) was measured to be approximately 30 Å thick. Disulfide forms in the upper part of zone B as a result of the oxidation of mono-sulfide by air. The sulfur does not migrate into the ferric oxyhydroxide layer; oxidation of mono-sulfide to disulfide and poly sulfide purely occurs in the region beneath zone A. Mycroft et al. (1995) suggest that oxidation occurs by the removal of electrons from the mono-sulfide of zone B and C and transport to the gas-mineral interface where the oxygen is reduced to the oxide. The oxide then reacts with Fe derived from the sulfur rich zone. The diffusion of Fe to the interface is promoted by the chemical potential gradient of Fe (III) or Fe (II). The formation of the ferric oxyhydroxide layer is controlled by the rate of diffusion of Fe to the mineral surface.

Mycroft et al. (1995) observed that after the formation of the thin ferric oxyhydroxide layer (5 Å) the reaction seems to be passivated. They further observed that diffusion of oxygen or water beyond a depth 10 to 15 Å seems to be inhibited by the formation of the ferric oxyhydroxide layer and/or the sulfur rich layer. Legrand et al. (2005a) observed that the rate of formation of the ferric oxyhydroxide layer with increase in thickness. However Cruz et al. (2005) found that pyrrhotite reactivity is affected more by the passivating sulfur layer than the diffusion barrier of the ferric oxyhydroxide layer.

Legrand et al. (2005a) studied the oxidation of both pentlandite and pyrrhotite surfaces at a pH of 9.3, because flotation of the ore is usually carried out at pH 9. They found that both minerals oxidise rapidly to form a thin ferric oxyhydroxide layer. However it was found that pyrrhotite oxidises more rapidly than pentlandite; after 5 minutes the oxidation extent of pyrrhotite is similar to that of pentlandite after 30 minutes.

2.3.3 Factors affecting oxidation

Oxygen

Knipe et al. (1995) confirmed that oxygen is the primary oxidant by showing that oxidation did not proceed in dehydrogenated water. Steger (1982) showed a direct increase of pyrrhotite reactivity with increasing relative humidity. This is consistent with reaction [2]

which shows that water must be present for oxidation by air to proceed (Knipe et al., 1995). Legrand et al. (2005b) showed that the rate of formation of the ferric oxyhydroxide layer is proportional to the amount of dissolved oxygen.

Ferric iron (Fe^{3+})

Both oxygen and ferric iron are important oxidants of pyrrhotite. Oxidation by ferric ion is dependent on pH; below pH 4 sulfides are mainly oxidised by ferric iron. Janzen et al. (2000) compared the reaction rates for oxidation by oxygen and ferric iron and found that oxidation rates with ferric iron as the oxidant exceeded those of oxygen. They went on to further suggest that pyrrhotite oxidation by ferric iron appears to follow an adsorption type mechanism. Ferric iron promotes continuous oxidation of pyrrhotite via reaction [5].

pH

Janzen et al. (2000) obtained oxidation rates of ferric iron and oxygen as oxidants at a pH of 2.50 and found that a slight increase in pH resulted in an increase of the oxidation rate by ferric iron as an oxidant. Non oxidative dissolution is promoted by low pH; therefore pH affects the nature of the oxidation products (reactions [1] and [2]). The formation of the insoluble ferric oxyhydroxide layer has been observed to be promoted in alkaline conditions (Legrand et al. 2005b; Huminicki and Rimstidt, 2009). Therefore under alkaline conditions the oxidation of pyrrhotite is repressed due to the formation of the passivating ferric oxyhydroxide layer.

Crystal structure

There is some conflict with studies which have been done on relating oxidation rate to crystal structure. Yakhontova et al. (1983) (as cited by Janzen et al., 2000) suggested that monoclinic pyrrhotite (magnetic pyrrhotite) is more reactive than hexagonal pyrrhotite (non-magnetic pyrrhotite) due to its vacancy layers which allow for electron transfer. Whereas Orlova et al. (1988) (as cited by Janzen et al., 2000), noted that non-magnetic pyrrhotite is more reactive than magnetic pyrrhotite. However Janzen et al. (2000) reported that there is no apparent correlation between pyrrhotite oxidation by oxygen or ferric iron as oxidants. Lehmann et al. (2000) however found larger rate constants for monoclinic pyrrhotite than hexagonal pyrrhotite and the activation energy was lower for monoclinic pyrrhotite than

hexagonal pyrrhotite. Becker et al. (2010a) measured the reactivity of different pyrrhotite ore bodies using cyclic voltammetry and found that magnetic pyrrhotite is more reactive than non-magnetic pyrrhotite.

Trace metal content

The effect of trace metal is uncertain, Janzen et al. (2000) found that the reaction rate seemed to decrease with increasing trace metal content but did not establish a relationship between the oxidation rate and individual trace metals (Co, Cu, Mn, Ni). However Kwong (1993) observed semi-quantitatively that monoclinic pyrrhotite types with high trace element content oxidised slower than those with lower trace element content.

Temperature

Effect of temperature over a range of 25 °C to 45 °C was studied by Janzen et al. (2000) the results indicated that oxidation followed the Arrhenius behaviour. A 10 °C increase resulted in a two fold increase in the oxidation rate (Janzen et al., 2000; Steger, 1982). The effect of temperature is reported to be more significant than the effect of pH (Kwong, 1993). On studies based on pyrite activation energies of oxidation by oxygen, activation energy ranged from 48 kJ/mol to 63 kJ/mol based on ferrous iron release and from 79 to 124 kJ/mol based on sulphate release (Janzen et al., 2000).

2.4 Flotation of pyrrhotite bearing ores

2.4.1 Principles of flotation

Flotation is a physico-chemical process that exploits the differences in surface properties between the valuable minerals and unwanted gangue. For flotation to take place, an air bubble must attach to a particle and lift it to the water surface. The process is applicable to relatively fine particles, within a range of about 500 μm to 10 μm (Fuerstenau et al., 2007). If the mineral particles are too large the adhesion between the particle and the bubble will be less than the particle weight thus the bubble will drop its load. Adhesion occurs if the mineral is water repellent or hydrophobic (Wills and Napier-Munn, 2006). To achieve these conditions flotation reagents are added to enhance the surface properties of the mineral.

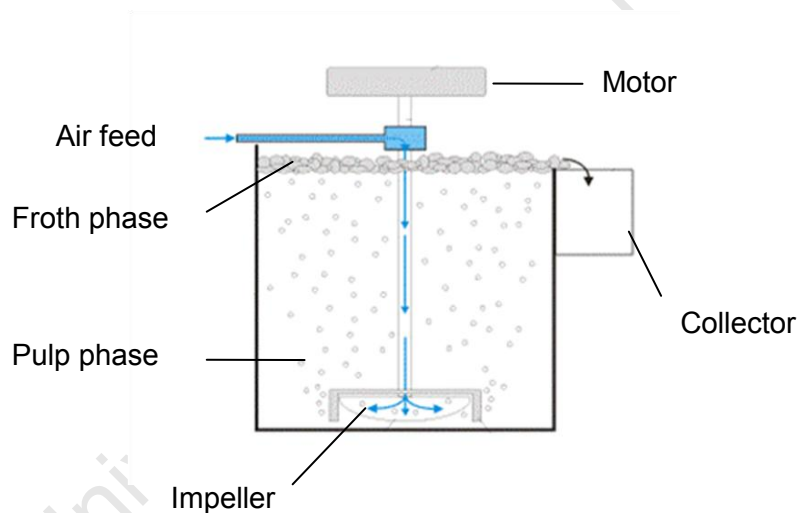


Figure 4: Schematic of a flotation cell (http://sic.ici.ro/sic2002_1/art09.htm).

Most minerals are not water repellent in their natural state thus reagents known as collectors are added to render the mineral surface hydrophobic. Collectors are organic compounds which render the minerals hydrophobic by adsorption of molecules or ions on to the mineral surface. The most widely used collectors are the sulphhydryls which are extremely selective to sulfide minerals, of these sulphhydryls the most widely used are the xanthogenates (technically known as xanthates). The other reagents added are depressants, which depress (or reject) unwanted hydrophilic gangue, and frothers, which help maintain the stability of the froth. Activators are may also be added to alter the chemical nature of the mineral surfaces to assist the collector to induce the hydrophobicity of the mineral (Wills and Napier-Munn,

2006). Activators are generally soluble salts which ionise the solution (Wills and Napier-Munn, 2006). Copper sulphate is commonly used as an activator to enhance the floatability of pentlandite (Senior et al., 1995). The pyrrhotite-pentlandite system contains Cu and Ni ions which can activate the pyrrhotite surface thus activation poses a problem to the separation of pentlandite and pyrrhotite as it increases recovery but reduces selectivity (Senior et al., 1995).

In a generic ore beneficiation flow sheet, the run of mine ore is crushed and subsequently milled or ground. During grinding or milling the size of the particles is reduced which allows liberation of the minerals from the ore. The particles are then classified into fine and coarse particles usually by a hydrocyclone. Coarse particles are recycled back to the grinding stage. Flotation is then performed on the fines to recover the valuable mineral. In traditional Cu-Ni flotation plants pyrrhotite is rejected (or depressed) to the tailings as a waste product (Wells et al., 1997; Wang, 2008).

2.4.2 Pyrrhotite rejection

Increase in nickel demand has been driven by the growth in the stainless steel market, whose production accounts for two thirds of the primary nickel demand (Kerr, 2002). In many nickel processing operations pyrrhotite is rejected to the tailings stream by flotation. This is due to the fact that in most magmatic nickel sulfide deposits, pyrrhotite is significantly more enriched than pentlandite and sending low grade Ni concentrates through to the smelter results in the inefficient use of smelter capacity and energy (Evans et al., 2011; Lawson et al., 2005). Of greater importance though is the fact that sending unwanted pyrrhotite to the smelter results in undesirable SO₂ emissions (Wells et al., 1997).

Improved pyrrhotite rejection produces a better pentlandite grade which in turn reduces the total energy requirements across the concentrator smelter process chain (Evans et al., 2011). Examples of this include the pyrrhotite rejection strategy that was implemented on many of the Sudbury Nickel such as the Clarabelle Mill and Strathcona Mill operations in the 1980's (Wells et al., 1997; Kerr, 2002; Lawson et al., 2005). Consequently, the recent focus for most nickel processing operations has been on the efficient depression of pyrrhotite and

the selective recovery of pentlandite and chalcopyrite (Wells et al., 1997; Kerr, 2002). Optimising rejection requires optimising depressant action on pyrrhotite.

Spectroscopy analyses conducted on the flotation products show that difficulty in pyrrhotite rejection arises from activation of the mineral by metal ions (eg. Cu^{2+} and Ni^{2+} and Fe^{2+}) present in process water (Yoon et al., 1995; Xu et al., 1997). Metal ions activate the surface of the pyrrhotite, forming complexes with the xanthate collector causing pyrrhotite to float and report to the concentrate. From X-ray Photoelectron spectroscopy analysis, Yoon et al. (1995) found that large amounts of Ni^{2+} , Cu^{2+} and Ag^{2+} ions adsorbed onto the pyrrhotite surface, even though the plant water initially contained small amounts of the ions. Similar findings were obtained by Xu et al. (1997) who further demonstrated that xanthate collector adsorbs onto the pyrrhotite surface in the presence of nickel ions. This renders the pyrrhotite hydrophobic causing it to report to the concentrate. This is an undesirable effect in the flotation cell as this reduces the grade of the nickel in the concentrate. A number of strategies have been investigated over the years in laboratory scale tests, however not all have been implemented; the following paragraphs give a discussion of these methods.

Rejection by magnetic separation

When magnetic pyrrhotite is present in the ore, magnetic separation is carried out to remove the magnetic fraction. At INCO's Clarabelle mill treating Sudbury ore in Canada (Figure 5), the overflow from the primary milling circuit is fed to magnetic drum separators where the magnetic fraction is separated out (Wells et al., 1997). Removal of the magnetic fraction is advantageous as the magnetic fraction has higher sulfur content and is more reactive so it can be processed separately and disposed accordingly (Lawson et al., 2005). The non-magnetic fraction reports to a rougher scavenger flotation circuit from which three concentrates are produced, A, B and scavenger concentrate.

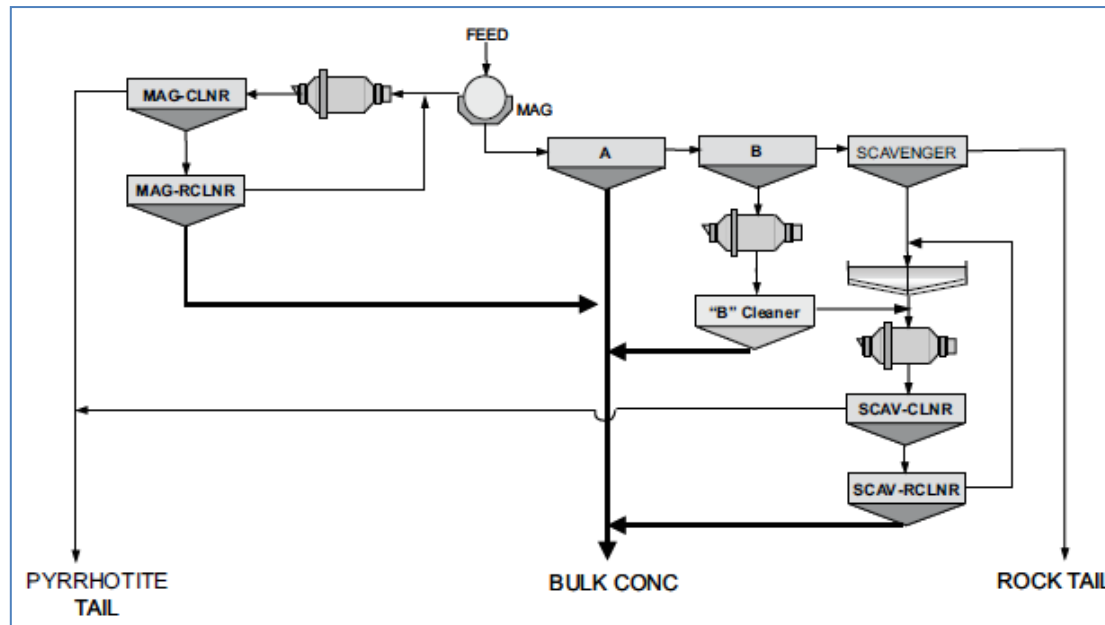


Figure 5: INCO Clarabelle circuit flow sheet (Lawson et al., 2005).

Magnetic separation simply separates the magnetic and non-magnetic pyrrhotite fractions hence flotation still needs to be conducted to separate pyrrhotite and pentlandite. The magnetic pyrrhotite is reground to improve liberation of pentlandite and the non-sulfide gangue is rejected in two stages of cleaning. The non-magnetic pyrrhotite is treated similarly with a regrinding stage and two stages of cleaning in the scavenger cleaning circuit (Lawson et al., 2005).

Oxygen depression

Oxidation of pyrrhotite by air causes Fe to diffuse from the interior to the gas-solid interface, where it reacts with oxygen to form a thin layer of iron oxyhydroxide. Due to the reactive nature of pyrrhotite its surface is oxidised rapidly upon exposure to air (Miller et al., 2005). Equation [6] corresponds to the initial oxidation of pyrrhotite to produce a hydrophilic ferric oxyhydroxide layer which inhibits collector attachment (Kelebek, 1993).

Above a pH of 4.5 it is expected that the natural floatability of pyrrhotite will not occur therefore, due to the hydrophilic nature of the surface, pyrrhotite will be depressed (Miller et al., 2005). In general floatability of sulfide minerals is depressed by excessive oxidation (Malysiak et al., 2002). The difficulty of depression by oxygen sparging is that pentlandite becomes less floatable with oxidation, while due to activation pyrrhotite becomes more

floatable (Wells et al., 1997; Kelebek, 2007). By taking advantage of the different rates of oxidation of pyrrhotite and pentlandite, Legrand et al. (2005b) showed using XPS (X-ray photoelectron spectroscopy) that at a given time different oxidation extents could be achieved for each mineral. Kelebek (1993) showed that by increasing the oxidation time of pyrrhotite prior to flotation in batch flotation tests a consistent decrease in pyrrhotite recovery can be achieved.

Becker et al. (2010a) compared the reactivity of different pyrrhotite samples by conducting oxygen uptake tests; magnetic pyrrhotite (Sudbury CCN), pure magnetic pyrrhotite (Sudbury Gertude west and Phoenix from Botswana) and inter grown magnetic and non-magnetic pyrrhotite (Nkomati MSB). The reactivity of the mixed magnetic and non-magnetic sample lay in between the non-magnetic CCN and Phoenix samples. Becker et al. (2010a) found that non-magnetic pyrrhotite was less reactive than magnetic pyrrhotite.

Nitrogen depression

Use of nitrogen as the flotation gas to prevent activation of pyrrhotite has been shown to be highly effective in separation of pyrrhotite from pentlandite under certain conditions. Dixanthogen formation is needed for pyrrhotite floatability, in oxygen deficient conditions pyrrhotite was found to develop rest potentials that are lower than the equilibrium potential for dixanthogen formation (Khan and Kelebek, 2004). By controlling the potential of the flotation system to avoid the oxidation of xanthate to dixanthogen, the flotation of pyrrhotite would be inhibited and so selective pentlandite flotation is promoted (Khan and Kelebek, 2004).

Cyanide depression

Use of cyanide in conjunction with ethyl xanthate was investigated as a method of increasing flotation selectivity at pH 9 (Prestidge et al., 1993). Cyanide addition was found to reduce the extent and rate of ethyl xanthate adsorption on iron both pyrite and pyrrhotite, however the results were more prominent for pyrrhotite (Prestidge et al., 1993). Laboratory scale tests with cyanide as a depressant produced promising results however use of cyanide has not been put into practise due to environmental concerns (Prestidge et al., 1993; Wells et al., 1997).

Depression with polyethylene polyamines

Previous studies have shown that pyrrhotite rejection is improved by the addition of polyethylene polyamines (Kelebek, 1995; Yoon et al., 1995). Different mechanisms of depression by DETA (diethylenetriamine) or TETA (triethylenetetramine) have been proposed, which either suggest that polyethylene polyamines absorb onto the pyrrhotite surface or indirectly depresses pyrrhotite by acting as a complexing agent (Kim, 1998).

Studies conducted by Xu et al. (1997) and Kelebek and Tukul (1999) showed that depression by the polyethylene polyamines, DETA or TETA, is greatly improved by adding a SO₂ derivative (eg. sodium metabisulfite i.e. SMBS). Whereas the study conducted by Yoon et al. (1995) showed that DETA is more effective when the mineral sample is oxidised. From the UV spectrophotometry and FTIR (Fourier transform infra red spectroscopy) studies done by Yoon et al. (1995), Xu et al. (1997) and Kim (1998), it was found that DETA does not adsorb onto the surface of pyrrhotite in the presence of metal ions, but acts as a complexing agent. Xu et al. (1997) concluded that the polyethylene polyamines depress pyrrhotite by acting as complexing agents, removing Cu and Ni ions which cause activation. DETA and/or TETA selectively remove Cu²⁺ and Ni²⁺ ions, but not Fe (III) ions from the pyrrhotite surface (Xu et al., 1997; Kelebek and Tukul, 1999). Xu et al. (1997) added different concentrations of DETA but still DETA was more selective to Cu and Ni than Fe, and suggested that this maybe the case due to the ferric hydroxide bond being more stable than ferric-DETA complex.

Xu et al. (1997) also studied the ability of DETA and a combination of DETA-SO₂ to remove metal ions from the pyrrhotite surface and found that, the DETA-SO₂ was more effective in removing the metal ions. Similarly Kelebek and Tukul (1999) studied the effect of TETA-SMBS (sodium metabisulfite), where SMBS is a derivative of SO₂. It was found that TETA-SMBS reagent combination was more effective as a depressant, than TETA alone. The role of SO₂ and its derivatives in the depression of pyrrhotite are not fully understood. The use of SMBS in combination with TETA has been proposed to assist in maintaining low redox potentials which enables inhibition the formation of hydrophobic sulfur species on pyrrhotite (Kelebek & Tukul, 1999). Lawson et al. (2005) varied the TETA to SMBS ratio and found that optimal pentlandite recovery and pyrrhotite rejection was obtained at a TETA to SMBS ratio of 1:4.

Polymeric depressants in flotation

Senior et al. (1995) studied the use of polymeric depressants in the selective flotation of pentlandite from a nickel ore and found that high additions of the depressant did not improve sulfide recovery, there was only improvement in the depression of talc. However Mbonambi et al. (2010) showed that the combination of a guar depressant with SNPX (sodium normal propyl xanthate) at high pH could cause some depression of pyrrhotite for selective pentlandite flotation in a low grade nickel ore.

University of Cape Town

2.5 Acid rock drainage generation

Acid rock drainage (ARD) is produced from the exposure of sulfide minerals to oxygen and water which cause oxidation. Although minerals weather naturally, human activity such as mining and excavations increase the exposure of sulfide bearing minerals to air. Waste which contains sulfides is a major source of ARD. Waste includes waste dumps, low grade ore stock piles, tailings and spent heap leach piles (Akcil and Koldas, 2006). Figure 6 illustrates the sources of waste from mining activity, structures such as underground pit mines are also a large contributor to ARD.

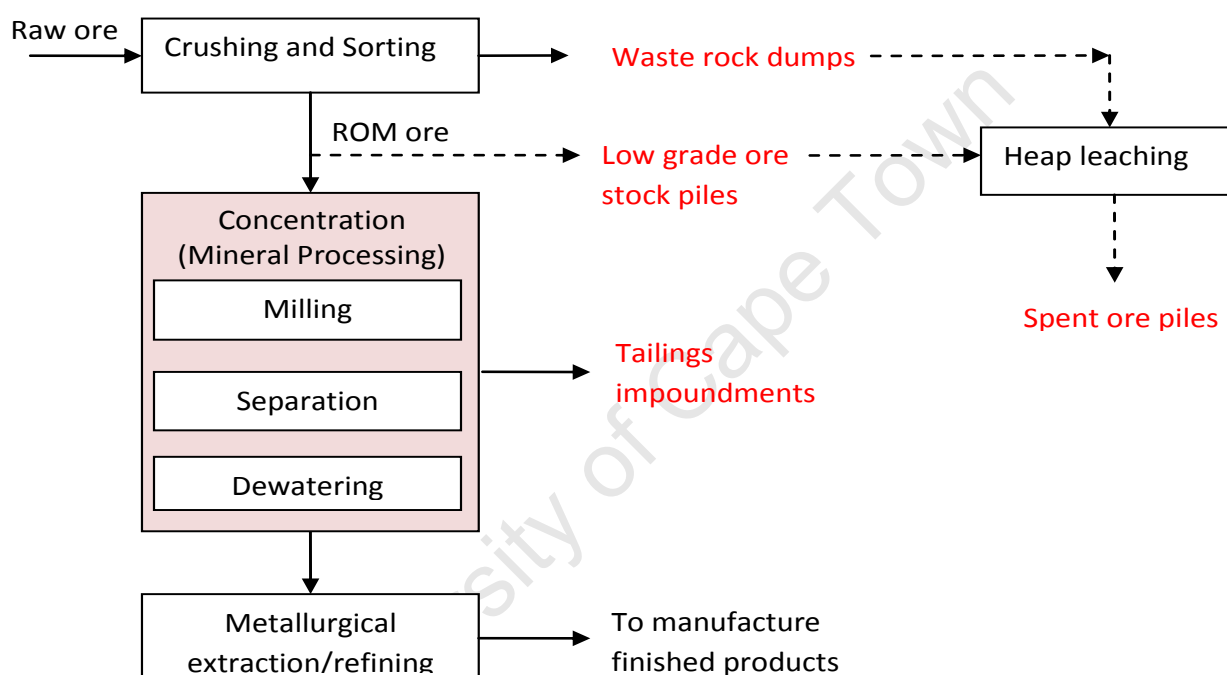


Figure 6: Typical mining and beneficiation flow sheet (Broadhurst, 2007).

Pyrite is the most abundant metal sulfide associated with the Earth's crust and thus contributes largely to the world's acid rock drainage. Pyrrhotite is also a significant ARD contributor, it is one of the most reactive sulfides (see section 2.3) and it is associated with a number of ore deposits (see section 2.1). ARD is characterised by low pH and high concentrations of heavy metals. Naturally occurring bacteria can accelerate ARD production by assisting in the breakdown of sulfide minerals, this is further discussed in the following section. ARD contaminates surface and ground water as well as soils. ARD production is a function of the mineralogy of the rock and the availability of oxygen and water (Akcil and Koldas, 2006). The extent of pollution depends on factors such as the size and buffering capacity of the receiving stream as well as the biogeochemical properties which will be later discussed in section 2.5.2. Acid mine drainage is site specific and metal contamination

depends on type of sulfide mineral. The mechanisms behind ARD generation will now be discussed.

2.5.1 ARD generation mechanisms

Acid generation from the oxidation of sulfide minerals is a complex function of whether oxygen or aqueous ferric iron is the oxidant (Plumlee and Logsdon, 1999). The formation of ARD from the oxidation of pyrrhotite occurs in 4 major steps;

1. Oxidative dissolution by oxygen of pyrrhotite (equation 2); Oxidation of pyrrhotite by oxygen releases ferrous iron (Fe^{2+}) and sulfuric acid.
2. Ferrous iron released in equation 2 is oxidised by oxygen to produce ferric iron (Fe^{3+}). In acidic conditions this reaction is mediated by Fe oxidising micro-organisms. The regeneration of ferric iron (equation 3 to 5) is the rate determining step (Singer and Stumm, 1970).
3. At high pH ($\text{pH} > 4$) ferric iron precipitates out as ferric hydroxide producing acidity in the form of H^+ ions (equation 4).
4. At low pH ($\text{pH} < 4$), ferric ion oxidises pyrrhotite (equation 5).

The overall production of acid by sulfide ores is a balance between acid producing sulfide minerals and acid buffering minerals. Minerals with effective acid neutralising capacity (ANC) or neutralising potential (NP) and pH buffering capacity are those containing calcium carbonate and magnesium carbonate including calcite, dolomite and ankerite (Lapakko, 2002; Plumlee and Logsdon, 1999). Generic reactions for the consumption of acid by the dissolution of carbonates can be written as;



**where Me represents a divalent cation such as calcium or magnesium*

Fe bearing carbonates such as siderite initially have the same neutralising capacity as calcite however upon dissolution oxidation of ferrous iron to ferric iron and its precipitation as ferric hydroxide produce acidity which reduces the net neutralising capacity. In the absence of carbonates nesosilicate minerals like olivine have neutralising capacity, whereas

aluminosilicate minerals such as chlorite, biotite, K-feldspar, only play a long term role in acid neutralisation (Weber et al., 2004). Most silicates provide much less neutralising capacity than carbonates because of their slow reaction kinetics and dissolution rates (Plumlee and Logsdon, 1999). However silicates like plagioclase and K-feldspars have potentially higher buffering capacity than carbonates when complete dissolution is assumed (see Table 2) (Lawrence and Scheske, 1997; Paktunc, 1999a).

Table 2: The silicate mineral neutralisation reactions, assuming complete dissolution (Paktunc, 1999a).

Silicate mineral	Neutralisation reaction	Moles needed to neutralise 1 mole sulfuric acid
Olivine	$\text{Mg}_2\text{SiO}_4 + 4\text{H}^+ \rightarrow \text{Mg}^{2+} + \text{SiO}_4$	0.5
K-feldspar	$\text{KAlSi}_3\text{O}_8 + 4\text{H}^+ \rightarrow \text{K}^+ + \text{Al}^{3+} + 2\text{H}_4\text{SiO}_4$	0.5
Ca-plagioclase	$\text{CaAlSi}_3\text{O}_8 + 8\text{H}^+ \rightarrow \text{Ca}^{2+} + 2\text{Al}^{3+} + 2\text{H}_4\text{SiO}_4$	0.25
Na-plagioclase	$\text{NaAlSi}_3\text{O}_8 + 8\text{H}^+ \rightarrow \text{Na}^{2+} + 2\text{Al}^{3+} + 2\text{H}_4\text{SiO}_4$	0.5

1 mole of calcite is needed to neutralise 1 mole of sulfuric acid whereas if complete dissolution of silicates is assumed, then the silicates have a higher potential buffering capacity (see Table 2). However when dissolution is taken into account, short term buffering capacity is provided by dissolving and fast weathering minerals whereas intermediate to slow weathering minerals will only provide a long term NP (Table 3).

Table 3: Weathering rates of typical minerals found in gangue (Kwong, 1993; Lawrence and Scheske, 1997).

Weathering rate	Typical minerals
Dissolving	calcite, aragonite, dolomite, magnesite
Fast weathering	olivine, diopside
Intermediate weathering	pyroxenes, epidote, enstatite, amphibole, chlorite, biotite, tremolite, Ca-plagioclase (anorthite)
Slow weathering	Na-plagioclase (albite), kaolinite,
Very slow weathering	K-feldspars, muscovite
Inert	Quartz, rutile, zircon

Smart et al. (2004) describes an ARD evolution trend which summarises the ARD generation mechanism (see Figure 7).

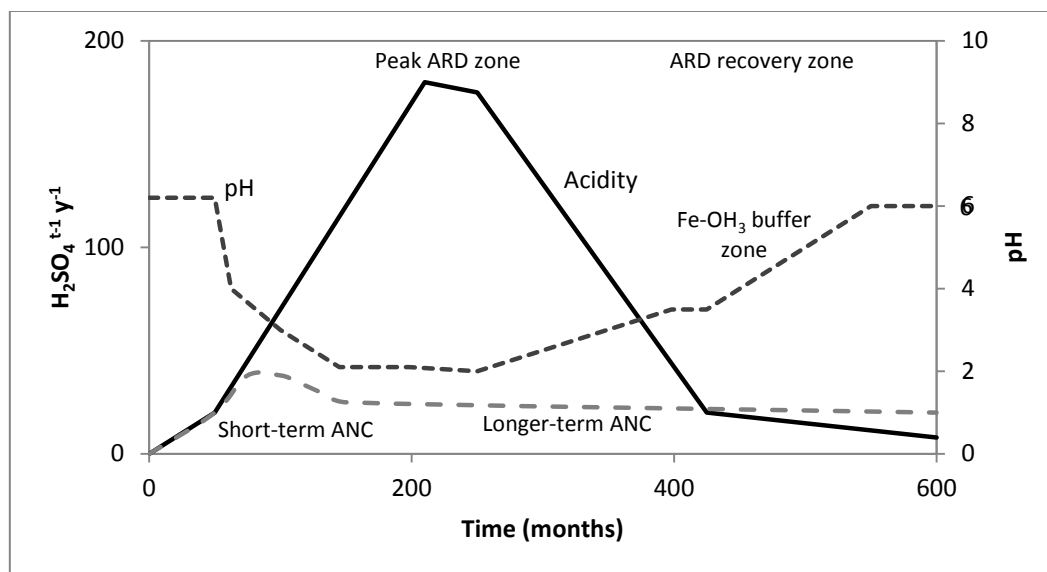


Figure 7: Acid rock drainage formation evolution trend (Smart et al, 2004).

- The peak zone is associated with sulfide mineral oxidation in excess of acid neutralisation by high sulfide oxidation and acid generation in excess of acid neutralising capacity (ANC).
- Short term ANC is derived from carbonates and cation exchange on silicate minerals
- Long term ANC may be determined by silicate dissolution kinetics after carbonate exhaustion
- ARD recovery zone occurs when the longer term aluminosilicate ANC is in excess of acid generation. It is characterised by decreasing sulphate and metal content.

2.5.2 Factors affecting ARD generation

The rate of acid generation is determined by chemical, biological and physical factors (Akciil and Koldas, 2006). The influence of biological factors is limited to sites where growth of acidophilic bacteria is promoted (Sampson et al., 2000). The factors that determine the rate of acid production can be summarised as shown in Figure 8. These factors form a complex interdependent environmental system. The chemical and biological factors have a greater effect on the rate of sulfide oxidation whereas the physical factors play a greater role in affecting the composition of the resulting drainage.

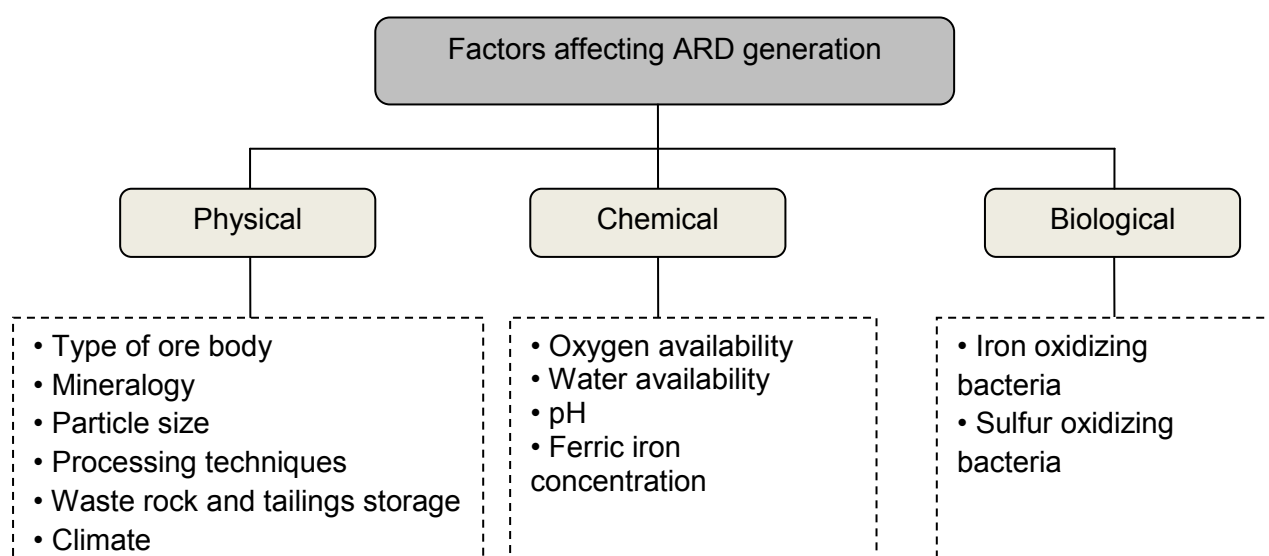


Figure 8: Factors affecting the rate ARD generation (Akciil, 2006).

Extensive studies have been done on these factors (Blowes et al., 2005; INAP, 2009). Chemical factors that affect the rate of pyrrhotite oxidation have been previously discussed in section 2.3.3. A brief discussion on physical factors and biological factors is given in the following paragraphs.

Mineralogy and mineral processing techniques

Different mineral processing methods are used for various ore bodies, which then affects particle size, extent of liberation and mineral composition of waste deposits. Comminution produces particle sizes less than 150 μm which increases liberation and the surface area of the sulfides (Wells et al., 1997). Separation efficiency in flotation affects the amount of sulfides and gangue that report to the tailings, which will then affect the balance between acid producing and acid neutralising minerals present in the waste deposits.

The rejection of pyrrhotite in Nickel processing was originally environmentally driven to reduce SO_x emissions from smelting (Wells et al., 1997). However the result is that the pyrrhotite rich tailings are deposited into shallow lakes where they are susceptible to oxidising agents (Peek et al., 2011). In solving one environmental problem another has been created over the years. In the Sudbury basin about 85 % of pyrrhotite rejection is achieved, from the early 1990s Xstrata and Vale Inco have released a combined amount of about 50 million dry metric tonnes of pyrrhotite tailings into shallow lakes and tailings dams

(Gunsinger et al., 2006; Peek et al., 2011). Figure 9 shows an example of a typical tailings dam.

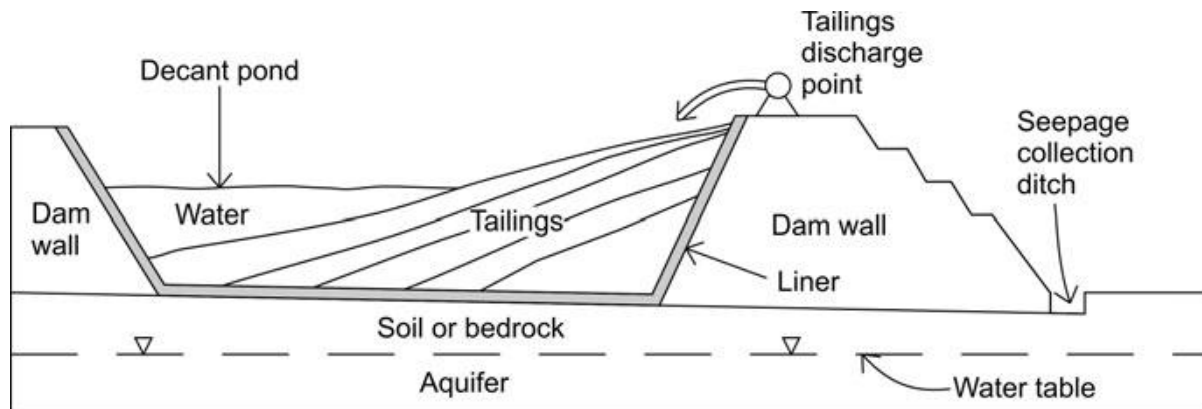


Figure 9: Cross section of a typical tailings dam (Lottermoser, 2010).

The manner in which waste is stored during mine operation and post closure affects the amount of sulfidic waste that is exposed to oxygen and water, and the rate at which mine drainage is released into the environment. The failure of tailing dam walls can lead to seepage of mine water into aquifers (Lottermoser, 2007). Infiltration from groundwater through weak dam walls into the tailings waste can accelerate oxidation of the sulfidic waste (Lei and Watkins, 2005). Excessive water levels in the decant pond can also lead to overtopping and the embankment collapsing exposing the sulfidic waste. Careful consideration of construction materials and monitoring of dams levels during operations are important to prevent dam failure.

Climate

Climatic conditions such as temperature and rainfall play an important role on the nature of mine drainage. Climatic conditions affect the amount of evaporation, water runoff and percolation. Regions with arid climates have a high level of evaporation which affects the saturation level. Rainfall and further addition to the deposit will then rewet these dry areas, creating perfect conditions for the generation of ARD. Areas with high levels of rainfall have larger quantities of water percolating through the deposits, causing higher levels of leaching.

Climate and seasonal effects determine whether mine discharge is continuous or intermittent, dilute or highly concentrated (INAP, 2009). Although climatic conditions are a key factor in mine water drainage quality, the shifts in pH and metal content of drainage from

a given deposit in different climatic conditions are more affected by differences in geologic characteristics (Plumlee and Logsdon, 1999).

Microbial activity

At acidic pH (pH below 4.5) certain species of bacteria can catalyse both the oxidation of sulfur and ferrous iron reactions (equations [3], [4] and [5]). The common ferrous iron-oxidising bacteria that are found in acid generating deposits include *Acidithiobacillus ferrooxidans*, *Acidithiobacillus thiooxidans*, *Leptospirillum ferriphilum* and *Leptospirillum ferrooxidans* (Johnson and Hallberg, 2003). Fe oxidising micro organisms generate ferric iron from the oxidation of ferrous iron and Sulfur oxidising microorganisms generate sulphate. *A. ferrooxidans* can catalyse both the oxidation of sulfur and ferrous iron and requires a pH range of 1.0 to 3.5 with the optimum near 2 at an optimum temperature of about 35°C (Gould and Kapoor, 2003). *A. thiooxidans* can only oxidise sulfur, and is more tolerant to a range of acid conditions, between pH 0.5 to 4.0 (Robertson and Broughton, 1992). Figure 10 shows the roles of iron and sulfur oxidising micro-organisms.

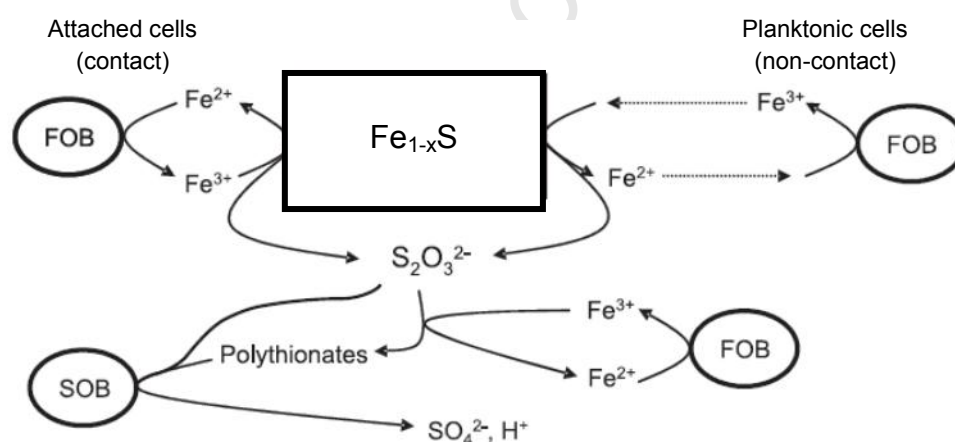


Figure 10: Schematic of pyrrhotite oxidation by acidophilic bacteria, adapted from Bryan (2006) FOB: ferrous oxidising bacteria, SOB: Sulfur oxidising bacteria.

The rate of acid generation and the bacterial activity is determined by the bacterial population density and the rate of the species' population growth. The population density and growth are governed by (Gould and Kapoor, 2003);

- Carbon availability (in the form of carbon dioxide)
- An electron donor (ferrous iron or sulfur)

- Nutrient availability (e.g. Nitrogen and phosphorous for production of biomass)
- Oxygen availability (enables growth of aerobic bacteria)
- Temperature

Above pH 4 the oxidation of ferrous iron is mediated by oxygen however below pH 4 the rate of oxidation of ferrous iron by oxygen is negligible (Stumm and Morgan, 1996). Therefore acidophilic iron oxidising micro-organisms play an important role in metal sulfide oxidation because they catalyse the conversion of ferrous iron to ferric iron.

2.5.3 Environmental impacts of ARD

The resultant effects of acid rock drainage on the environment depend on the sources, pathways and the sinks (i.e. receiving environment). Mine drainage is transported by various pathways (see Figure 11) into the environment where it contaminates water sources and degrades the quality of the water to a point where it is unfit for human and animal consumption or crop irrigation. The receiving environment can alter the nature of the mine drainage and its overall impact on the environment (INAP, 2009).

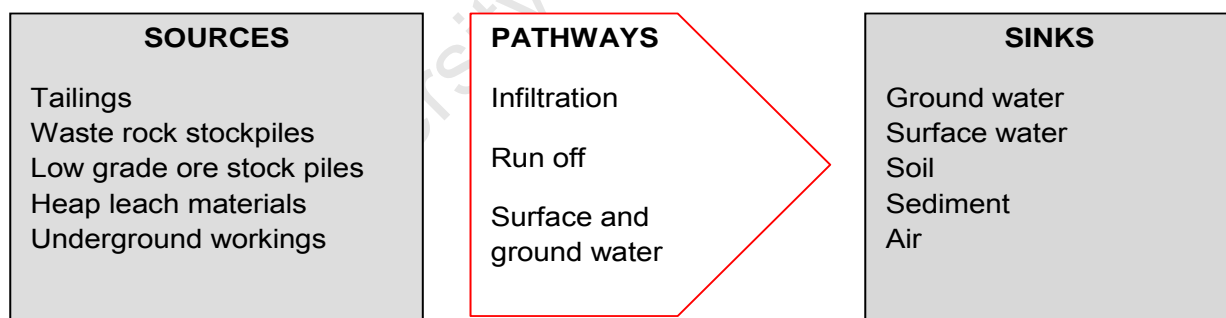


Figure 11: Conceptual model of Sources, Pathways and Sinks (adapted from INAP, 2009).

The resultant effect of mine drainage on the environment can be either acidic drainage (ARD), neutral mine drainage (NMD) or saline drainage (SD), all depending on the pathways and receiving environment of the mine drainage. Above pH 6, mine drainage is classified as NMD and SD whereas below pH 6 it is ARD. ARD has elevated sulphate and metal ion concentration whereas NMD and SD have moderate to low metal ion and sulphate concentrations (INAP, 2009). Mine drainage from mine waste sources may contain suspended solids, dissolved contaminants such as acid, salts, heavy metals, metalloids and

sulphate. Table 4 gives the characteristics of ARD and the associated environmental impacts of low pH, high heavy metal concentrations and dissolved solids concentrations.

Table 4: Main characteristics of ARD water and environmental impacts (Lottermoser, 2007; Ritchie, 1994).

Property	Chemical species	Conc in solution	Environmental impact
Acidity	H^+	$pH < 4.5$	<ul style="list-style-type: none"> • Mobilisation of metal ions • Reduction in potable water quality • Corrosion of man-made structures
Iron precipitates	Fe^{2+} , Fe^{3+} , $FeOH_3$	100 to 1000 mg/l	<ul style="list-style-type: none"> • Discoloration and turbidity in receiving water as pH increases
Dissolved heavy metals and metalloids	Cu, Pb, Zn, Cd, Co, Ni, Hg, As, Sb	0.01 to 1000 mg/l	<ul style="list-style-type: none"> • Soil and sediment contamination • Reduction in potable water quality
Total dissolved solids (TDS)	Ca, Mg, K, Na, Fe, Al, Si, Mn, SO_4^{2-}	100 to more than 1000 mg/l	<ul style="list-style-type: none"> • Form salts precipitates • Soil and sediment contamination • Further reduction in potable water quality

The low pH environment resulting from acidic drainage promotes the mobility of acid soluble and ion exchangeable metals from stable phases (John and Leventhal, 1995). ARD does not only contribute to surface and ground water pollution it can also result in degradation of surrounding soil quality and allows dispersion of heavy metals into the environment (Hallberg, 2010). The release of these metal elements into the environment can have severe effects to flora and fauna through bioaccumulation (Hallberg, 2010).

2.6 ARD mitigation

ARD is one of the major environmental issues facing the world's water resources and it has various consequences and multigenerational ramifications. Prevention of the formation of ARD or the migration of acidic mine water from its source is considered to be the preferable option (Johnson and Hallberg, 2005). The poor management of ARD can have detrimental effects on the communities surrounding the mining area, now and for generations to come. ARD treatment can be classified into prevention and control methods. Prevention methods focus on source control to eliminate the risk of ARD formation. Whereas control methods aim to remove the risk, either by treating resultant waste or by generating benign waste. However a lot of the methods currently in use focus on an end-of pipe level approach, by treating resultant drainage or managing waste.

2.6.1 Current disposal techniques

Current disposal methods aim to prohibit the contact of water and oxygen with the potentially acid forming (PAF) waste (Romano et al., 2003). The control measures currently in use include flooding or sealing underground mines, underwater storage of mine tailings and solidification of tailings (Johnson and Hallberg, 2005). The limitation however, of backfill and sealing of underground mines is that the mines may be susceptible to flooding by underground water, and unstable mines may collapse exposing PAF waste to water and air. Another technique in waste disposal includes blending sulphidic waste with neutral waste. However due to the different dissolution rates of various neutralising minerals it will be hard to predict the ARD mitigation provided by such a method (Weber et al., 2004). In light of the limitations and practicality of inhibiting contact of waste with oxidising agents, most mitigation methods aim to minimise the impact of ARD waste on the receiving environment. Therefore most approaches involve minimising the impact of waste on the environment by treating the waste and resultant acid water.

2.6.2 Current ARD treatment technologies

Current treatment methods are focused on remediation of resulting drainage by pH adjustment and removal of metals ions by precipitation. There are different methods available for remediation of ARD which can be classified into chemical methods (abiotic) and biological systems (biotic). Both systems include methods which can be described as

“active” (require continuous input to sustain the process) and “passive” (input once in operation) (Johnson and Hallberg, 2005). Mitigation is site specific as factors such as physical, biological and climatic conditions will differ from site to site. The following diagram (Figure 12) gives examples of some of the remediation options available:

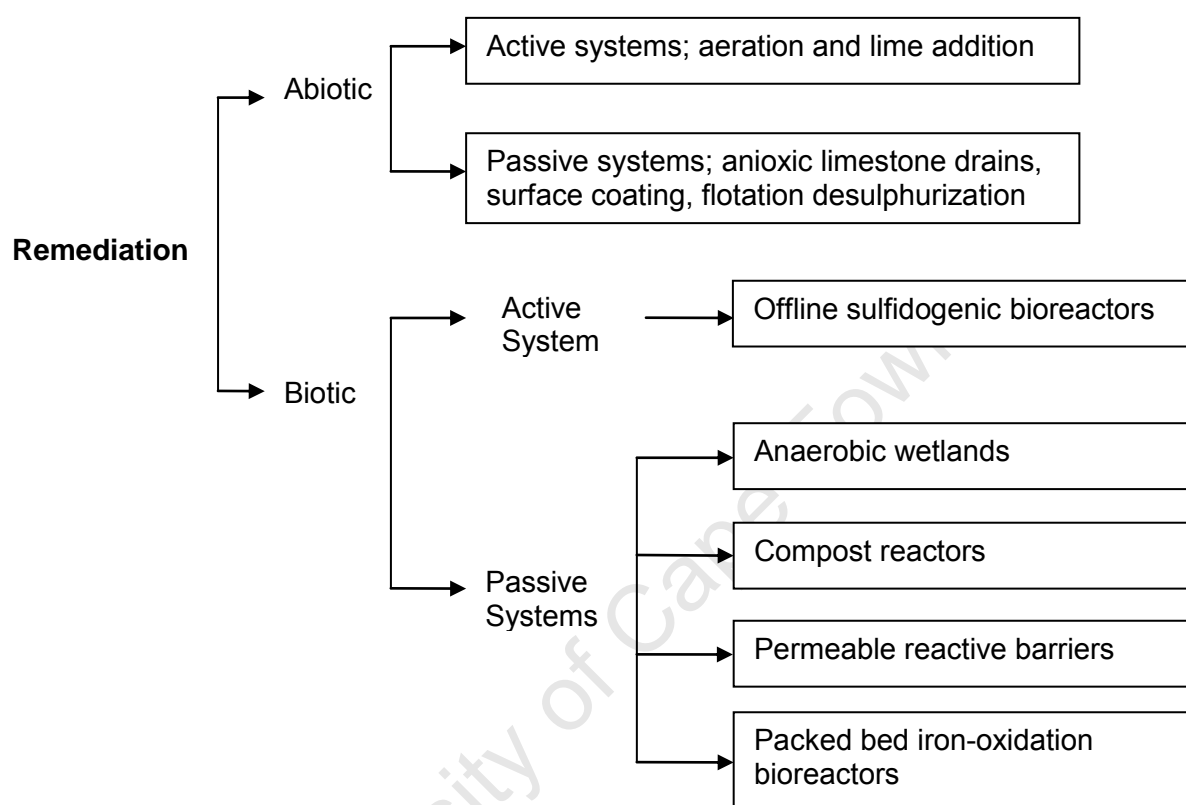


Figure 12: Examples of ARD remediation options (adapted from Johnson and Hallberg, 2005).

The remediation options shown in Figure 12 are end-of-pipe level measures. These measures are implemented to prevent ARD migration and manage ARD waste rather than deal with ARD at a source level. In the Sudbury area in Canada, Inco limited (currently Vale-Inco) and Falconbridge limited (now Xstrata), two of the largest nickel producers in the area, use about a quarter of the pyrrhotite tailings as underground backfill in mines (Crawford, 1995; Benzaazoua et al., 2000). Currently the majority of the tailings are disposed of in shallow lakes which hold the solids but allow water to flow to treatment plants (Peek et al., 2011). Once the dams are filled to capacity the tailings deposits are revegetated. Limestone is spread onto the surface to neutralise surface acidity and further mixed with fertiliser to provide a medium for the seeds. Further limestone mixed with fertiliser is added as required; this can be classified a biotic active system (Crawford, 1995). Currently in South Africa ARD

is largely treated by adding lime to neutralize the acid and precipitate out the heavy metals as hydroxides (Akciil and Koldas, 2006). Even though treatment methods may be effective, high costs are incurred to sustain them therefore prevention at the source is more promising. Prevention methods will not require treatment facilities after mine closure, thus they are deemed as a more cost-effective management approach (Johnson and Hallberg, 2005).

With a push for industry to move towards more sustainable development, which requires an integrated, balanced and responsible approach that accounts for short-term and long-term environmental, social and economic considerations long after mining operations have stopped (MMSD, 2002). The production of benign waste is in line with the concept of cleaner production and sustainable development, which aims to identify options within a mineral beneficiation process flow sheet to minimise waste. Currently in Sudbury Nickel processing operations magnetic pyrrhotite, which is more reactive and has high sulfur content, is removed in magnetic drums before the concentration circuit. Magnetic separation simply separates the magnetic and non-magnetic pyrrhotite fractions. Flotation still needs to be conducted to separate pyrrhotite and pentlandite (Lawson et al., 2005). However this process step is advantageous because a high sulfide stream and a low sulfide stream are produced which enables effective management of PAF waste.

A form of cleaner production of tailings known as environmental desulphurisation, has been investigated by Benzaazoua et al. (2000) and Hesketh (2010c). This process employs selective froth flotation to produce desulphurized tailings and is to be used at the end of primary process treatment before tailings disposal. With this process it is possible to produce two distinct fractions, a sulfide concentrate and desulphurized non-acid generating tailings. The sulfide rich concentrate can then be disposed by cement paste backfilling and the desulphurized fraction can be used in layering existing sulfide tailings deposits. However this approach can only be implemented if it is economically comparable to ARD mitigation techniques in use as it will require installation of new flotation equipment (Benzaazoua et al., 2000). Even though desulphurisation has been proven to be feasible, additional costs may be prohibitive in some cases. Passivation also known as surface coating has presented a possibly cost effective remediation option as it employs reagents which are already used in mineral processing. Surface coating takes advantage of the surface characteristics of pyrrhotite, and will now be further discussed.

2.6.3 ARD mitigation by passivation or “surface coating”

Passivation of pyrrhotite and pyrite by surface coating has been identified as a possible means of mitigating acid rock drainage. The objective of surface coating is to coat sulfide minerals with a substance that will prevent oxidative attack. A number of chemicals have been tested on pyrite and proved to significantly reduce the oxidation rate (Belzile et al., 1997; Lan et al., 2002). Lan et al. (2002) by use of a strong insoluble chelating agent, 8-hydroxyquinoline, as a coating agent, were able to drastically reduce the oxidation of pyrite; a 97% decrease was reported. Chen et al. (2006) used polyethylene polyamines as coating agents on both pyrite and pyrrhotite and found oxidation was greatly reduced after coating. Passivation of sulfide surfaces by the ferric oxyhydroxide layer has been observed; at a certain thickness the layer inhibits further oxidation. Passivation by polyethylene polyamines and O₂ sparging will now be focussed on, due their current application in the depression and rejection of pyrrhotite, which means that limited costs would be incurred in their possible usage as passivating agents.

Passivation by polyethylene polyamines

Polyethylene polyamines are basic substances and they neutralise protons during oxidation processes. The presence of several nucleophilic nitrogen atoms in the structure of polyamines (Figure 13) allows them to provide electrons and act as a reducing agents thus preventing oxidation.

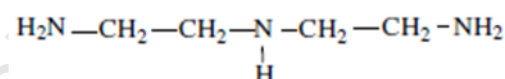


Figure 13: Polyethylene polyamine structure (Kirk-Othmer, 1984).

In the study by Cai et al. (2005) pyrrhotite particles were coated with TETA and exposed to different oxidising conditions (air, Fe³⁺ and *Acidithiobacillus ferrooxidans*). Oxidation of two different pyrrhotite bearing ore samples and pure pyrrhotite, were drastically reduced. In the study conducted by Chen et al. (2006) coating effectiveness was compared between pristine and pre-oxidised samples of both pyrite and pyrrhotite. In both studies solutions of either TETA or DETA were added directly to the samples; different concentrations of the solutions were tested ranging from 0.2 % to 1 % (v/v). To compare the effectiveness of the passivation of different coating agents the parameter oxidation extent was introduced:

$$\text{Oxidation extent (\%)} = \frac{\text{weight of oxidised sample}}{\text{weight of sulfide sample}} * 100 \quad [10]$$

Another parameter, passivation efficiency, was also introduced to compare different coating conditions where;

$$\text{Passivation efficiency (\%)} = \frac{\text{Oxidation extent}_{\text{control}} - \text{Oxidation extent}_{\text{coated}}}{\text{Oxidation extent}_{\text{control}}} * 100 \quad [11]$$

To obtain the oxidation extent the coated samples were filtered through a membrane and flame atomic absorption (FAAS) was used to measure the iron content of the filtrate. Chen et al. (2006) found that the passivation efficiency was improved when the samples were pre-oxidised. Belzile et al. (1997) studied the inhibition of pyrite oxidation by surface treatment and found that the formation of the oxide layer improves coating efficiency. Chen et al. (2006) tested the passivation efficiency of pyrrhotite from two different regions (Garson and McCreedy in Sudbury) and found that the coating effectiveness varied. Chen et al. (2006) attributed this variation to differences to surface, chemical and mineralogical properties.

Further coating experiments were done by Chen et al. (2006) in which mixtures of DETA and potassium amyl xanthate (PAX) were used as the coating agents. The passivation efficiencies obtained with DETA alone and DETA + PAX were approximately the same for both pristine and pre-oxidised samples of pyrite. Chen et al. (2006) did not observe any degradation of the coating layer after 33 days of experiment under 85 ± 15 % humidity and 30 ± 5 °C. They concluded that DETA or TETA adsorb strongly onto the surface of sulfide ores. As pointed out by Cai et al. (2005), the use of TETA/DETA as passivating agents is advantageous as the reagents are already utilised in flotation therefore limited cost will be incurred.

Passivation by the ferric oxyhydroxide layer

Huminicki and Rimstidt (2009), and Schumann et al. (2009) studied the possibility of using iron oxyhydroxide coating for acid rock drainage control of pyrite. It was found that when

pyrite is oxidized at alkaline pH, as the oxyhydroxide layer thickens it is possible to reduce the oxidant's diffusion coefficient by more than five times. Huminicki and Rimstidt (2009) proposed a mechanism for the oxyhydroxide layer growth; the reaction rate results suggested that the coatings grow in two stages (1) an initial stage of colloid deposition followed by stage (2) the densification and inward propagation of the coating (Figure 14).

In the first stage a thin, highly porous and permeable Fe oxyhydroxide layer deposits on the pyrite surface (see section 2.3.2). This layer is a weak barrier to oxidation transport causing the oxidation rate to only decline slightly. In the second stage the Fe oxyhydroxide coating becomes denser, further precipitating in the pores of the first layer producing a more effective oxidation barrier. After the second stage Huminicki and Rimstidt (2009) found the rate of pyrite oxidation decreases more rapidly.

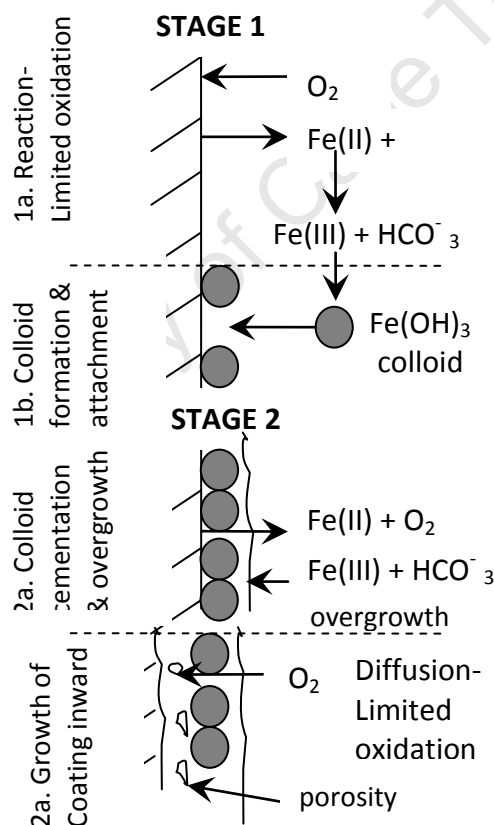


Figure 14: Schematic showing the steps of Fe oxyhydroxide coating formation on pyrite (Huminicki and Rimstidt, 2009).

However hydrodynamic conditions were found to play a crucial role in the initial stages of the development of the coating. With high flow rates the colloidal oxyhydroxide formed in stage 1

were swept away. The model developed by Huminicki and Rimstidt (2009) showed that in alkaline conditions the growth of the oxyhydroxide coating is promoted and can potentially forestall runaway ARD development. Schumman et al. (2009) from their study postulated that under conditions of a neutral pH the oxidation rate of pyrite can be reduced by the development of a multi-layered coating of goethite-like material of iron oxyhydroxide reaction products that incorporate sulfate, silicate and carbonate.

2.7 ARD potential prediction

Efficient ARD potential prediction and characterisation of waste is crucial to preventing ARD and managing potential acid generating waste. There are a number of procedures that have been developed to determine the acid generating potential of mine waste. These methods can be characterised as static methods or kinetic methods. Static methods involve a single measurement in time whereas kinetic methods involve a number of measurements over time. Commonly used static tests include (Smart et al., 2002);

- Acid base accounting (ABA)
- Single addition and sequential net acid generation tests (NAG)
- Electrical conductivity EC_{1:2} and pH_{1:2} tests

Static tests are initial screening tests and they provide information on the absolute potential of a sample but however do not take into account reaction kinetics. Static tests give information on the balance of acid forming and acid neutralising minerals within waste material. The recommended particle size for static tests varies from -23 µm to -240 µm. Electrical conductivity EC_{1:2} and pH_{1:2} tests measure the inherent acidity or alkalinity of the material and its potential to release salinity elements when initially exposed to water. The most widely used are acid base counting (ABA) and net acid generation (NAG) potential test.

Kinetic tests provide information on the reactivity of waste material and are usually conducted over longer periods. Commonly used kinetic tests include (Smart et al., 2002);

- Kinetic Net acid generation (KNAG)
- Humidity cells and leach columns
- Biokinetic tests

Kinetic tests take into account weathering rates. Humidity cells are packed with material into a reactor with air inlet and outlet flow and are intended to simulate changes in atmospheric conditions with periodic rainfall events. Subsequently the leachate is collected and analysed for pH, acidity, alkalinity, redox potential and cation and anion concentrations. Humidity cells may be inoculated with iron and sulfur oxidising microorganisms. Leach columns are an extension of the humidity cell concept, the difference being that leach columns are typically packed with a greater mass of minerals or tails than a typical humidity cell. Water is flushed at regular intervals through the column to create a wet-dry cycle which mimics oxidation and flushing events (Harrison et al., 2010). However humidity cells and leach columns have to be run over long periods of time to obtain substantial results, and for the time frame of the study these were not used. Batch biokinetic tests can provide data in a shorter period of time. Current application of ARD prediction tests has been largely focused on pyrite bearing waste. Limited work has been reported in the literature on the ARD prediction of pyrrhotite bearing waste. A selection of tests commonly used, will now be reviewed.

2.7.1 Acid base accounting (ABA)

Acid base counting involves static procedures which evaluate the balance between acid generation processes (oxidation of sulfide minerals) and acid neutralising processes. ABA reports the maximum potential acidity (MPA) and the acid neutralising capacity (ANC) or neutralising potential (NP). The difference between the MPA and ANC is referred to as the net acid producing potential (NAPP). The MPA generated by a sample is determined from the total sulfur content of the sample (Smart et al., 2002). The NAPP is a theoretical calculation used to indicate if a sample has the potential to generate AMD.

$$\text{NAPP} = \text{MPA} - \text{ANC} \quad [12]$$

The ANC of a sample is quantified as the buffering capacity of a sample, which is the ability of acid produced from oxidation to react with neutralising minerals contained within the sample (Smart et al., 2002). If the MPA is less than the ANC then the NAPP is negative which indicates that the sample may have sufficient ANC to prevent acid generation. If the MPA is greater than the ANC, then the resulting NAPP is positive, hence the material is acid generating.

There are different ANC tests which have been developed to better estimate the neutralising potential of samples such as the Sobek test, Lapakko and the BRCI initial. The more commonly used is the Sobek test and its modifications which are shown in Table 5.

Table 5: Commonly used ANC tests.

ANC test	ANC (NP) determination	Minerals possibly dissolved
Sobek (Sobek et al., 1978)	Uses Fizz test and heated with HCl (ca. 80 to 90°C). NaOH titration end point 7.0	Mineral carbonates Ca-feldspar, pyroxene, olivine (forsterite-fayallite) pyroxene, hornblende, augite, biotite
Modified Sobek (Lawrence and Wang, 1996)	Uses Fizz test and heated with HCl at ambient temperature. NaOH titration end point 7.0	Ca + Mg carbonates Some Fe carbonate, biotite, chlorite, amphibole olivine
Sobek Siderite correction (Skousen, 1997)	Uses Fizz test and heated HCl. 30 % H ₂ O ₂ added prior to titration to oxidise Fe ²⁺ to Fe ³⁺	Ca + Mg carbonates, excludes Fe + Mn carbonates. Otherwise as per Sobek.

The Sobek ANC test has been criticised for its tendency to overestimate the neutralising capacity as a result of the use of strong acid and the heating of the sample (see Table 5). The modified ANC test involves extended reaction time and does not involve heating of the sample (Lawrence and Wang, 1996), which is an improvement to the Sobek test, but may also still overestimate neutralising capacity. Different ANC tests dissolve different minerals which results in either an overestimation or underestimation of the neutralising capacity. Due to the aggressive nature of ANC tests, non-carbonate neutralising potential measured during static tests may or may not be available in mine wastes (Paktunc, 1999b). Therefore interpretation of the neutralising capacity of waste requires taking mineralogical composition into account (Lawrence and Scheske, 1997; Paktunc, 1999b). The computation of ANC from mineralogy (ANC_{MN}; equation 12) enables interpretation of ANC results and assessment of the neutralising capacity of different minerals that contribute to the ANC (Paktunc, 1999a, 1999b).

$$ANC_{MN} = \sum_{i=1}^k \frac{w_a * 10 * X_i * c_i * n_s}{n_i * w_i} \quad [13]$$

Where ANC_{MN} is the summation of the mineralogical ANC contributed by k number of neutralising mineral i, in kg sulfuric acid equivalent per ton,

w_a = molecular weight of acid H_2SO_4 ,

10 = conversion factor to $kg.t^{-1}$

X_i = amount of mineral i in wt%

c_i = number of non-oxidizable cations in one formula unit of neutralised mineral i

n_s = moles of sulfuric acid formed by the oxidation of one mole of sulfide mineral s

n_i = moles of mineral required to consume n_s

w_i = molecular weight the neutralising mineral

When conducting static tests the MPA is measured by LECO tests which give a bulk sulfur concentration of the sample. The method currently used to compute MPA assumes all the sulfur is available as reactive pyrite, and is determined as follows (Smart et al., 2002);

$$MPA \text{ (kg } H_2SO_4/\text{ton of sample)} = \text{wt\% total sulfur} \times 30.6 \quad [14]$$

This maybe an overestimation as this does not account for different types of sulfide minerals present that contribute to the acid producing potential of the sample (Paktunc, 1999b). To take into account the different sulfide minerals the MPA can be computed from mineralogy using equation 13 (Lawrence and Scheske, 1997; Paktunc, 1999b);

$$MPA_{MN} = \sum_{s=1}^m \frac{w_a * 10 * X_s * n_s}{w_s} \quad [15]$$

Where MPA_{MN} is the summation of the mineralogical ANC contributed by m number of sulfide mineral s, in kg sulfuric acid equivalent per ton,

w_a = molecular weight of acid H_2SO_4 , w_s = molecular weight the sulfide mineral

10 = conversion factor to $kg.t^{-1}$

X_s = amount of sulfide mineral s in wt%

n_s = moles of sulfuric acid formed by the oxidation of one mole of sulfide mineral s

The ANC is a function of mineralogy hence using mineralogical calculation can address the shortcomings of chemical tests (Lawrence and Scheske, 1997; Paktunc, 1999b). This can enable more practical estimates of the neutralising potential of mine wastes. Methods which incorporate mineralogical analysis are important in understanding the mechanisms behind mineral weathering. Equation [12] and [14] however are based on modal mineral concentration, and this may be an over estimation of ANC or MPA. Parbhakar-Fox et al. (2011) have developed an acid mine drainage index (ARDI) which predicts acid formation based on intact rock texture which incorporates geochemistry and mineralogical analysis. Textural effects such as liberation, association and grain size etc were taken into account in the ARDI method.

2.7.2 Net generating potential (NAG)

NAG determines the acid generating potential of a sample. In this test the sample is reacted with H_2O_2 which oxidises the sample to produce acid allowing it to react simultaneously with neutralising materials. The pH (NAG pH) of the reaction solution is measured; a NAG pH of less than 4.5 indicates the sample is acid forming whereas a pH of more than 4.5 indicates that the sample is not acid producing (Smart et al., 2002).

There are number of variations of the NAG test which include the single addition NAG, sequential and the kinetic NAG. In the sequential NAG test when the sample is filtered at the end of the first test the solids are not discarded, but are retained to be used as the starting material for the second NAG test. Sequential NAG tests are conducted when samples have a sulfur content of more than 1% to ensure complete oxidation of the sulfide minerals (Smart et al., 2002). The kinetic NAG test is similar to the single addition test the difference is that the temperature, pH and the electric conductivity of the liquor are measured. Observation of these parameters with time gives an indication of the kinetics of sulfide oxidation and acid generation. This test provides some understanding on the behaviour of the mineral in field conditions.

2.7.3 ARD potential classification

Samples can be classified as non acid forming (NAF) and potentially acid forming (PAF) or uncertain (UC). Non-acid forming (NAF) samples are defined as samples that have sufficient

acid neutralising capacity to neutralise all the acid that theoretically can be produced by the sulfide content of the mineral. A sample is defined as NAF when the NAPP is negative and the final NAG pH = 4.5. PAF samples are defined as having an acid generating potential exceeding the inherent acid neutralising capacity of the material. A sample is usually defined as PAF when the NAPP is positive and the final NAG pH < 4.5. Samples are classified as UC when there is disparity between the NAPP and NAG results. Table 6 shows a summary for ABA and NAG test classifications.

Table 6: The ARD classification guidelines (Stewart, Miller and Smart, 2006).

Test	Result	Units	Classification guideline
Acid Base Account	NAPP > 20	kg H ₂ SO ₄ /ton	Acid forming
	-20 < NAPP < 20		Potentially acid forming (PAF)
	NAPP < -20		Non acid forming (NAF)
Net Acid Generation	NAG pH < 4.5 & NAG _{pH7} >10	kg H ₂ SO ₄ /ton	Acid Forming
	NAG pH > 4.5 & NAG _{pH7} =5-10	pH	Potentially acid forming (PAF)
	NAG pH > 4.5		Non acid forming (NAF)
Kinetic NAG	Temp peak lag > 3 hrs		PAF with slow reaction kinetics
	Temp peak lag < 15 min		PAF with fast reaction kinetics
Combined static tests	NAG pH < 4.5 and NAPP > 0		Potentially acid forming (PAF)
	NAG pH > 4.5 and NAPP < 0		Non acid forming (NAF)
	If either of these criteria fail, the results are considered uncertain and further testing is required for classification		

The results from the ABA test and NAG test can be combined and put on a geochemical plot (Figure 15) which summarises the guidelines shown in Table 6.

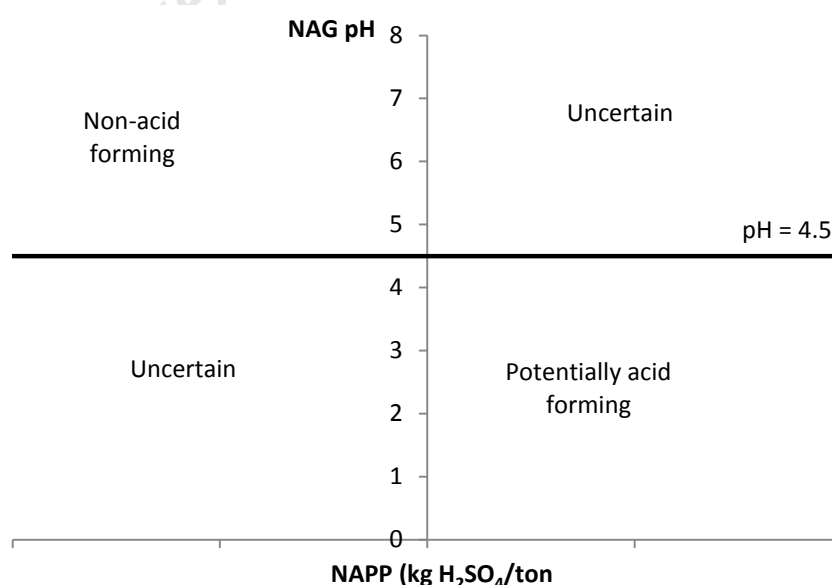


Figure 15: ARD classification plot showing the boundary regions (Stewart et al., 2006).

2.7.4 Biokinetic prediction test

Microbial tests which employ microbial colonisation in shake flasks have been used previously for the prediction of ARD generation such as the British Columbia Research Confirmation Test which was first developed by Duncan and Bruynesteyn (1979). In the British Columbia Research Confirmation Test, an iron oxidising bacterium, *Acidithiobacillus ferrooxidans*, is added to an acid stabilised suspension of mineral particles crushed to an average size of 200 μm and the solution pH is tested regularly. However the limitation to this test is that it employs a single microbial species whereas the Biokinetic test developed at the University of Cape Town (Hesketh et al., 2010b) employs a mixed culture containing both iron oxidising and sulfur oxidising microbes which are commonly found in mine wastes.

In the work done by Hesketh et al. (2010b) a refinement of the microbial shake flask test is presented. The modified test employs the use of finely milled ore or tailings (35 to 75 μm) on which the potential for microbially-mediated ARD formation is characterised while minimising the duration of the test (Harrison et al., 2010). This test is usually used as a follow up to static tests. The tests are conducted on samples which were determined to be acid producing by static tests; static tests assume all the sulfur in the sample is oxidised whereas with the shake flask test the extent of oxidation can be determined. Biokinetic tests provide information on microbial activity and its role on the mechanism of ARD generation (Hesketh et al., 2010b).

2.8 Summary and objective of the study

Pyrrhotite has been observed to exist in two forms commonly referred to as magnetic and non-magnetic pyrrhotite. Pyrrhotite is one of the most reactive sulfides due to its vacancy layers, making it highly susceptible to oxidation. Magnetic pyrrhotite has been observed to be more reactive than non-magnetic pyrrhotite. Lower rates of oxidation have been observed on non-magnetic pyrrhotite due to its less reactive nature. Current nickel processing flow sheets reject pyrrhotite to the tailings streams due to concerns of SO_x emissions from smelter gas emissions. Different rejection schemes have been explored (Wells et al., 1997) but not all have been implemented. Currently Nickel processing circuits operations tend to favour the use of chemical depressants (Wells et al., 1997; Lawson et al., 2005).

Pyrrhotite rich tailings are disposed of in shallow tailings dams where they potentially result in the formation of acid rock drainage (ARD). ARD mitigation methods currently in place deal with ARD by managing waste disposal or treating the waste streams e.g. backfill and lime addition. Thus there arises a need to incorporate into the mineral processing flow sheet a measure of dealing with the sulfide mineral tailings prior to disposal. This is line with the sustainable development concept of cleaner production which aims to minimise waste by mitigating environmental impacts at the source. Cleaner production methods such as desulphurisation flotation have been explored as a possible measure to separate high sulfide and low sulfide waste during flotation, but this requires additional equipment to be added to flotation circuits which may be costly. Thus there is still a niche to study possible cost effective ways in which sulfide mineral processing flow sheets can be manipulated to produce benign waste.

Passivation enables surface coating of the sulfide inhibiting attack by oxidising agents. Promotion of passivation of pyrrhotite during flotation to produce un-reactive tailings has not been explored. Polyethylene polyamines (DETA/TETA), which are already used as depressants in flotation, have been proved to be effective coating agents, effectively reducing the oxidation of pyrrhotite and pyrite in both abiotic and biotic systems (Cai et al., 2005; Chen et al., 2006). However passivation by polyethylene polyamines (DETA and TETA) has only been explored on waste rock and pristine pyrrhotite. The advantage of use of polyethylene polyamines as passivating agents is that they are used as depressants in current nickel processing flow sheets. It has been suggested that DETA/TETA remove

metal ions from the surface of pyrrhotite leaving the hydrophilic ferric oxyhydroxide layer enabling pyrrhotite to be rejected to the tailings. Also the rejection of pyrrhotite has been observed to be greatly improved when TETA/DETA are used in conjunction with sulfur derivatives e.g. SO_2 or SMBS. Although DETA/TETA have been reported to only act as chelating agents during flotation, there is still some uncertainty whether the reagents absorb onto the metal surface.

From studies of the mechanism of oxidation of pyrrhotite, the formation of a ferric oxyhydroxide layer has been reported to inhibit the further oxidation of the pyrrhotite surface. Passivation of sulfides by the ferric oxyhydroxide layer has only been explored in leach columns (Huminicki and Rimstidt, 2009; Schumann et al., 2009). Huminicki and Rimstidt (2009) showed that the growth of this layer can be promoted in alkaline conditions which results in a thick ferric oxyhydroxide layer which can greatly retard further oxidation of the sulfide. There also the possibility of passivating the surface by promoting growth of the ferric oxyhydroxide layer during flotation. Use of oxygen as a depressant in pyrrhotite rejection has been explored on laboratory scale in the past, but was never implemented.

This project has identified a possibility of manipulating rejection mechanisms in flotation to possibly produce passivated pyrrhotite tailings. To date, the promotion of passivation of pyrrhotite during flotation to produce un-reactive tailings appears to have been unexplored. The depression schemes to be investigated in this study will be limited to depression by oxygen and depression by polyethylene amines (TETA) due to their capability of promoting passivation. The aim of this study is to investigate the feasibility of mitigating the ARD generating potential of pyrrhotite tailings through the formation of passivation layers on the pyrrhotite surface during flotation. An additional objective is to review and compare the two pyrrhotite rejection methods.

2.9 Thesis Approach

In light of the complex reagent mineral interaction in the separation of pyrrhotite and pentlandite in the flotation process, this project aims to explore the possibility of depressing pyrrhotite and promoting its passivation to remediate the potential ARD production from pyrrhotite rich tailings, while maintaining a sufficient pentlandite recovery.

Using knowledge from mineralogical analysis (QEMSCAN, PXRD and Optical microscopy) and current ARD characterisation and nickel processing separation techniques (i.e. flotation), the project aims at providing an integrated approach (Figure 16) to the mitigation of ARD from pyrrhotite rich tailings. This is in line with the Minerals to Metals Initiative at the University of Cape Town which aims to combine cross disciplinary knowledge to address sustainable development issues in mineral beneficiation.

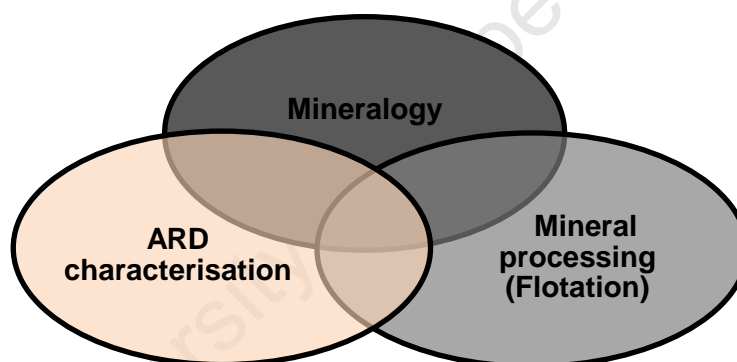


Figure 16: Thesis approach by integrating cross disciplinary knowledge.

Based on the summary of the literature and the scope of the project presented in the introduction, the key questions will be stated again;

- i. Is it plausible to simultaneously depress and passivate pyrrhotite during flotation?
- ii. Which depressant mechanism is more effective at pyrrhotite depression?
 - (c) TETA or TETA/SMBS
 - (d) Artificial oxidation

- iii. Which depressant is more effective at pyrrhotite passivation?
 - (b) TETA or TETA/SMBS
 - (b) Artificial oxidation

This study aims to also review the two rejection methods and to compare their rejection efficiency. The efficiency of passivation is determined by static and biokinetic ARD prediction tests. ARD characterisation methods documented in literature have been largely focused of pyrite bearing wastes. Very few authors have documented application of existing ARD prediction test methodology to pyrrhotite bearing ores. In addition, this study reviews the application of existing ARD prediction test methodology to pyrrhotite bearing ores. Figure 17 summarizes the detailed integrated approach to the test methodology used in this study. Mineralogical characterisation of the feed and tails samples is measured by several methods - including QEMSCAN, SEM imaging analysis and optical microscopy. The reactivity of the sample is measured by conducting oxygen uptake tests prior to flotation. The TETA dosages and oxidation times are varied to determine their effect on pyrrhotite depression and passivation. Prior to collection the tailings are further treated either by further oxidation or dosing them with TETA to promote further formation of passivation layers. ARD static and biokinetic tests are used to determine the acid producing potential of the samples.

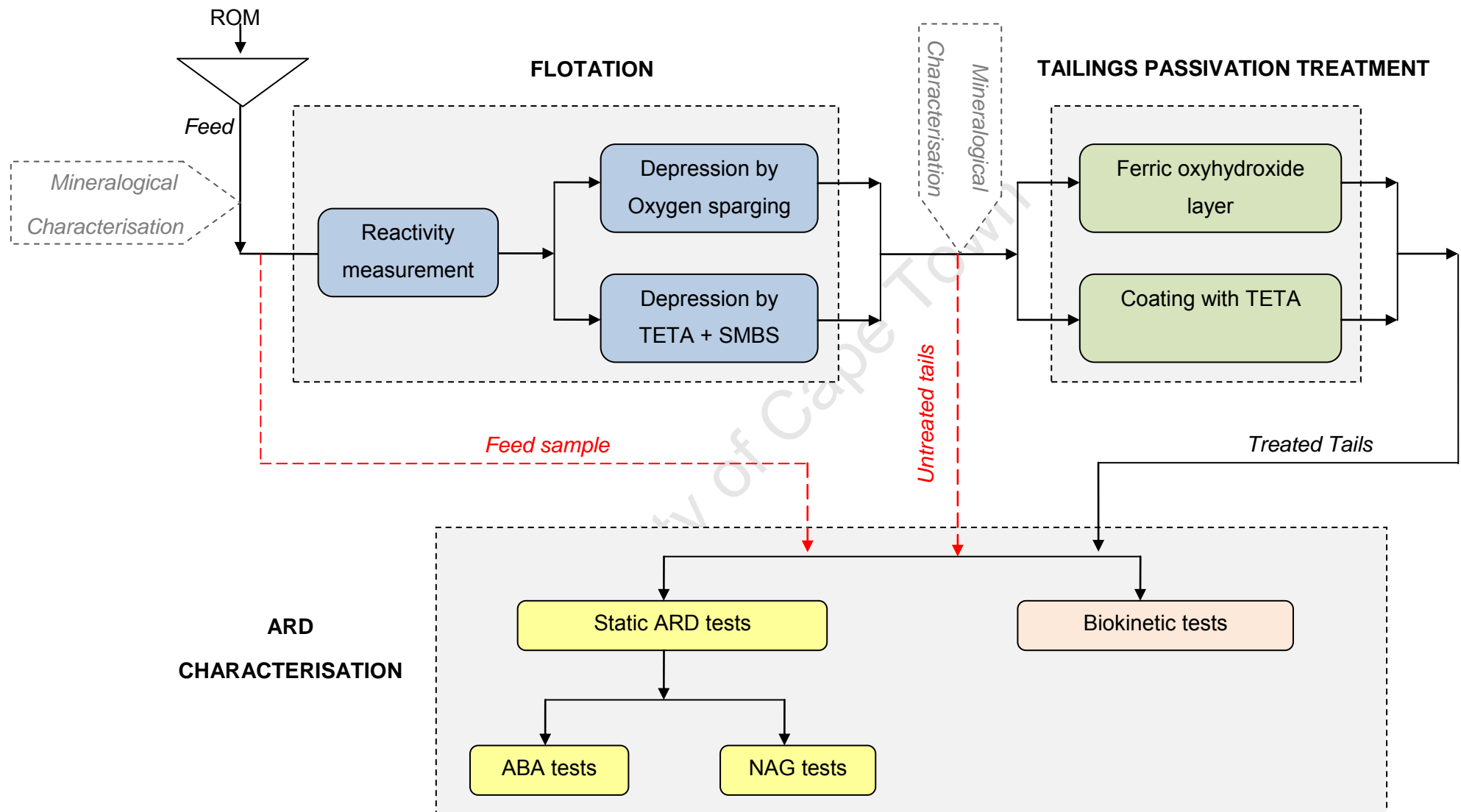


Figure 17: Flow sheet summary of test methodology approach.

3 EXPERIMENTAL METHODS AND MATERIALS

To determine the feasibility of simultaneously rejecting and promoting passivation layers on pyrrhotite rich tailings during flotation, the two rejection methods, TETA and artificial oxidations were investigated. Tests conditions were varied for both rejection methods and their flotation performance were reviewed. Thereafter the pyrrhotite rich tailings samples were characterized using ARD static and biokinetic tests to determine passivation efficiency. This chapter describes in 4 sections, the methods employed during the study.

Section 3.1 describes the sample selection and preparation. The ore was obtained as small rocks so it was crushed into a smaller particle distribution suitable for flotation. Section 3.2 describes the mineralogical characterisation methods employed in this study. Mineralogical characterisation methods were employed to determine the magnetic pyrrhotite content and bulk mineralogical composition and liberation of the ore. Section 3.3 describes the reactivity measurements and flotation tests work. Oxygen uptake tests were conducted to measure the reactivity of the sample before flotation. Flotation tests were then conducted where the rejection test conditions were varied for both methods; TETA and artificial oxidation. Section 3.4 describes the ARD characterisation methods used to determine the acid producing potential of the samples. The tailings were further dosed with either TETA or further oxidized, after which the acid producing potential of treated and untreated tailings and feed samples was characterized using static and biokinetic ARD tests.

3.1 Sample selection and preparation

The ore selected for this study contains magnetic pyrrhotite. It is a low nickel grade disseminated nickel ore sourced from a main mineralized zone. This ore was selected for the study as it contains magnetic pyrrhotite which is more reactive thus more responsive to oxidation.

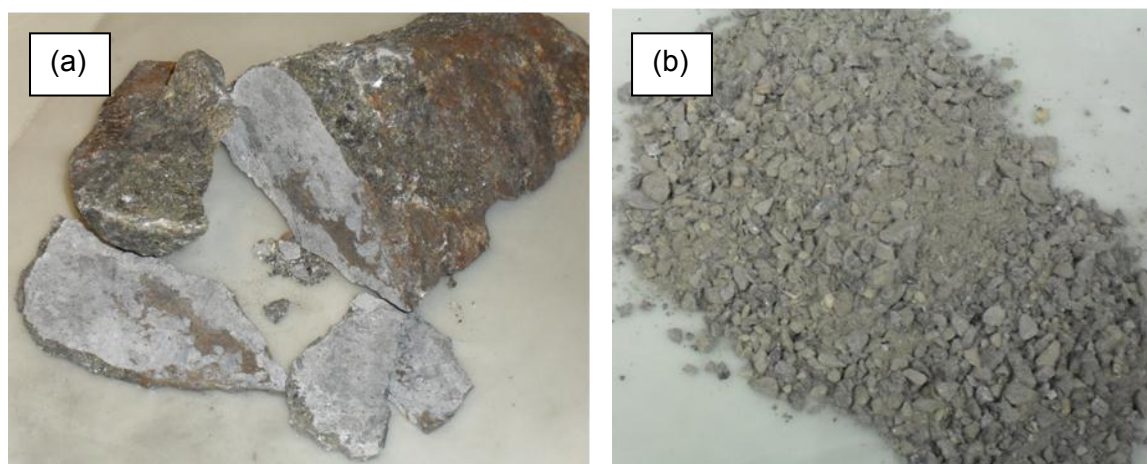


Figure 18: Photographs of the ore (a) rock samples (b) crushed sample

The ore was obtained as rock samples shown in Figure 18a, which were extracted from the mine in 2009. Preparation of the samples was carried out in the Centre for Minerals research (CMR) labs at UCT. The bulk ore samples were crushed to 100% passing 3 mm (Figure 18b), subsequently blended, riffled and split into representative 1 kg portions for further experimental tests.

3.2 Mineralogical characterisation

3.2.1 Optical microscopy

A standard Zeiss petrographic microscope was used to investigate the petrography of the pyrrhotite samples. Discrimination of the two pyrrhotite types was achieved by using a magnetic colloid; the magnetic colloid adheres to the magnetic pyrrhotite, thus differentiating magnetic pyrrhotite from non-magnetic pyrrhotite. The colloid was prepared by mixing FeCl_2 and FeCl_3 particles to form an insoluble black magnetite precipitate which was stored in a solution of sodium oleate (Craig and Vaughan, 1981). The colloid was placed over the surface of the ore mount and given a few seconds to interact and adhere to the magnetic pyrrhotite without letting the colloid dry. The sample was observed under the microscope and images were captured using a digital camera.

3.2.2 QEMSCAN

The bulk modal composition of the ores was conducted on a size by size basis (+106 μm , +75 μm , +53 μm , +25 μm , +10 μm , -10 μm) using a QEMSCAN based on a LEO SEM platform at the University of Cape Town. Representative samples were obtained by sub-sampling with a microriffler and were mounted in resin and carbon coated. Bulk mineralogy analysis (BMA) which gives linear analysis of the minerals and Specific mineral search (SMS) which identifies specific minerals of interest present in the grains were conducted. BMA was used to obtain the bulk modal mineral composition and SMS was used to obtain sulfide liberation data.

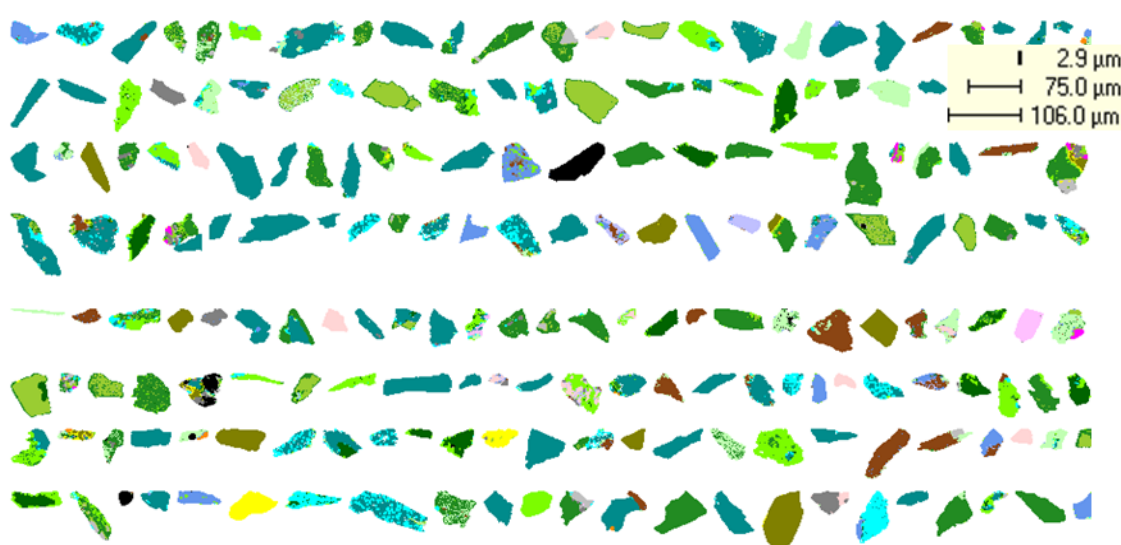


Figure 19: Image showing SMS analysis of various particles grains. Each colour represents a different mineral.

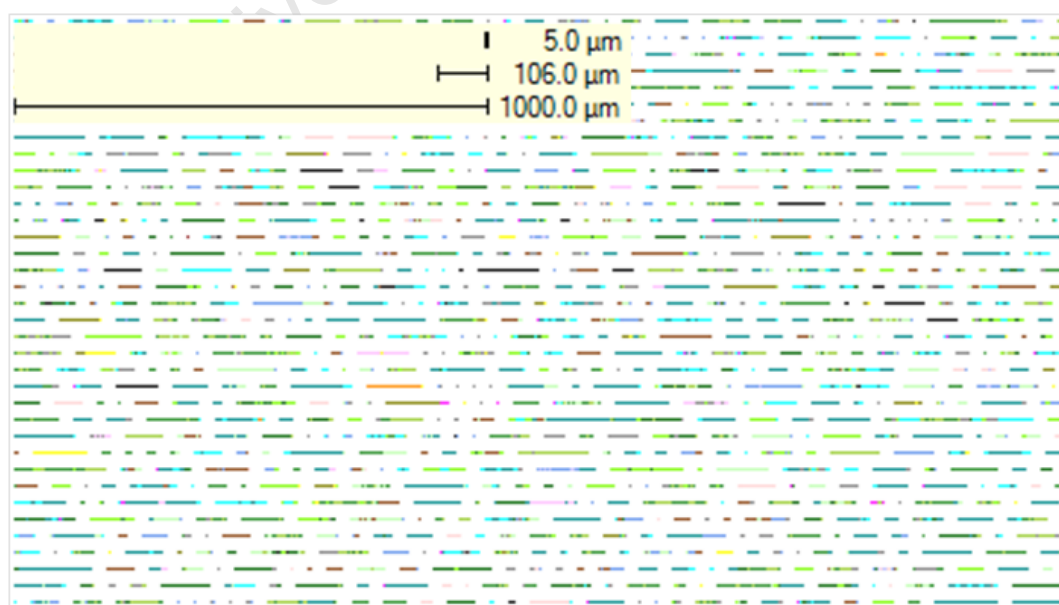


Figure 20: Image showing a section of BMA analysis. Each colour represents a different mineral.

Appendix A shows the bulk mineral composition of the feed obtained by QEMSCAN. Data validation of QEMSCAN data was obtained by comparing elemental chemical assays from ICP-OES (inductively coupled plasma optical emission spectrometry) and QEMSCAN (Figure 21).

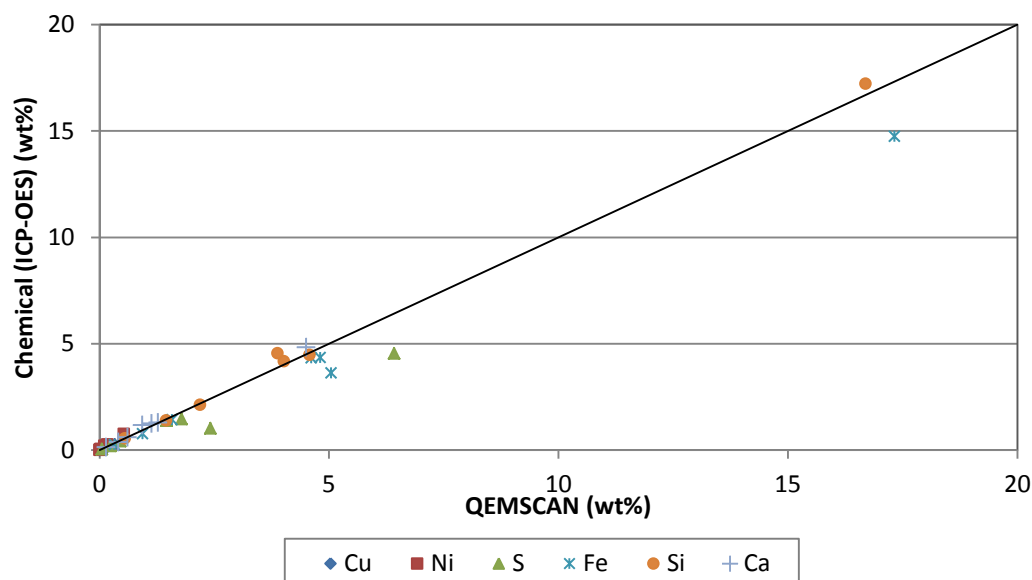


Figure 21: Graph showing the correlation between ICP-OES chemical assay and QEMSCAN data for the major elements present in the feed sample. The x=y shows 1:1 relation.

3.2.3 Chemical assays

All the chemical assays were conducted in the analytical laboratory in the Department of Chemical engineering at the University of Cape Town. Copper and Nickel assays of feed and tailings samples were done using a Bruker S4 Explorer XRF spectrophotometer. The total sulfur content was determined by combustion infrared spectrophotometer LECO analysis on a LECO DR 423 sulfur analyser. The total sulfur was assumed to be a contribution from sulfur in pentlandite, chalcopyrite and pyrrhotite.

3.2.4 Scanning electron microscopy (SEM)

SEM images were obtained on an FEI Nova Nano SEM machine using secondary electron images. The stubs were prepared by dispersing a pinch of a sample evenly on a metallic 1 mm diameter stub and coating the sample with carbon. An electron beam of 5 Kev was used and pictures were taken at a magnification of 10000x.

3.3 Flotation experiments

3.3.1 Pyrrhotite reactivity

To compare the reactivity of the pyrrhotite samples, the rate of oxygen uptake of the pyrrhotite slurry was measured. This measurement was adapted from Becker (2010a) who used the method developed by Afrox to determine oxygen uptake factors (reactivity) of pyrrhotite slurry. Prior to flotation the slurry was sparged with a controlled amount of air and the rate of decay of dissolved oxygen was measured. Below is a schematic of the apparatus, both the dissolved oxygen (DO) probe and the pH probe were immersed in the slurry. The DO probe was connected to a TPS meter and a PDA computer, the pH probe was only connected to a TPS to monitor the pH during flotation.

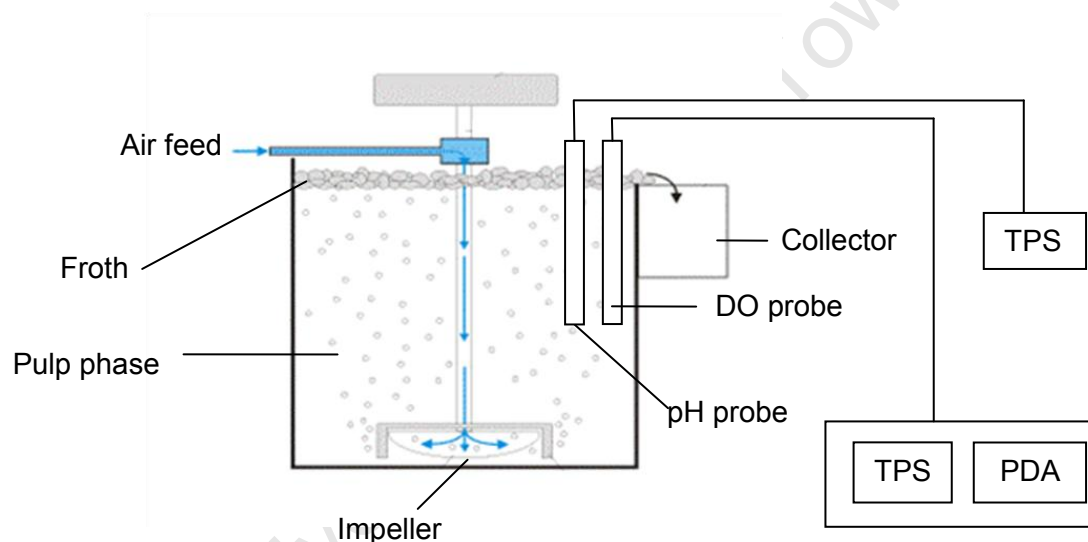


Figure 22: Schematic of the experimental set up

The dissolved oxygen content of the slurry was measured with a YSI 5739 probe fitted with a YSI high speed membrane, connected to a TPS W91 dissolved oxygen meter. The slurry was sparged with air for 10 seconds at a flow rate 7 l/min, which was the air flow rate used for flotation. The dissolved oxygen decay was then measured every 2 seconds for 2 minutes. The reactivity of the sample was quantified by the reactivity number (RN) which is calculated from the rate constant by assuming first order rate kinetics by fitting an exponential curve to the dissolved oxygen concentration versus time data. (Appendix B shows the method used to obtain the reactivity number)

3.3.2 Pyrrhotite rejection

Batch flotation tests were conducted to obtain the conditions at which maximum pyrrhotite depression could be achieved while maintaining nickel grade. The focus of the project was on the pyrrhotite rich tailings so typical plant reagent dosages were maintained to obtain a sufficient recovery of pentlandite where as depressant dosages were varied based on current plant dosages (Lawson et al., 2005) in the tests to maximize pyrrhotite rejection or depression.

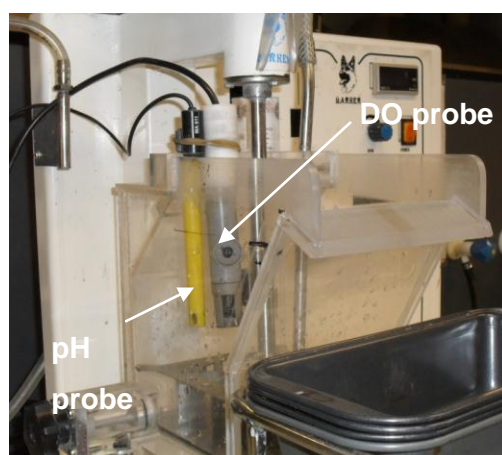


Figure 23: 3 L LEEDS Flotation cell at the CMR research lab at UCT.

The 1 kg feed sample portions of the ore were milled at 66 % solids in synthetic plant water (Wiese et al., 2005) (Table 8) using a laboratory stainless steel rod mill at a speed of 90 rpm to achieve a grind of 80 % passing 75 μm . Figure 24 shows the milling curve obtained. (Appendix C.1 shows the milling time required)

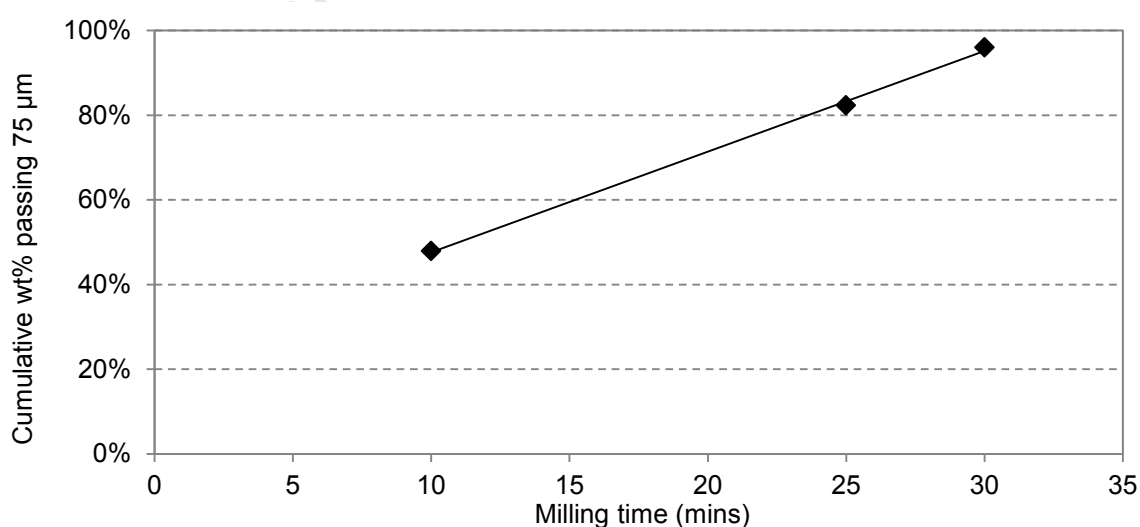


Figure 24: Milling curve obtained at a milling speed of 90 rpm at different milling times

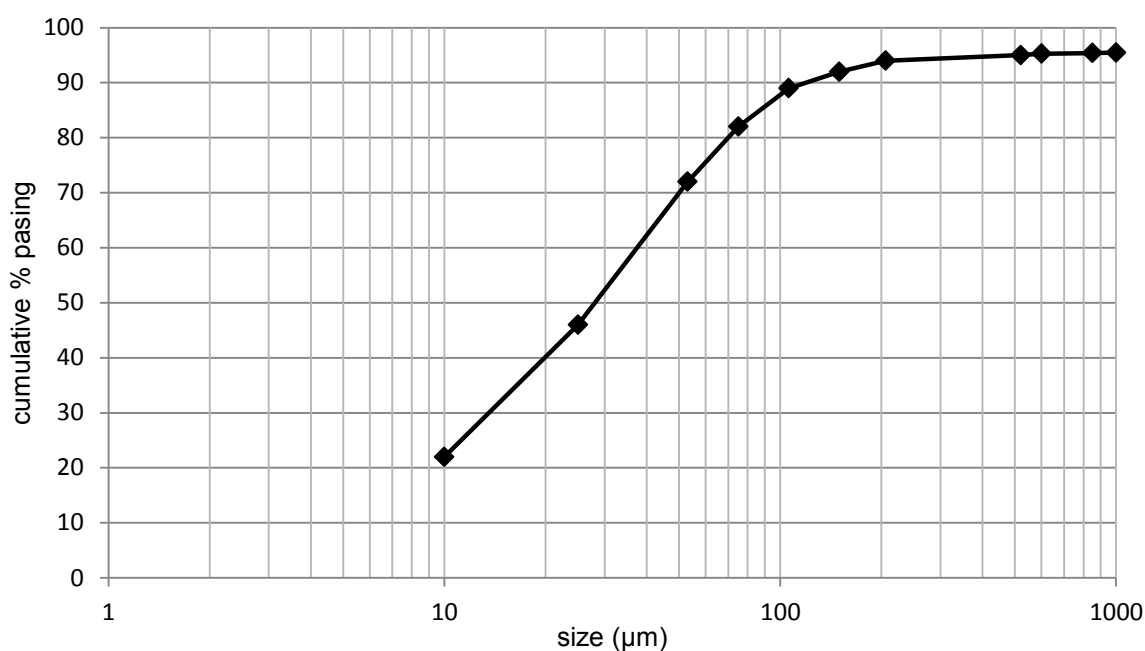


Figure 25: Particle size distribution (PSD) of the sample

The milled slurry was then transferred to a 3 L Leeds flotation cell, where the volume was made up to 35 % solids using the synthetic plant water (Table 8) and the pH adjusted to a value of between 9 and 10 with lime, whilst agitating at a speed of 1200 rpm. The reactivity of the ore sample was subsequently measured by conducting oxygen uptake tests using the Afrox Lab-Oscar device, prior to the addition of flotation reagents. Standard flotation was carried out for a period of 20 minutes at airflow rates of 7l/min. The pH was maintained between pH 9 and 10 by addition of lime, and the level of the pulp was controlled manually by the addition of synthetic plant water. Three types of flotation tests were conducted on each of the viz:

- Standard or baseline flotation tests in which no depressant was added. These tests used sodium isobutyl xanthate (SIBX) as a sulfide collector at dosages of 50 g/t, and (DOW 200) as a frother at a dosage of 35 g/t.
- Flotation tests using oxygen as a depressant. In these tests the ore slurry was sparged with air at a rate of 7 L/min for periods of 5, 10 or 15 minutes, prior to flotation under standard conditions.
- Flotation tests using TETA and SMBS, at a mass ratio of 1:4, as a depressant. Tests were carried at three different depressant dosages, viz 125 g/t TETA and 500 g/t SMBS; 250 g/t TETA and 1000 g/t SMBS; 350 g/t TETA and 1400 g/t SMBS.

Depressant ratios and total dosages were selected on the basis of plant practise as reported by Lawson et al. (2005). Concentrated TETA was handled with care while making the dilute solution. A mask was worn to prevent inhalation of the fumes from the concentrated amine. (see appendix C.2 for detailed flotation procedure)

Table 7 below summarises all the reagents used and the conditioning times needed.

Table 7: A summary of the reagent dosages and the conditioning times.

Reagent	Reagent name	Dosages (g/t)	Conditioning Time (minutes)
Frother	DOW 200	35	2
Collector	SIBX	50	2
pH control	Lime	400	5
Depressant	TETA	125 to 350	2
Depressant	SMBS	500 to 1400	2

Table 8: The concentration of the ions present in the synthetic plant water used in the batch flotation tests (Wiese et al, 2005).

Ion	Ca ²⁺	Mg ²⁺	Na ⁺	Cl ⁻	SO ₄	NO ₃	CO ₃	TDS
Concentration (ppm)	80	70	153	287	240	176	17	1023

Concentrate samples were collected after periods of 2, 4, 6 and 8 minutes, and subsamples were submitted for nickel, copper and sulfur analysis along with representative subsamples of the flotation feed and tailings. Assays were conducted on the samples as described in section 3.2.4. Nickel and copper assays were conducted using a Bruker S4 Explorer XRF. Total sulfur was determined using a LECO DR 423 total sulfur analyzer. The concentration of the minerals pentlandite, chalcopyrite and pyrrhotite were subsequently calculated.

3.3.3 Tailings passivation treatment

Selected tailings samples with sufficient pyrrhotite depression and pentlandite recovery, were then further treated to enhance pyrrhotite passivation. The two methods of passivation explored were passivation artificial oxidation to promote the formation of the ferric oxyhydroxide layer and surface coating with TETA. The tailings were further treated in the

flotation cell, with the impeller speed maintained at 1200 rpm to ensure thorough mixing during treatment. Table 9 and Table 10 show the further treatment applied to the tailings.

Table 9: Tailings passivation experimental matrix.

Test	Treatment	Oxidation as depressant	TETA as depressant	No depressant tails
1	No action	√	√	√
2	Oxidation	√	x	
3	TETA	x	√	

In test 2 the tailings from each depressant mechanism were further oxidized, to promote the formation of the ferric oxyhydroxide passivating layer. Legrand et al. (2005a) showed that it takes 5 minutes to form an appreciable ferric oxyhydroxide layer whereas it takes 30 minutes to achieve the same extent of oxidation on pentlandite. In test 3, the tailings from each depressant mechanism were further dosed with increasing concentrations of TETA and 2 minutes were allowed for conditioning after each dosage. Table 10 summarises the further oxidation and TETA dosages applied on the tailings.

Table 10: Further treatment dosages.

Test	Oxidation time (minutes)	TETA dosage (g/t)
1	-	-
2	10 – 120	-
3	-	120 – 1400

After each oxidation time interval and TETA dosage, representative samples were taken on which ARD potential tests were conducted. ARD potential tests were conducted on tailings in which no depressant was used and no treatment was done on the tails (Test 1). This test was used as a control to determine the acid producing potential prior to any further treatment by the depressant. The further treatment methods were conducted on tailings from the respective depression mechanism to isolate either effect i.e. passivation by ferric oxyhydroxide layer and passivation by TETA thus the treatments were not combined.

3.4 ARD prediction tests

ARD potential of the feed sample, treated and untreated tailings was determined by static tests and biokinetic tests. The methods used are subsequently described.

3.4.1 ABA (Acid base accounting)

Maximum potential acidity

The MPA was calculated stoichiometrically from the total sulfur (S_T) found by LECO tests. The MPA is reported in units of kg H_2SO_4 /ton of ore based on the assumption that all the sulfur in the form of pyrrhotite and pyrite in the sample forms H_2SO_4 . The MPA is calculated as follows (sec 2.7.1, equation 14);

$$MPA = S_T \times 30.6$$

Acid neutralising capacity

Different ANC test methodology exists which quantifies neutralising potential by varying reaction time which results in dissolution of different buffering minerals. Thus the acid neutralising capacity (ANC) or the neutralising potential (NP), was determined using the different test procedures to compare the accuracy of methods. The Standard Sobek ANC test, Skousen ANC test and ANC mineralogical calculations were conducted to compare the NP obtained. The detailed procedures are shown in appendix D.

Standard Sobek test

2 g of dry sample was digested in HCl in an Erlenmeyer flask according to the fizz rating guidelines (Sobek et al, 1978). The test was done in duplicate along with a blank test which has no sample. 20 ml of deionised water was then used to flush the sample to the bottom of the flask and the sample was heated at 90 °C for 1 to 2 hours and subsequently cooled for 1 hour. The reaction was complete when no gas evolution was observed and the solid particles settle at the bottom of the flask. Deionised water was again added to obtain a total volume of 125 ml, after which the pH of the mixture was measured. The sample was then filtered and back titrated using standardised NaOH to pH 7. The NaOH volume was recorded

to determine the final ANC of the samples in equivalent kg H₂SO₄/ton of sample according to the following equation;

$$ANC = \frac{[Vol_{HCl} - Vol_{NaOH} \times C] \times M_a \times 49}{W} \quad [16]$$

where M_a is the molarity of HCl (M), W is weight of sample (g) and $C = (Vol_{HCl} \text{ in blank}) / (Vol_{NaOH} \text{ titrated in blank})$ to take into account the differences in molarity between the acid and base solutions. A stoichiometric conversion factor of 49 gives results in kg H₂SO₄/ton. The step by step procedure is given in appendix D.1.2.

Skousen test

The Skousen H₂O₂ siderite correction test (Skousen, 1997) is a modification of the standard Sobek test to improve the efficiency of the test by minimising incomplete Fe hydrolysis on samples containing significant Fe content or siderite (FeCO₃). The procedure is similar to the standard Sobek test, except that the boiling step is for 5 mins and the solution is allowed to cool. After filtering, 30 % H₂O₂ was added to the filtrate to promote oxidation of dissolved Fe(II) and precipitation of Fe(III) thereafter the solution is further boiled for 5 min. After cooling the samples were back titrated to pH 7 and the NaOH volume added is recorded. After 24 hours a further 5 ml of H₂O₂ is added, and any resultant drop in pH is corrected with further back titration. This is repeated over 72 hours. The ANC is again computed using equation 14. The step by step procedure is given in appendix D.1.3.

ANC mineralogy

The ANC from mineralogy was obtained using the formula from section 2.4 from Paktunc (1999a, 1999b). The wt% composition of the minerals with a neutralising capacity was obtained from QEMSCAN data. The minerals considered in the calculation were dissolving and fast weathering. Appendix D.2 presents the calculations use to obtain the ANC from mineralogy using equation 13 from section 2.7.1.

3.4.2 NAG (Net acid generation) tests

Single addition and sequential NAG tests were conducted on the tailings samples. Sequential NAG tests were conducted because the samples have a sulfur content of more than 1% (Smart et al, 2002).

Single Addition NAG test

1.25 g of sample was weighed into an Erlenmeyer flask. Then 125 ml of 15% H₂O₂ at pH 4.5 was added at room temperature, and the flask was covered and placed in a fume hood.

The samples were allowed to react for 24 hours after which the pH is measured, and the samples are then heated for a minimum of 2 hours or until no sign of effervescence was noted. The sample was cooled and the after-boil pH was recorded. The sample was filtered and the filtrate was back titrated with 0.1 M NaOH to pH 4.5 and then to pH 7, noting the volume of NaOH added at each instance. The residues were analysed for total sulfur with LECO. The NAG_{pH 4.5} and NAG_{pH 7}, were calculated from back titration volumes in units of kg H₂SO₄/ton of ore.

$$\text{NAG} = \frac{49 \times V \times M}{W} \quad [17]$$

where V is the volume of NaOH (ml); M is the molarity of NaOH and W is the weight of sample (g).

Sequential NAG tests

The sequential NAG test is carried out following the same procedure as the single addition NAG test. However, after filtering, the residues were retained and air dried, the addition NAG test procedure is then repeated until no further reaction with H₂O₂ was noted and the after-boil pH was above pH 4.5. The remaining solids were sent for LECO total sulfur analysis. The sequential NAG was calculated with equation 17, using the cumulative volume of sequential additions of NaOH.

3.4.3 Biokinetic test

To assess the passivation efficiency under microbial leach conditions, batch shake flask leach tests were conducted on samples of flotation feed, treated tailings and untreated tailings. Samples of 7.5 g were added to 150 ml autotrophic basal salts medium at pH 4 (Bryan, 2006). Both abiotic tests and inoculated tests were conducted in triplicate. A mixed culture of *Acidithiobacillus ferrooxidans*, *Leptospirillum ferriphilum*, *Sulfobacillus benefaciens* and *Acidithiobacillus caldus*, was used. The flasks were maintained at 37°C on an orbital

shaking bench at 150 rpm for 90 days and the redox potential, pH and Fe in solution were measured at regular 2 to 4 day intervals. The redox potential was measured using a Crison ELP 21 Eh meter against a silver/silver chloride reference electrode (+199 mV vs. SHE). The pH was measured using a Metrohm 713 pH probe and the ferrous and the total iron in solution were determined colorimetrically using the 1-10 phenanthroline method (Komadel and Stucki, 1988). Appendix E.1 and E.2 show the detailed biokinetic test procedure used.

University of Cape Town

4 PYRRHOTITE CHARACTERISATION AND REJECTION

4.1 Introduction

The aim of this work is to explore the possibility of depressing pyrrhotite during flotation and promoting its passivation to remediate potential ARD production from pyrrhotite rich tailings, while maintaining a sufficient pentlandite recovery during flotation. This chapter describes the mineralogy of the nickel ore and provides the results obtained during oxygen uptake and batch flotation tests.

The chapter is divided into 4 sections. Section 4.2 describes the mineralogy of the ore obtained by QEMSCAN and optical microscopy. Section 4.3 presents the reactivity of the ore obtained by oxygen uptake measurements at the different test conditions (no depressant, oxygen as a depressant, TETA as a depressant and TETA and SMBS as a depressant). The depressant dosages used were based on plant dosages of TETA between 125 to 350 g/t, and with TETA at a 1:4 ratio with SMBS and pre-oxidation times were varied between 5 to 10 minutes. Section 4.4 presents these results obtained from the batch flotation tests.

4.2 Ore characterisation

As seen from literature pyrrhotite flotation differs with mineralogy. To understand the effect of mineralogy on flotation performance and ARD potential, mineralogical characterisation is needed to determine the magnetic or non-magnetic nature of the sample. Mineralogical composition of the feed sample is needed to understand the effect of mineral composition of ARD production. Therefore the results from optical microscopy, mineral chemistry and liberation of the ore samples are presented in this section.

4.2.1 Discrimination between magnetic and non-magnetic pyrrhotite

Discrimination between magnetic and non-magnetic pyrrhotite was done qualitatively by optical microscopy using a magnetic colloid, as described in Chapter 3. The photomicrographs are shown in Figure 26 and 27. The relative proportions of magnetic phase and non-magnetic phase in the sample was determined by inspection. The magnetic colloid was allowed to spread evenly over the samples so as to eliminate possible preferential attachment by the colloid. The photomicrographs (Figure 26a and 26b) confirmed that pyrrhotite is mainly in the form of magnetic (Fe_7S_8) pyrrhotite. A previous study conducted by Becker et al. (2010b) on ore from a similar deposit showed that both magnetic and non-magnetic pyrrhotite exist in the deposit, however magnetic pyrrhotite was found to be the dominant phase in this ore.

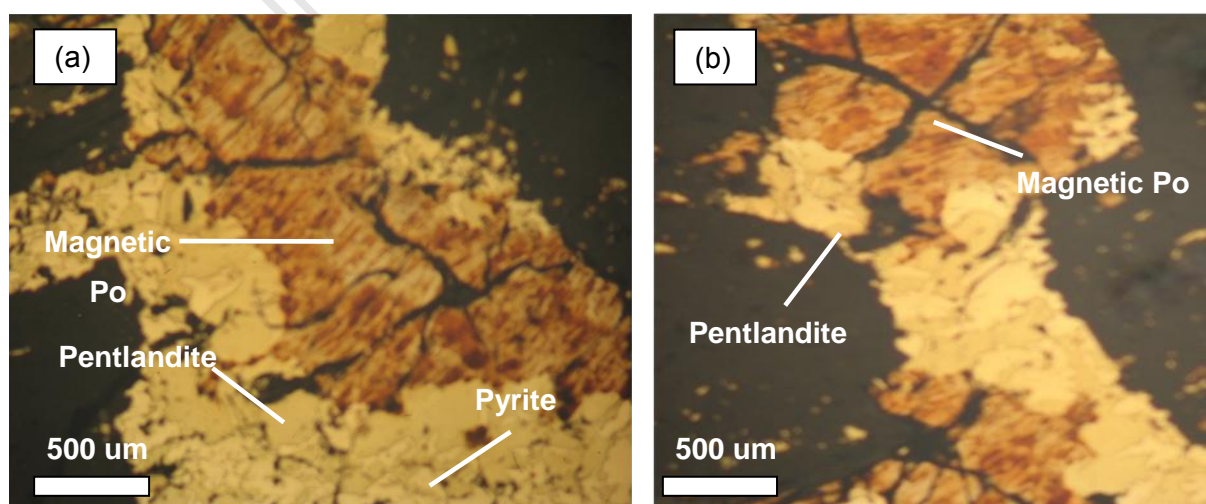


Figure 26: Reflected light photomicrographs of the ore; (a) Magnetic colloid adheres to magnetic pyrrhotite (b) Pentlandite inter-grown with pyrrhotite.

Pentlandite was found to be present in the sample as both granular (Figure 27a) and flame pentlandite; other sulfides present were chalcopyrite, and slight amount of pyrite.

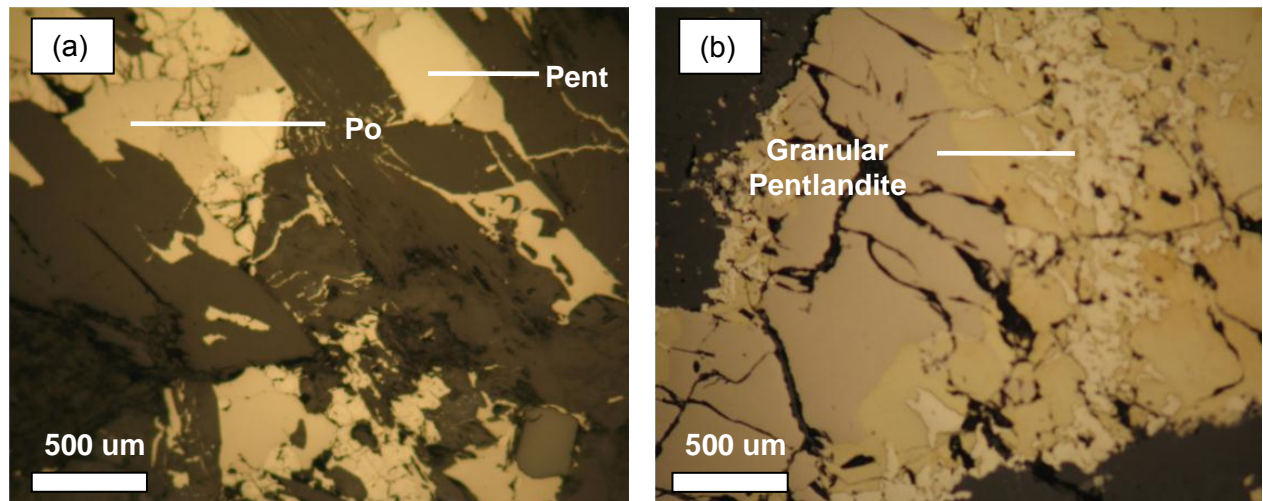


Figure 27: Reflected light photomicrographs of the ore; (a) photomicrograph showing the different sulfide minerals present in the ore (b) Granular pentlandite.

4.2.2 Mineral composition and Liberation

The mineralogical characteristics of the batch flotation feed sample was characterized by QEMSCAN. The bulk mineral composition of the sample is shown in Figure 28.

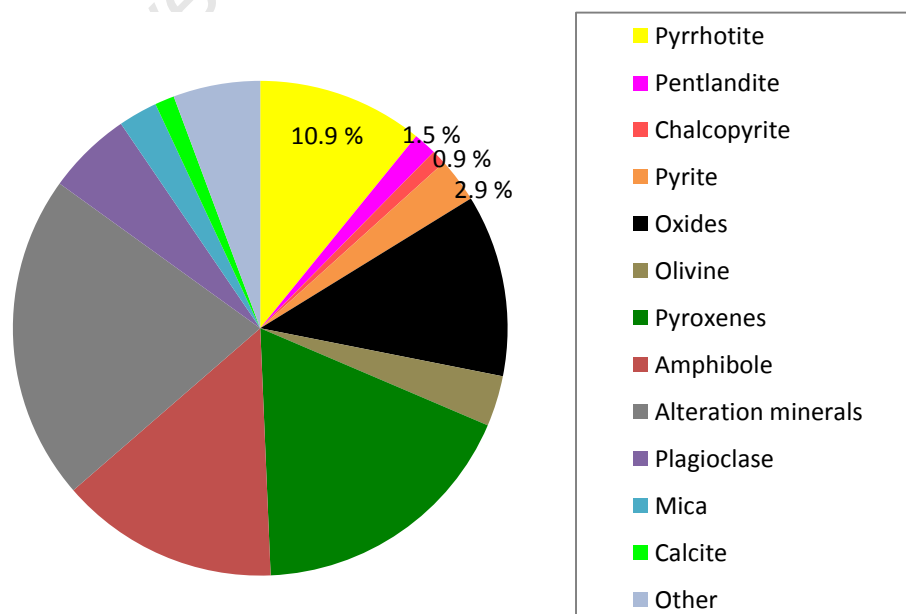


Figure 28: Summary of the feed mineral composition (wt %) as determined by QEMSCAN.

The ore has a total base metal sulfide (BMS) content of 16 wt %. The base metal sulfides are comprised mainly of pyrrhotite (10.9 wt %) , with minor to trace amounts of pyrite (2.9 wt %), pentlandite (1.5 wt %) and chalcopyrite (0.95 wt %). The ore contains about 27 wt % silicate gangue comprising mainly of amphibole, plagioclase and talc.

Table 11 shows the liberation of pyrrhotite and pentlandite achieved by grinding. Analysis of pyrrhotite liberation and association indicates that 74 % and 71 % of the pyrrhotite and pentlandite respectively, in the ore is liberated. The amount of pyrrhotite and pentlandite associated with other minerals is also shown.

Table 11: The percentage liberation and association of the minerals in feed sample.

Mineral	Pyrrhotite (%)	Pentlandite (%)
Liberated	74	71
Association with other sulfides		
Pyrrhotite	-	17.5
Pentlandite	3.83	-
Pyrite	15.2	2.85
Chalcopyrite	0.31	0.89
Association with other minerals		
Olivine	0.93	10.5
Calcite	-	0.05
Plagioclase	0.01	0.15

4.3 Pyrrhotite reactivity

Pyrrhotite is considered to be one of the most reactive sulfide minerals due to its vacancy layers which allow electron transfer, thus it is very susceptible to oxidation. The hydrophilic hydroxide surface oxidation product affects the flotation performance of pyrrhotite. And as seen from previous studies (e.g. Becker et al., 2010a) mineralogy affects the reactivity of pyrrhotite. Therefore the aim of this section is to compare the reactivity of the ore under the different flotation conditions. The pH was maintained at 9 for all the tests, the depressant conditions were the only variation. The reactivity was measured under three different reagent conditions, with no depressant, with oxygen as a depressant, TETA as a depressant and TETA/SMBS reagent combination. All tests were done in duplicate.

4.3.1 No depressant

In this test the dissolved oxygen content was measured before reagents were added to the slurry. The reactivity number was obtained by fitting first order rate kinetics to the rate of decay of dissolved oxygen in the slurry. The dissolved oxygen content of the slurry before sparging was at 1.85 ppm with the ambient oxygen content ranging between 10 ppm to 12 ppm. Figure 29 compares the reactivity number obtained for the ore used in this case study with those reported by Becker et al. (2010a) for other nickel sulfide ores with similar test conditions as the no depressant test in this study.

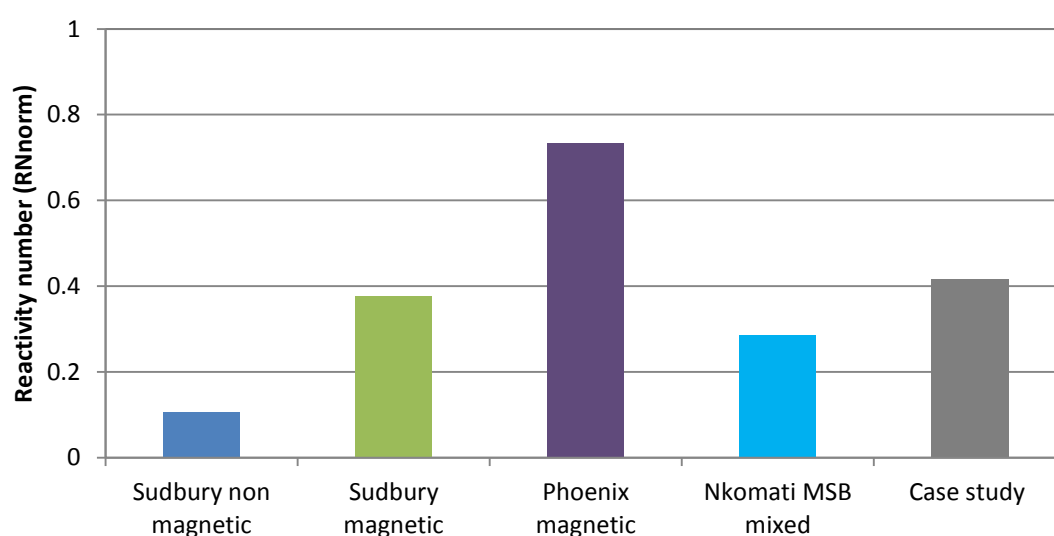


Figure 29: Comparison of the reactivity number (RN_{norm}) of different nickel sulfide ores (Becker et al. 2010a) with the ore used in this case study.

The other pyrrhotite ores had pyrrhotite content higher than 75 wt % whereas the case study ore has 11 wt %. Thus to compare the case study to the other ores the reactivity numbers had to be normalised as per their pyrrhotite content, Figure 29 reports the normalised RN i.e. RN_{norm} . The results in Figure 29 show that the magnetic pyrrhotite bearing case study ore has a high reactivity number ($RN_{norm} = 0.42$) in comparison to the other nickel sulfide ores (Becker et al., 2010a). From Figure 29, Phoenix magnetic has the highest reactivity number ($RN_{norm} = 0.73$), and Sudbury non-magnetic has the lowest reactivity number ($RN_{norm} = 0.106$)

4.3.2 Oxidation as a depressant

The oxidation time was varied for 5, 10 and 15 minutes for the different tests where oxygen was used as a depressant as per described in Chapter 3. The rate of decay of dissolved oxygen was measured to obtain the reactivity number after sparging for these specified times. The reactivity numbers obtained after 5 minutes, 10 minutes and 15 minutes of oxidation show no significant difference.

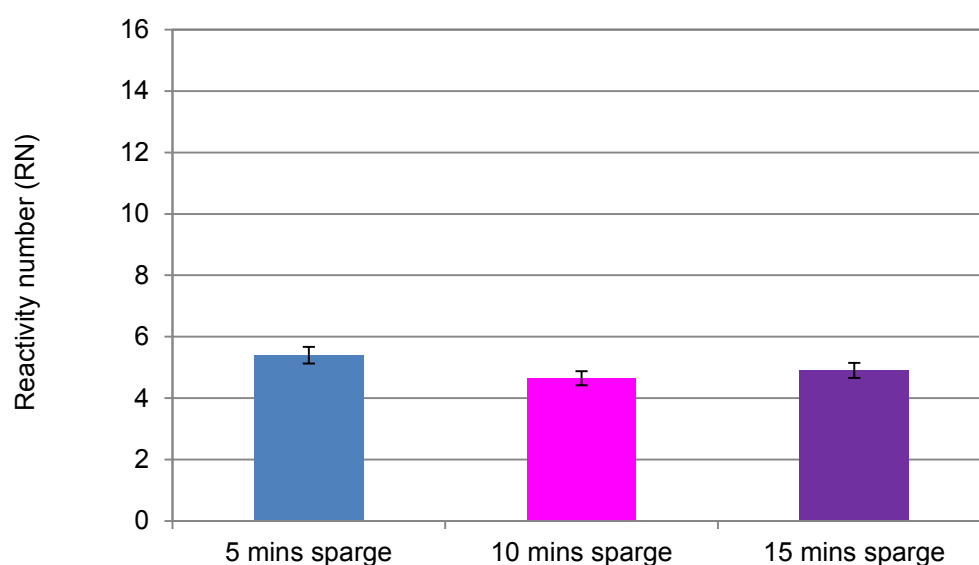


Figure 30: Reactivity number (RN) with oxygen as a depressant. Standard error is shown.

As seen from Figure 30, the reactivity number (RN) for the ore did not vary significantly with a change in oxidation time. This shows that the rate of decay does not change with increase in oxidation, so the ore may have been passivated after 5 minutes making it un-reactive thereafter.

4.3.3 TETA + SMBS as a depressant

(a) TETA only

Oxygen uptake tests were conducted when TETA alone was used as a depressant. As the TETA dosage is increased a slight decrease in the RN is observed, the RN number achieved is at TETA 125 g/t with RN = 9.9, however at 250 g/t the RN = 8.6 which is slightly higher than at TETA 350 g/t (RN= 6). The reactivity numbers obtained when TETA only (Figure 30) was used as a depressant was higher than when no depressant was used (RN =5).

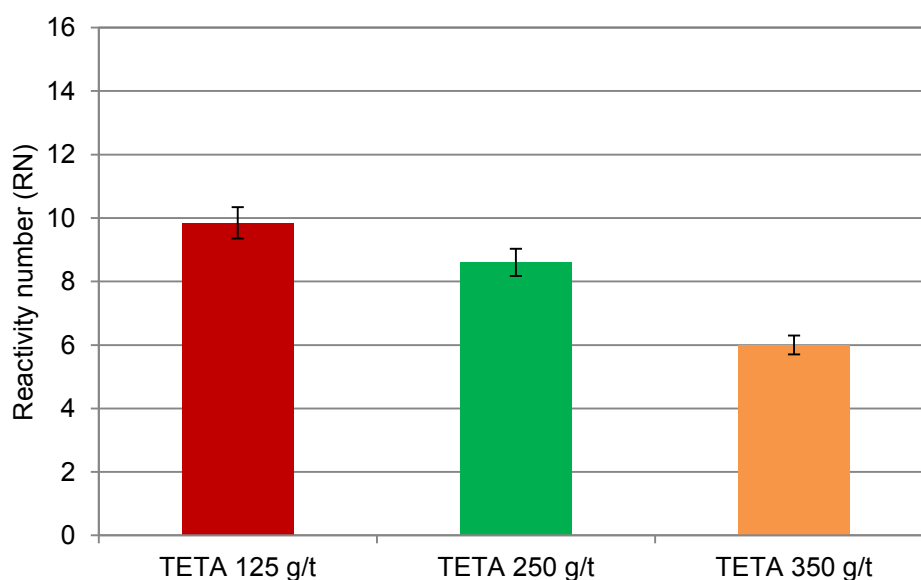


Figure 31: Summary of reactivity numbers (RN) obtained when TETA was used as a depressant. Standard error is shown.

(b) TETA + SMBS depressant combination

The slurry in this case was sparged after adding SMBS to determine the effect of SMBS on the reactivity of the ore. As the dosage of SMBS is varied from 500 g/t to 1400 g/t an increase in the rate of decay of dissolved oxygen content in the slurry is observed. Tests were done with and without SMBS to compare the effect of SMBS and TETA depressant combination. When SMBS and TETA were used as a depressant combination, the reactivity number was measured after addition of SMBS. The dissolved oxygen content is greatly

reduced with the increase of the addition of SMBS; the RN increased from 5 to approximately 14. This significant increase in RN infers that SMBS has an effect on the reactivity of the ore. Upon addition of SMBS the pH in the flotation cell was observed to drop to between pH 7 – pH 8, and increased again to pH 9 when TETA was subsequently added. Also on addition of SMBS the dissolved oxygen content of the slurry decreased, from about 4 ppm to 0.8 ppm.

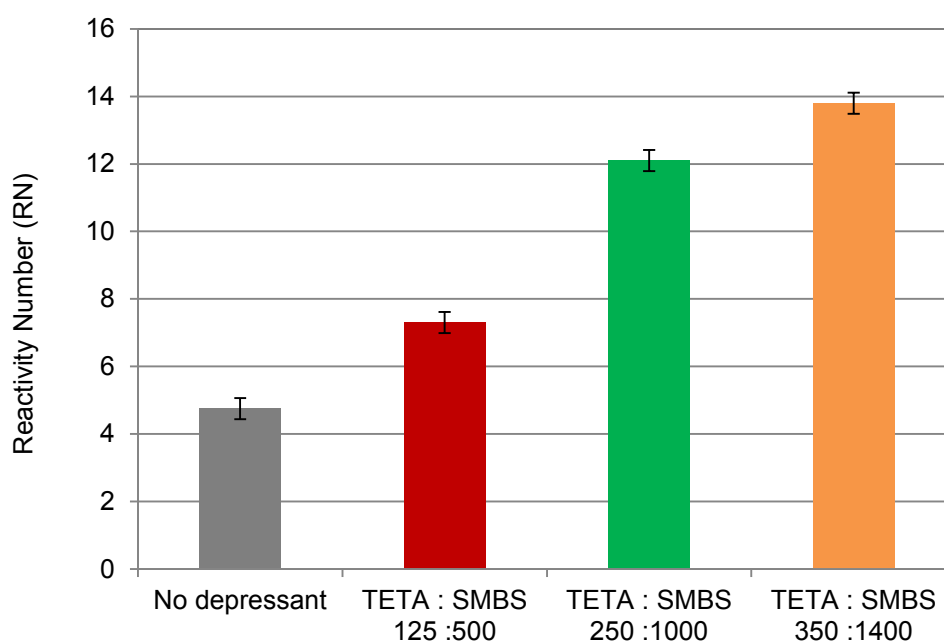


Figure 32: Comparison of the reactivity number (RN) with TETA and SMBS as a depressant. Standard error is shown.

4.3.4 Summary of reactivity numbers

Table 12 is a summary of the reactivity numbers obtained for all the test conditions. The R^2 values are close to 1 for the tests, showing that the first order kinetics give a good fit to the rate of decay of dissolved oxygen in the slurry.

Table 12: Summary of the reactivity numbers and the associated R^2 values obtained to calculate the reactivity numbers.

Conditions	Reactivity number (RN)	
	RN	R^2
No pre-treatment	4	0.988
5 mins air sparge	5	0.998
10 mins air sparge	5	0.986
15 mins air sparge	5	0.996
TETA 125 g/t	10	0.992
TETA 250 g/t	9	0.993
TETA 350 g/t	6.0	0.989
TETA: SMBS - 250 g/t :500 g/t	7	0.987
TETA: SMBS - 250 g/t :1000 g/t	12	0.991
TETA: SMBS - 350 g/t :1400 g/t	14	0.994

A comparison of reactivity numbers before and after pre-treatment with oxygen, indicates that the rate of oxygen uptake did not vary significantly after oxidation by air sparging, the RN values being approximately 5 (Table 12). Pre-treatment with SMBS resulted in an increase in the reactivity number, the RN increasing as the dosage increased in the range 500 g/t to 1400 g/t. These results indicate that SMBS acts as a reductant, thereby enhancing the rate at which the pyrrhotite surface is oxidised in the presence of oxygen.

4.4 Flotation test work

This section presents the results from the batch flotation tests. To determine the performance of the two depression mechanisms used in the study, the pentlandite recovery is plotted against the pyrrhotite recovery. The percentage pyrrhotite rejected is also used to evaluate the performance of the tests.

4.4.1 Oxygen as a depressant

Figure 33 shows the pentlandite recovery against the pyrrhotite recovery for the no depressant test and the tests in which oxygen was used as a depressant. The 5 mins oxidation test gives the best performance where the pentlandite recovery to the concentrate is high and the pyrrhotite recovery to the concentrate is low.

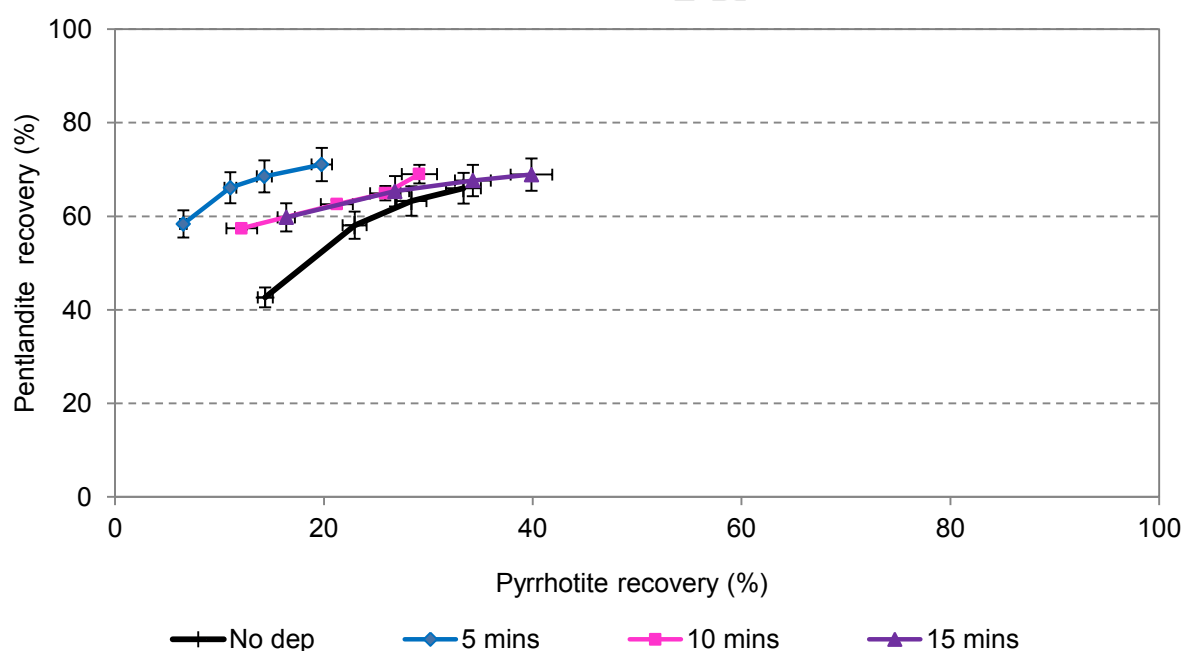


Figure 33: Pentlandite and pyrrhotite recovery with oxygen as a depressant. Standard error is shown.

Figure 33 shows that as the oxidation time increases the pyrrhotite recovery to the concentrate increases and the inverse occurs with pentlandite. This is line with findings of

Legrand et al. (2005a and 2005b) who after 5 minutes of oxidation observed increased formation of the hydrophilic layer on the surface of pentlandite which decreases floatability.

4.4.2 TETA + SMBS as a depressant

Figure 34 shows the effects of TETA: SMBS depressant combination on the relative extents of pentlandite and pyrrhotite recovery to the flotation concentrates. Figure 34 shows the results obtained when TETA alone was used and when TETA and SMBS were used together.

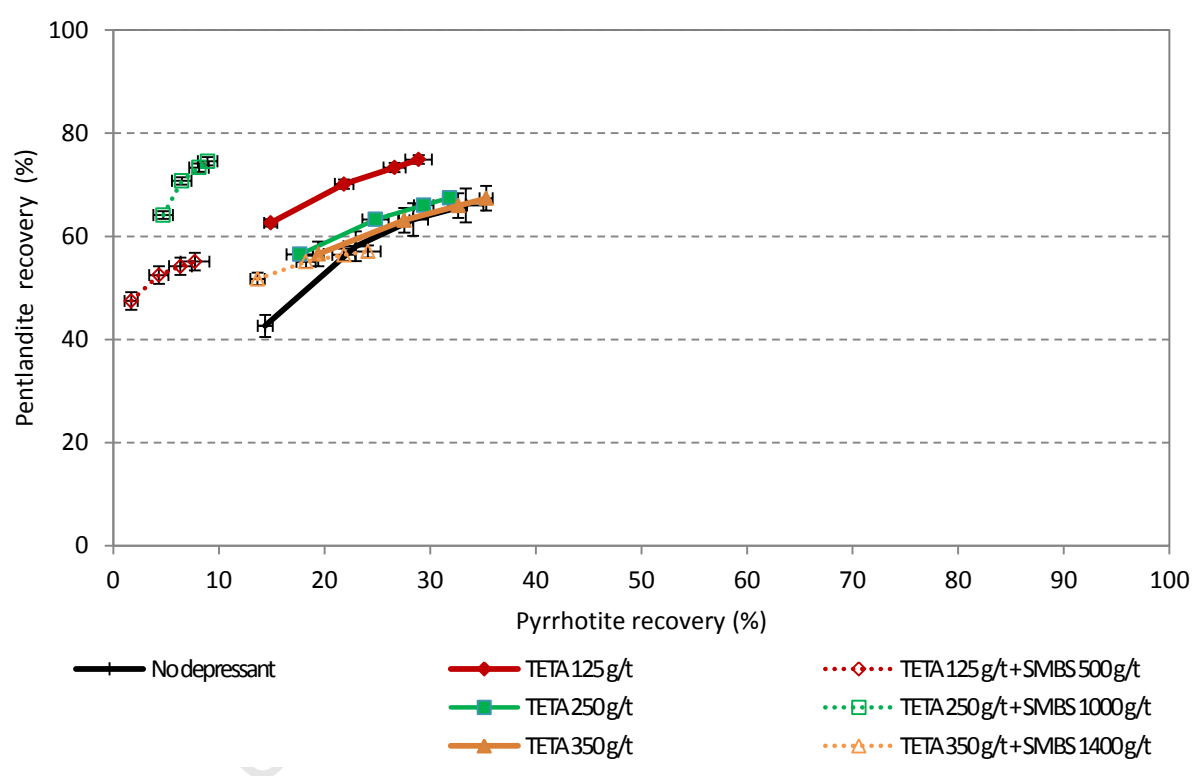


Figure 34: Pentlandite and pyrrhotite recovery using TETA only and TETA/SMBS as a pyrrhotite depressant. Standard error is shown.

Figure 34 illustrates that as the TETA dosage increased the pentlandite recovery decreased and the pyrrhotite recovery increased. Thus at a dosage of 125 g/t the highest pentlandite and lowest pyrrhotite recoveries are achieved; thus more pyrrhotite is rejected to the tailings at this dosage. At the higher TETA dosages the recovery curve is similar to that obtained with no depressant.

Using TETA with SMBS results in a significant reduction in pyrrhotite recovery to the concentrate as compared to when TETA was used alone. The highest pentlandite recovery

to the concentrate is achieved with 250 g/t of TETA and 1000 g/t of SMBS. The least recovery of pyrrhotite to the concentrate is achieved with 125 g/t of TETA and 500 g/t of SMBS, which is desirable effect as the aim is to obtain maximum pyrrhotite rejection but still maintaining a sufficient pentlandite recovery.

4.4.3 Summary of pentlandite and pyrrhotite recovery

Table 13 summarizes the cumulative recovery obtained for the flotation test work for all the depressant dosages.

Table 13: A summary of the cumulative recovery to the concentrate of pentlandite and pyrrhotite.

Test conditions	Pentlandite recovery	Pyrrhotite rejection
	(%)	(%)
No depressant	66	70
5 minutes oxidation	68	85
10 minutes oxidation	69	69
15 minutes oxidation	69	72
TETA 125 g/t	75	79
TETA 250 g/t	68	71
TETA 350 g/t	67	66
TETA 125 g/t + SMBS 500 g/t	55	92
TETA 250 g/t + SMBS 1000 g/t	74	91
TETA 350 g/t + SMBS 1400 g/t	57	78

Table 14 shows the selectivity ratio of all flotation conditions. The selectivity ratio $\text{Selectivity}_{\text{Pn}/\text{Po}}$ is obtained by cumulative recovery pentlandite over that of pyrrhotite after time, t of concentrate collection;

$$\text{Selectivity}_{\text{Pn}/\text{Po}} = \frac{\text{Recovery}_{\text{Pn}}(t)}{\text{Recovery}_{\text{Po}}(t)}$$

Table 14: Selectivity ratio of Pentlandite (Pn) : Pyrrhotite (Po)

Test conditions	Selectivity Pn/Po			
Concentrate Collection time	2 min	6 min	12 min	20 min
No depressant	3.0	2.5	2.2	2.0
5 minutes oxidation	9.5	6.2	4.8	3.7
10 minutes oxidation	4.7	3.0	2.5	2.4
15 minutes oxidation	3.6	2.4	2.0	1.7
TETA 125 g/t	4.2	3.2	2.7	2.6
TETA 250 g/t	3.2	2.5	2.2	2.1
TETA 350 g/t	2.9	2.0	2.0	1.9
TETA 125 g/t + SMBS 500 g/t	28.0	12.2	8.5	7.1
TETA 250 g/t + SMBS 1000 g/t	13.6	10.9	9.0	8.4
TETA 350 g/t + SMBS 1400 g/t	3.8	3.0	2.6	2.8

From Table 13, 5 minutes of oxidation results in the highest rejection of pyrrhotite (85 %) and gives a sufficient recovery of pentlandite (68 %) as compared to the other oxidation tests. When TETA and SMBS were used for pyrrhotite depression, at a dosage of 125 g/t and 500 g/t respectively, the highest pyrrhotite rejection (92 %) was achieved. Although at a dosage of TETA 125 g/t a higher pentlandite recovery was obtained than the parallel test where SMBS was used, a lower pyrrhotite rejection was obtained. Overall better pyrrhotite rejection was achieved when TETA and SMBS were used together than when TETA was used alone. ARD characterisation was conducted on the tests where the highest pyrrhotite rejection was achieved and a sufficient pentlandite recovery was obtained.

Thus the 5 minutes oxidation test and the TETA 125 g/t and SMBS 500 g/t test were used in further ARD characterisation as they gave the highest pyrrhotite rejection and a sufficient pentlandite recovery. The tailings from these tests were further treated and ARD characterisation was done on the tailings before and after treatment. The results from the ARD characterisation tests are presented in the next chapter as well as mineralogical analysis of the tailings samples.

5 ARD CHARACTERISATION

5.1 Introduction

One of the key questions of the study is to determine if pyrrhotite can be simultaneously rejected and passivated using the two rejection mechanisms. The tailings from the tests which gave the best rejection of pyrrhotite and a sufficient recovery of pentlandite were treated by further oxidation or adding TETA. Thus the 5 minutes oxidation test and the TETA 125 g/t and SMBS 500 g/t test were further treated. As a gauge of the passivation efficiency of the tailings, ARD characterisation tests were employed to determine if passivation was achieved and to quantify the extent of potential reduction of acid production by the passivated pyrrhotite rich tailings. ARD characterisation tests were conducted on untreated tailings and treated tailings.

This chapter is divided into 5 sections. Section, 5.2, starts by describing the mineralogy of the tailings. Mineralogical analysis was conducted on the tests in which the best pentlandite recovery and pyrrhotite depression was achieved to interpret the results of the ARD prediction tests based on the mineral content of the samples. As described in chapter 2, mineralogy strongly influences ARD production, thus it is imperative to know the mineral composition of samples. Section 5.3 goes on to present the acid base accounting results, which reports the net acid producing potential (NAPP). In addition, section 5.3 will present a comparison between results obtained from chemical tests and theoretical mineralogical calculations. Section 5.4 then goes on to present the net acid generation results for untreated and treated tailings. This is followed by section 5.5 that presents the biokinetic test data.

5.2 Tailings mineralogy

QEMSCAN was used to obtain the mineral composition of the tailings which gave the highest pyrrhotite rejection and a sufficient pentlandite recovery. The mineral compositions for the tailings of the tests which gave the best pyrrhotite rejection are presented in Figure 35 and a summary of the BMS content is given in Table 15.

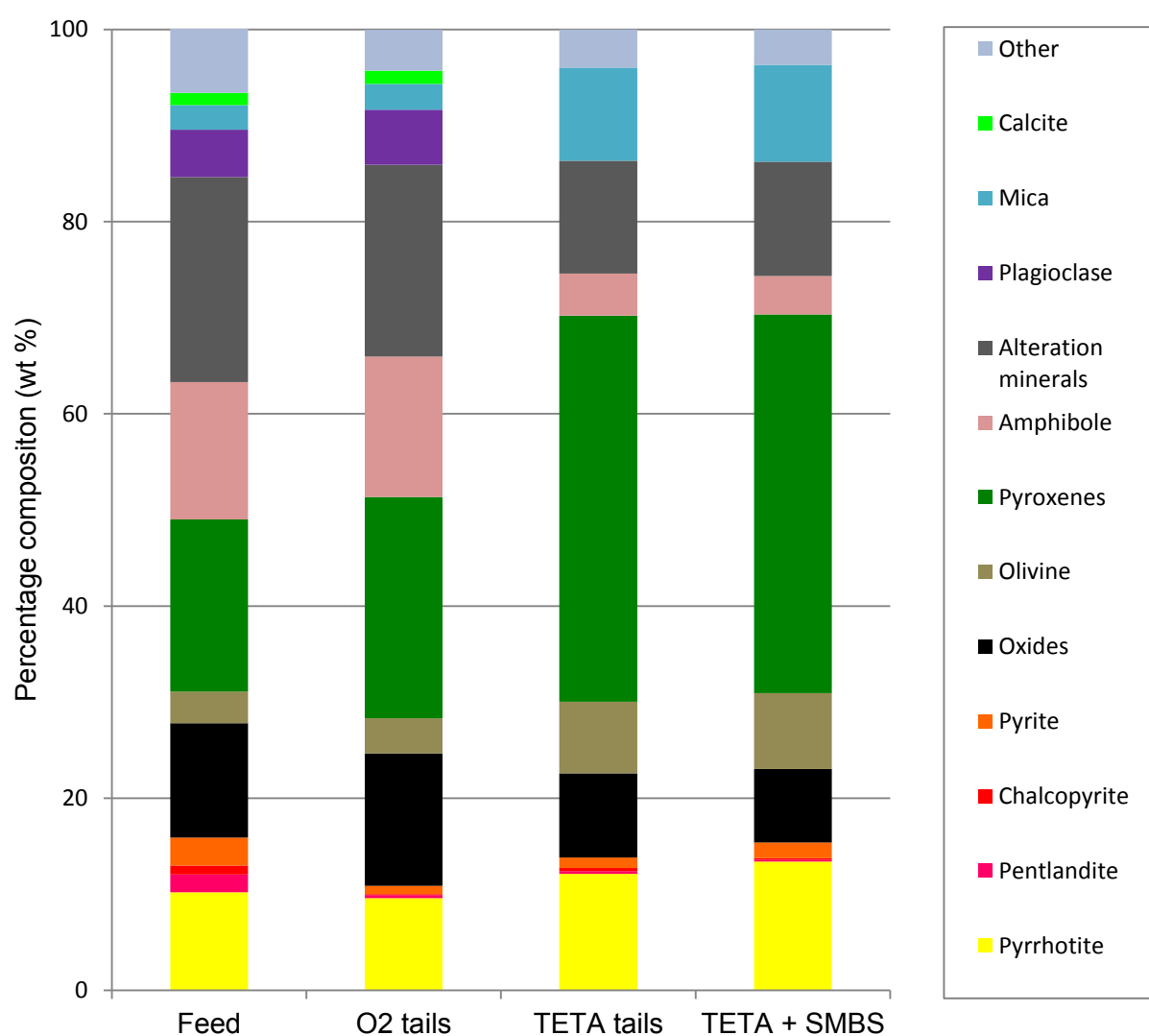


Figure 35: Mineral composition for the feed, oxygen as a depressant tails (5 minutes oxidation), TETA (125 g/t) only tails, TETA + SMBS (125 g/t : 500g/t) tails.

Table 15: The base metal sulfide (BMS) wt% composition of the tailings from the selected flotation tests.

Mineral	Sample			
Mineral wt % composition	Feed	O ₂ tails	TETA tails	TETA +SMBS tails
Pyrrhotite	10.9	9.6	12.1	13.4
Pentlandite	1.5	0.1	0.3	0.2
Chalcopyrite	1.0	0.1	0.3	0.2
Pyrite	2.9	0.9	1.1	1.6

As expected the TETA and SMBS test in which 92 % pyrrhotite rejection was obtained, contains the most pyrrhotite. The pyrite composition of the tailings is about 1 wt %; pyrrhotite and pyrite are reactive sulfide minerals and primarily contribute to the acid producing potential of the samples.

5.3 Acid base accounting (ABA) results

ABA tests were conducted on the feed and untreated tailings. It was assumed that MPA and ANC are not a function of passivation, thus MPA and ANC were computed for tailings without treatment. ANC and MPA are a function of buffering minerals and total sulfide content respectively, thus it was assumed passivation will not affect these quantities. The MPA and ANC were both computed by chemical test analysis and by mineralogical calculations to compare, theoretical calculations and chemical analysis.

5.3.1 MPA

The MPA (MPA_{ST}) was obtained from the total sulfur content measured by LECO using the standard method from Smart et al. (2002). Whereas the MPA from mineralogy was obtained by using the sulfide mineralogical compositions (Table 15) obtained from QEMSCAN (Paktunc, 1999b). Table 16 summarizes the MPA values obtained and shows the total sulfur content of the tailings samples.

Table 16: The maximum potential acidity (MPA) of the tailings samples.

Ore sample	Total sulfur content	MPA _{ST}	MPA _{MN}
Tailings sample	S _T %	MPA (kg H ₂ SO ₄ /ton)	MPA (kg H ₂ SO ₄ /ton)
Feed	4.45	136	161
O ₂	3.81	117	121
TETA + SMBS	5.34	163	177

The MPA (MPA_{MN}) obtained from mineralogy is higher than that obtained from the total sulfur content. The value obtained by mineralogical calculations assumes that pyrrhotite and pyrite will be the main sulfides contributing to acid producing potential of the tailings. From Table 15 the BMS of the tailings samples comprises mainly of pyrrhotite and pyrite. The standard MPA measurement does not take into account the different proportions of sulfides present in a sample.

5.3.2 ANC

From the literature review (Section 2.6.1) different ANC chemical test methodology exists which affect the minerals which get dissolved as the test is conducted (Smart et al., 2002; Weber et al., 2004). Two different chemical tests were used in this study to obtain the ANC for the tailings samples. The standard Sobek test (Sobek et al, 1979) and the Skousen test (Skousen, 1997) were used. The standard Sobek test dissolves mineral carbonates, pyroxene and olivine whereas the Skousen test is a modification and will dissolve Ca and Mg carbonates and excludes Fe carbonates as they are acid producing (see Table 5).

Table 17 gives the mineralogical composition of the neutralizing minerals contained in the feed and the tailings samples. To compute ANC from mineralogy; dissolving, fast weathering minerals were used, of which calcite is dissolving and olivine and plagioclase are fast weathering minerals. The neutralising minerals present do not occur in composite particles with the pyrrhotite due to its good liberation (Table 11); pyrrhotite has limited surface association to calcite, olivine and plagioclase. Therefore the capacity for the neutralising minerals to consume acid produced in a particle is reduced. The plagioclase contained in the ore has a sodium end member (Pillay et al., 2011) (NaAlSi₃O₈) which has a slower dissolution rate than Ca end member (CaAl₂Si₂O₈) (Paktunc, 1999a), thus plagioclase was

excluded when calculating the ANC mineralogy. Thus only calcite and olivine were used to obtain the ANC mineralogy values.

Table 17: Mineralogical composition (wt %) of the acid neutralising minerals contained in the feed and tailings samples.

Composition	Classification	Sample (wt %)		
Mineral	Weathering rate	Feed	O ₂ tails	TETA+SMBS
Calcite	dissolving	1.28	1.4	-
Olivine	fast weathering	4.6	3.6	7.88
Pyroxene	Intermediate weathering	18	23.0	39.4
Na-Plagioclase	slow weathering	5.5	4.4	-

Figure 36 shows the ANC values obtained from the chemical tests and mineralogical calculations. The Sobek test gives the highest values, whereas the Skousen test and mineralogical values are close. The Sobek test may be an overestimation because of extensive boiling times resulting in longer reaction times, minerals which would not normally weather under natural conditions may have been dissolved. Intermediate weathering minerals such as pyroxenes and amphibole (see Table 3) may have been dissolved.

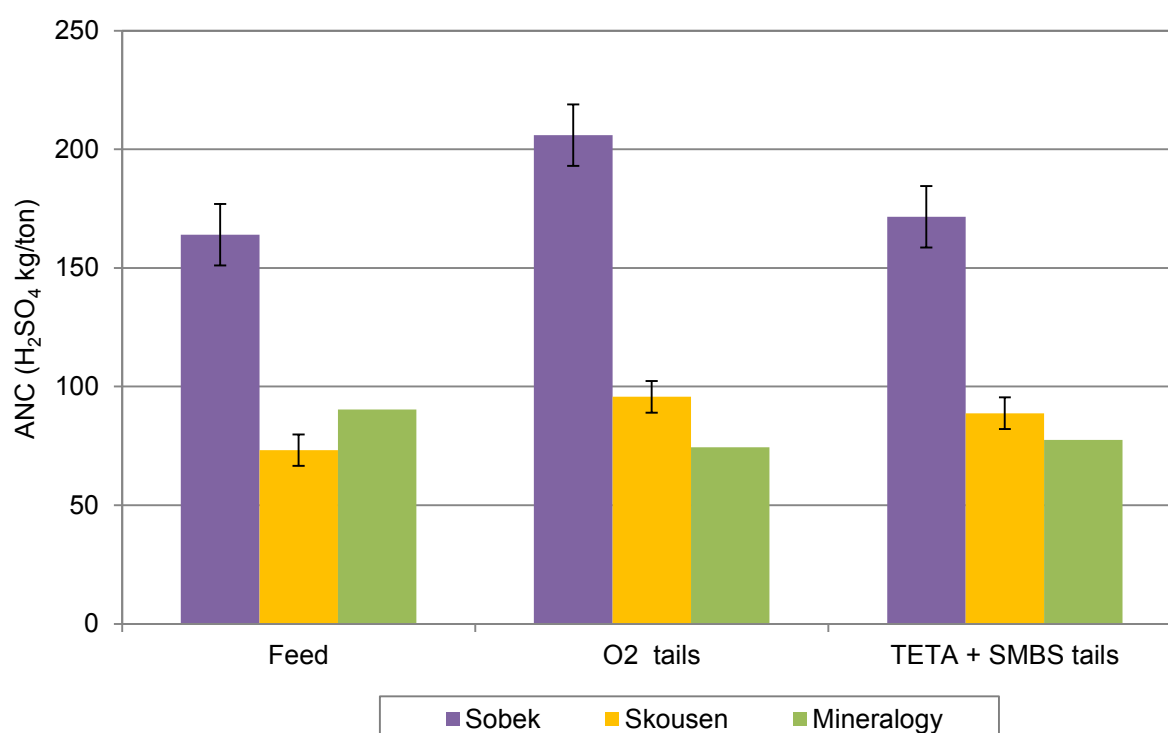


Figure 36: ANC values from chemical tests and mineralogical calculations. Standard error is shown.

5.3.3 NAPP

The net acid producing potential was obtained for the different chemical tests used as well as a mineralogical value was calculated (Figure 37). The NAPP is the difference between the MPA and the ANC. The NAPP was obtained using MPA_{MN} , because this value takes into account the acid producing potential from the different sulfides present in a sample.

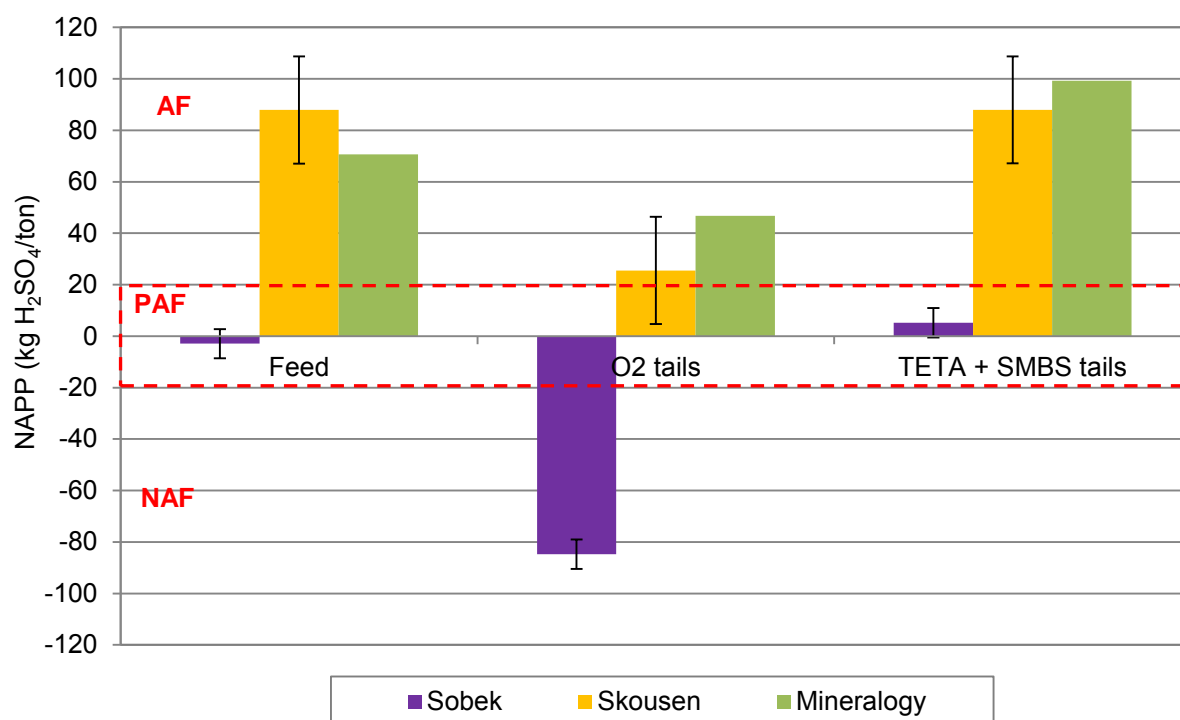


Figure 37: The NAPP (net acid producing potential) values obtained from chemical tests and mineralogical calculations. Standard error is shown.

The boundary regions, acid forming (AF), potentially acid forming (PAF) and non-acid forming (NAF) (see Table 6) are marked on Figure 37 based on the ARD classification guidelines from Stewart et al. (2006). The NAPP predicted by the Sobek test is much lower than that predicted by the chemical tests; this is because the ANC values are higher than the other tests (Figure 36). The test methods give conflicting results, the Sobek test gives a NAPP < -20 kg H₂SO₄/ton for the oxygen tails, which classifies them as NAF whereas the feed sample and TETA/SMBS tails sample are classified as PAF. The NAPP obtained from mineralogical calculations is close to that obtained by the Skousen test; though the samples are all classified as acid forming as the NAPP is above 20 kg H₂SO₄/ton. It is important to note the differences obtained from the different methodology depending on the sulfur content of the sample, this could affect prediction of the acid potential of an unknown sample at the boundary of the classification limits.

5.3.4 Net acid generation (NAG) results

Net acid generation tests were conducted to further understand the acid generating potential of the samples before and after treatment. Single addition NAG tests were conducted on all the treated samples and sequential NAG tests were conducted on the untreated tailings, and two treated samples for each method of treatment. To isolate each passivation treatment effect, further treatment was done as per the depression mechanism. Thus tailings where oxygen was used as the depressant were further treated by oxidizing them further and tailings where TETA and SMBS were used, tailings were further treated by TETA. The next sections present the results from the single addition NAG tests and the sequential NAG tests.

5.3.5 NAG of the tailings after treatment by oxidation

Tailings from which oxygen was used as a depressant were further treated before dewatering the tailings and collecting them from the flotation cell. The tailings were oxidized for 10, 20, 30, 40, 60 and 120 minutes and representative samples were collected before further oxidation and after each interval. Figure 38 shows the single addition NAG results obtained for samples taken at each interval, where at time 0 minutes is the tailings sample before further oxidation.

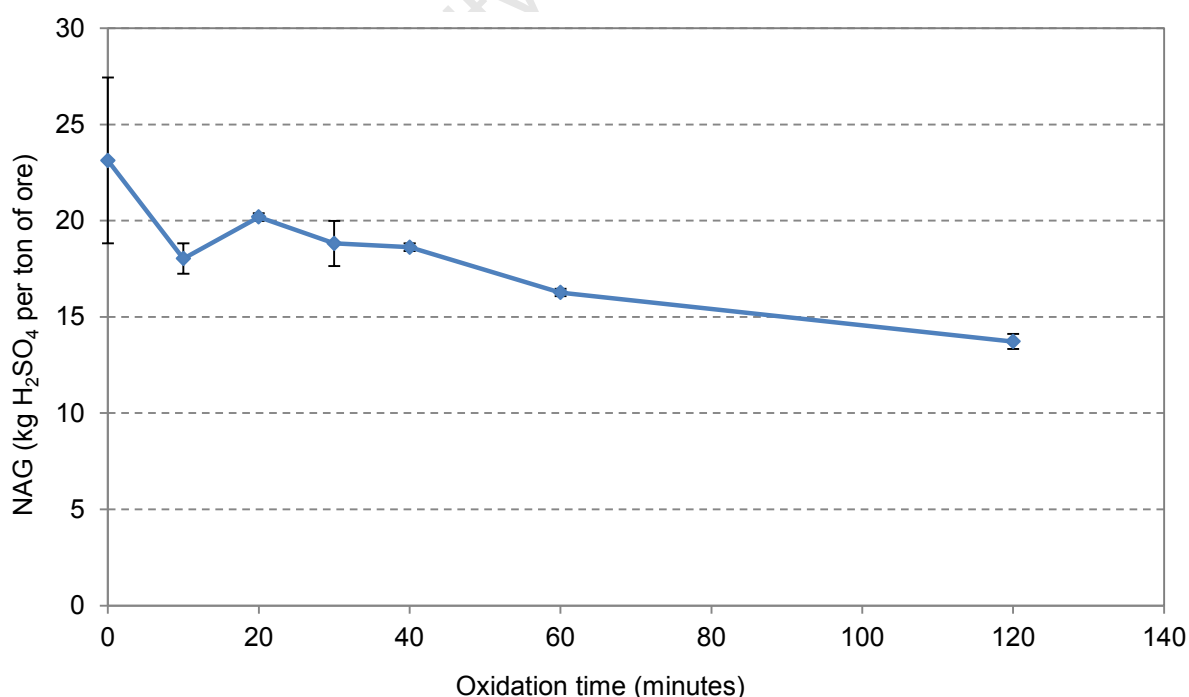


Figure 38: Net acid generation profile of tailings after they were further treated by oxidation. Standard error is shown.

Table 18: The NAG pH of the tailings samples (T_n = Tailings at time n minutes of oxidation).

Sample	Feed	T_0	T_{10}	T_{20}	T_{30}	T_{40}	T_{60}	T_{120}
NAG	3.70	3.16	3.15	3.00	3.24	2.96	3.56	3.80

From Figure 38, a clear trend is observed that as the tailings were further oxidised the NAG decreased. The feed NAG of the sample before flotation is 29 kg H_2SO_4 /ton, and the tails before treatment have a NAG of 23 kg H_2SO_4 /ton and after 120 minutes of oxidation the NAG decreases to 13 kg H_2SO_4 /ton. Even though there is a decrease in the NAG according to the guidelines if the NAG is above 10 kg H_2SO_4 /ton and the NAG pH is less than 4.5, the sample is classified as acid generating. The sulfur content of the tailings samples is more than 1 % so sequential NAG tests were needed to ensure that the sulfide minerals were oxidized to get a more accurate net acid generational potential prediction (Smart et al., 2002).

Table 19: The NAG pH and cumulative NAG of selected samples treated by further oxidation, after 2 stage sequential NAG test.

Sample	NAG pH (after 2 stages)	Cumulative NAG (kg H_2SO_4 /ton)
T_0	4.53	57.7
T_{60}	4.61	40.7
T_{120}	4.66	34.9

Single addition NAG tests were repeated until no further reaction was noted. Table 19 shows the results obtained, 2 more stages were needed to ensure complete oxidation of the sulfide minerals and to achieve an after boil NAG pH above 4.5. The NAG is above 10 kg H_2SO_4 /ton thus the samples are still classified as acid producing.

5.3.6 NAG of the tailings after treatment by TETA

Similarly tailings from which TETA and SMBS were used as a depressant were further treated before dewatering the tailings and collecting them from the flotation cell. The tailings were conditioned with TETA at incremental dosages of 120, 240, 470, 700 and 1400 g/t, and representative samples were collected after flotation and after each dosage of TETA was added. Figure 39 shows the single addition NAG results obtained for samples taken after each dosage, where at volume 0 g/t of TETA is the tailings sample before further dosing with TETA.

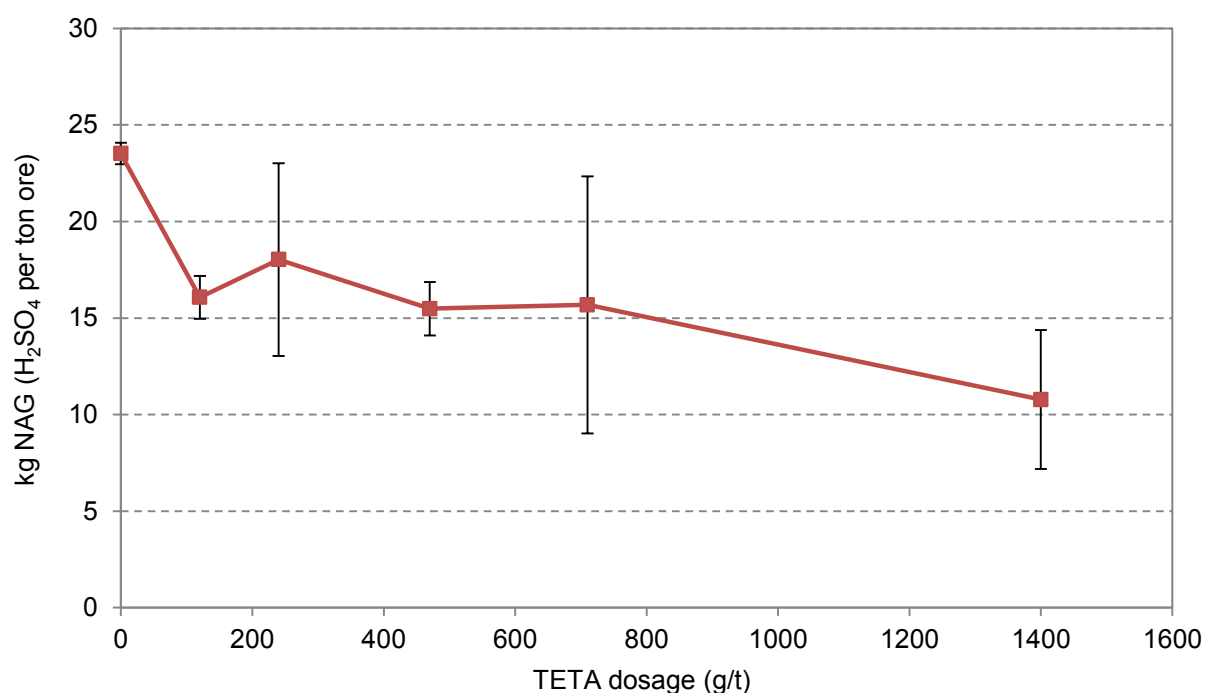


Figure 39: Net acid generation profile of tailings as they were further treated further addition of TETA. Standard error is shown.

Table 20: The NAG pH of the tailings samples (TT_n = Tailings at n dosage (g/t) of TETA).

Sample	TT_0	TT_{120}	TT_{240}	TT_{470}	TT_{700}	TT_{1400}
NAG pH	3.16	3.20	3.26	3.61	3.07	3.67

From Figure 39, similarly it is observed that as the tailings were further dosed with TETA the NAG decreased. However, the standard deviation is an average of ± 4.3 kg H_2SO_4 /ton. The feed NAG of the sample before flotation is 32 kg H_2SO_4 /ton, and the tails before treatment have a NAG of 22.1 kg H_2SO_4 /ton and after 120 minutes of oxidation the NAG decreases to 12 kg H_2SO_4 /ton. Even though there is a decrease in the NAG according to the guidelines, if the NAG is above 10 kg H_2SO_4 /ton and the NAG pH is less than 4.5 (see Table 6), the sample is still classified as acid generating. Table 21 shows the results obtained, 2 more stages were needed to ensure complete oxidation of the sulfide minerals and to achieve an after boil NAG pH above 4.5.

Table 21: The NAG pH and cumulative NAG of selected samples treated with TETA after 2 stage sequential NAG test.

Sample	NAG pH (after 2 stages)	Cumulative NAG (kg H ₂ SO ₄ /ton)
TT ₀	4.49	54.5
TT ₇₀₀	4.56	42.1
TT ₁₄₀₀	4.51	32.6

5.4 Biokinetic test results

Hesketh et al. (2010b) showed that static tests do not account for microbial factors and relative kinetic rates of acid generating and acid consuming reactions. The biokinetic test provides insight into the findings from static tests and gives an indication into the effect of microbial activity on the kinetics involved in ARD production (Hesketh et al., 2010b). For this study biokinetic tests with no pH control were conducted on the feed sample and the tailings samples before and after treatment with TETA and further oxidation. The focus was on the effect of microbial activity thus the majority of the tests were conducted under biotic conditions.

5.4.1 Time course results

The results are shown for the feed sample, the tailings samples before and after treatment. The tailings samples on which the maximum amount of treatment was applied were used for the biokinetic tests i.e. oxygen tailings after 120 minutes of oxidation and TETA tails after 1400 g/t of further dosage with TETA. Results are shown for the variation in pH (Figure 40), ferric iron (Figure 41) and redox potential (Figure 42) with time. The experiments were run in triplicate, and the error bars of standard error are shown.

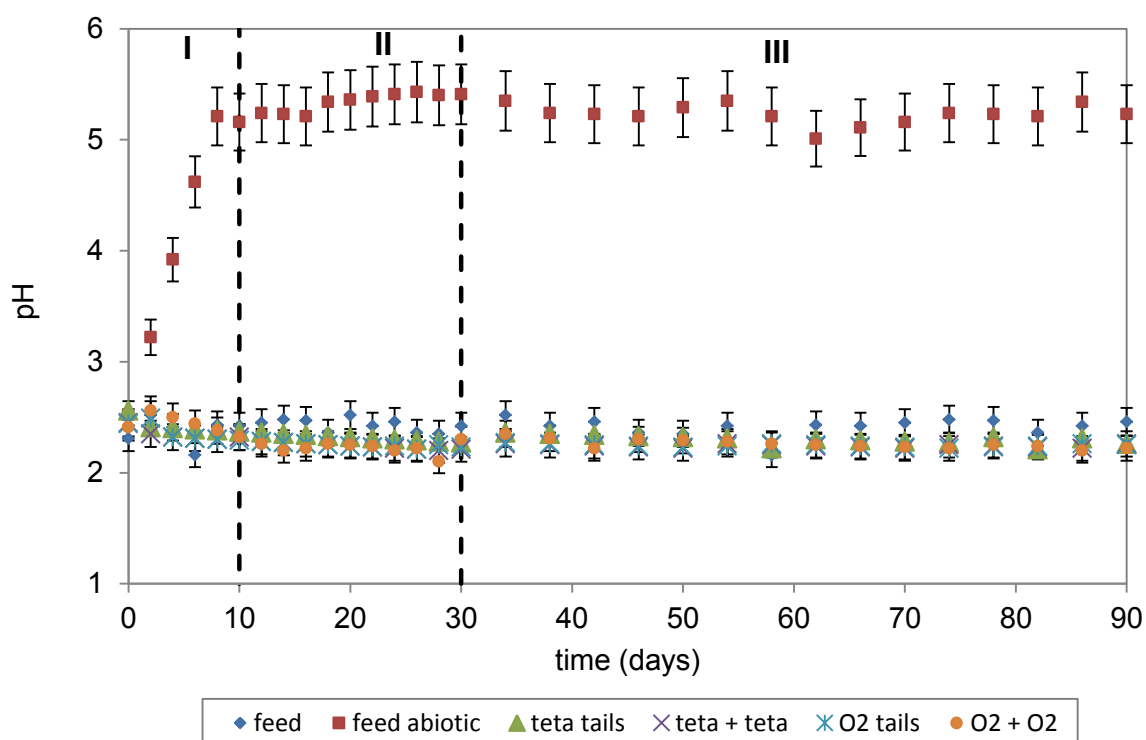


Figure 40: Change in pH with time for the biokinetic test for feed sample and tailings sample

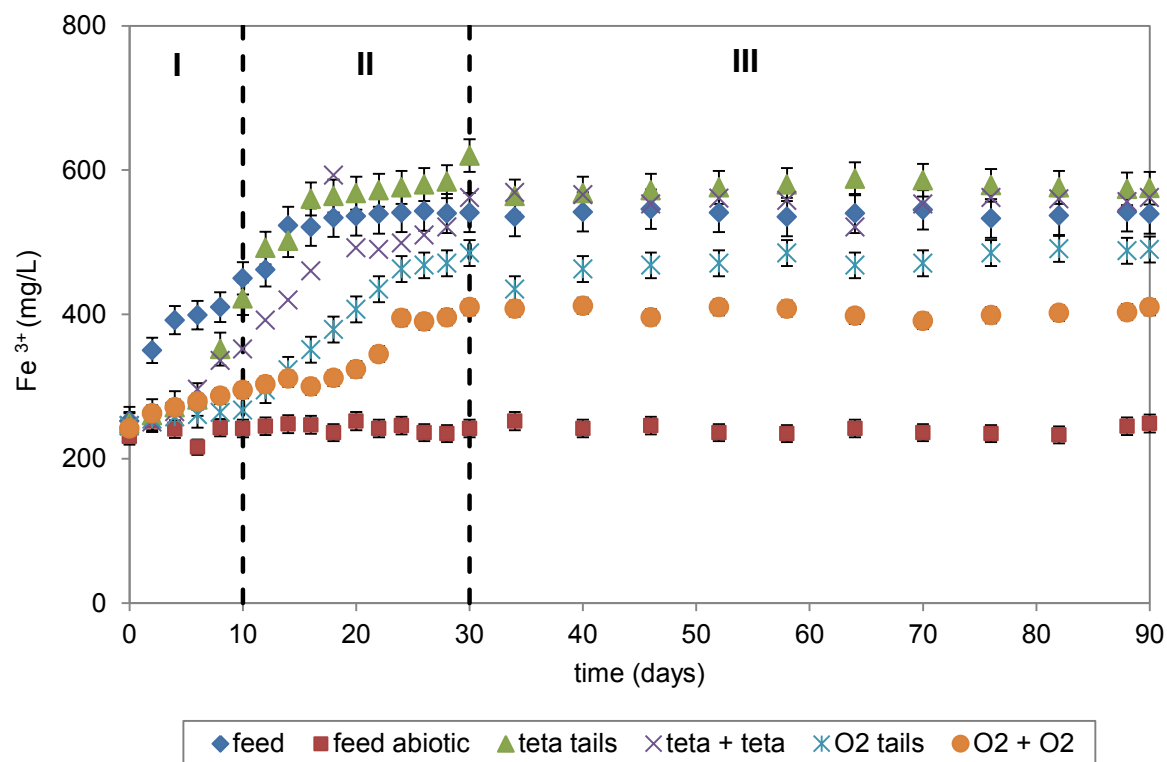


Figure 41: Change in Ferric iron concentration with time for biokinetic tests for the feed samples and tailings samples

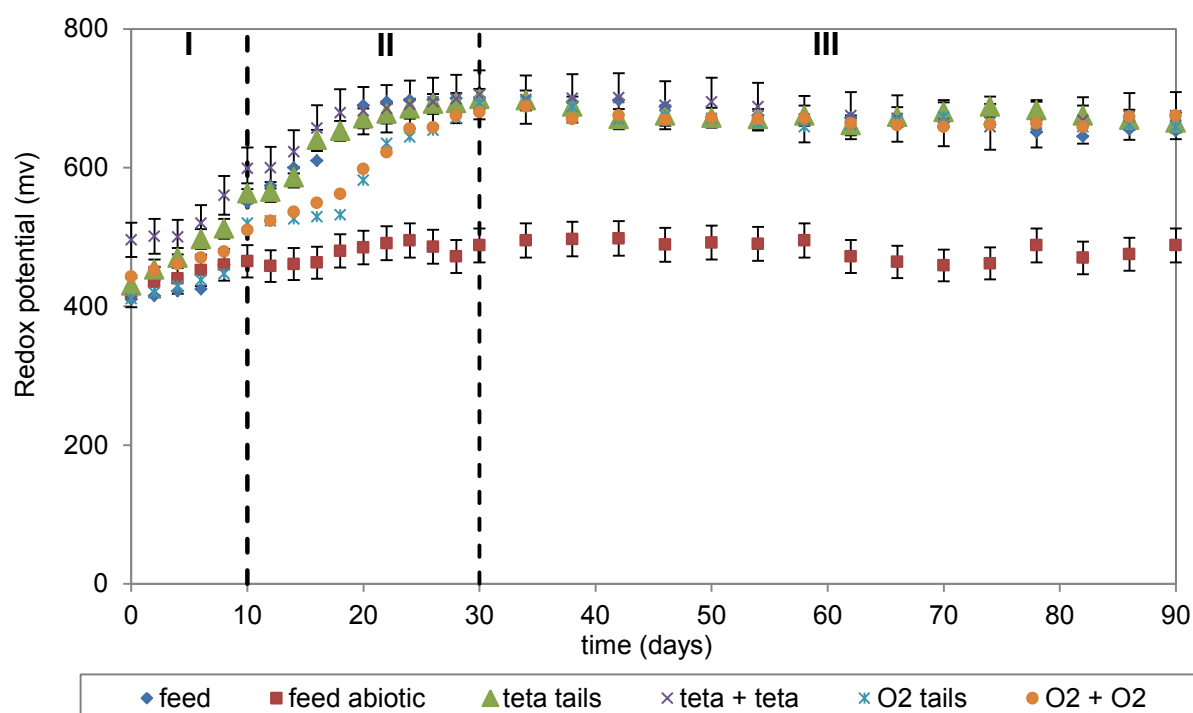


Figure 42: Change in Redox potential with time for the for biokinetic tests for the feed samples and tailings samples (reference electrode +199 mV vs. SHE)

The 3 regions shown I (< 10 days), II (10 - 30 days) and III (> 30 days), show distinct different changes with time for pH, ferric iron concentration and redox potential. In Figure 40 the pH of the abiotic tests decreases slightly from the initial average test pH of 2.44 in region I and II. In region III the pH levels off at an average pH of 1.9. This is consistent with the static tests which show the sample has a high acid producing potential. The feed sample was conducted under biotic and abiotic conditions. It is interesting to see in Figure 40, that at abiotic conditions the pH of the feed sample increases in region I to about 5.3, after which the pH stays almost constant at around this value.

From region I in Figure 41 an increase in the Fe^{3+} concentration for the biotic tests is observed which shows the onset of microbial activity which increases the rate of oxidation of Fe^{2+} to Fe^{3+} . In region II the Fe^{3+} concentration further increases and then reaches a maximum, and stays almost constant in region III. For the abiotic feed test sample, the Fe^{3+} concentration stays low at about 240 mg/l. The redox potential for all the biotic tests increases in region I and II to about 700 mV and stays high after 30 days (region III), indicating microbial activity. As for the abiotic test the redox potential slightly increased from the initial value of 420 mV in region I and II to about 480 mV, where it remained constant in

region III. Overall the biokinetic tests are consistent with the static tests, the biotic tests stayed at a low pH showing the high acid generation potential of the samples.

5.4.2 SEM image analysis

SEM images were taken of the sample surfaces to examine surface of the particles, and determine if passivation layers were present. SEM imaging was conducted on treated samples before and after they were subjected to biokinetic conditions for 35 days. Figure 43 shows the SEM images taken of the samples which were treated with further oxidation and Figure 44 shows the samples which were treated with TETA.

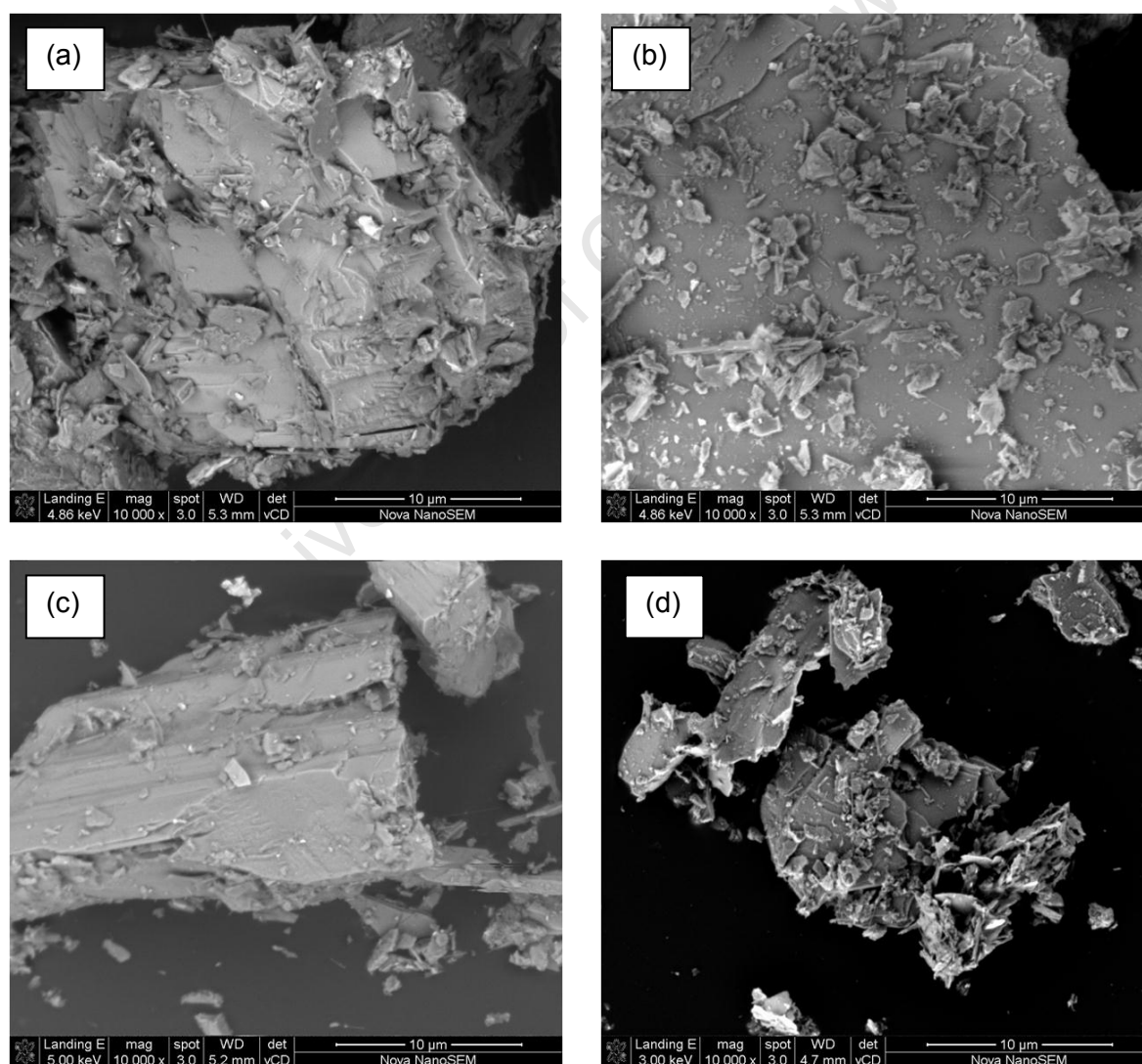


Figure 43: SEM images of tailings treated with further oxidation before biokinetic tests [(a), (b)] and during biokinetic tests (after 35 days) [(c),(d)].

It is important to note that SEM imaging was conducted at the end of the study to try and understand the results obtained by the static tests and biokinetic tests, and to see if the surface had been coated. From Figure 43, picture (a) and (b), the ferric oxyhydroxide layer, could not be detected by SEM imaging. After 35 days of undergoing biokinetic test conditions, the surface of the particles appears clean showing dissolution of small reactive minerals (Figure 43; (c) and (d)).

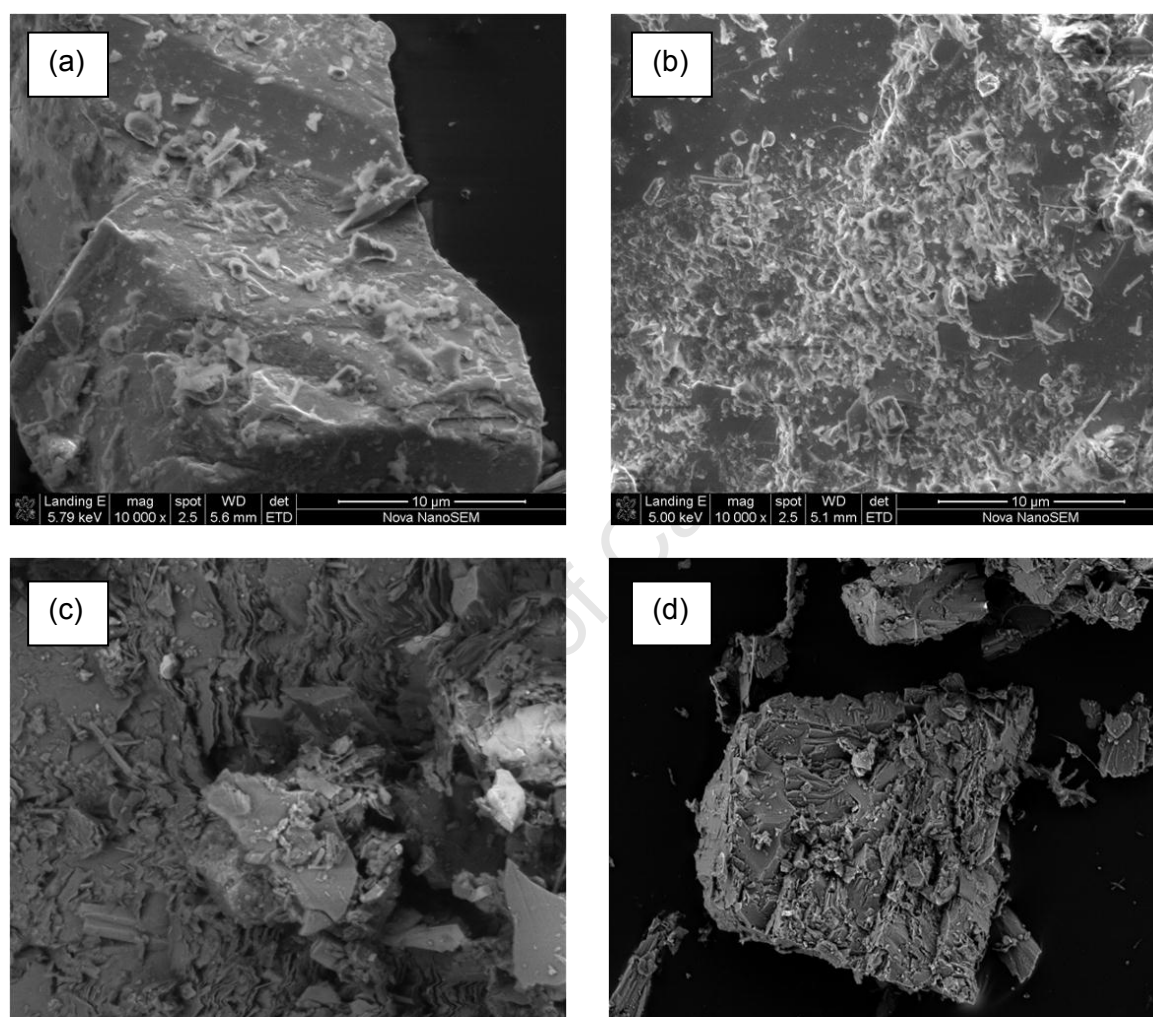


Figure 44: SEM images of tailings treated with TETA before biokinetic tests [(a), (b)] and during biokinetic tests (after 35 days) [(c), (d)].

Figure 44 (a) and (b) represent the original sample which had been dosed with 1400 g/t of TETA before conducting biokinetic tests. From observing the particle in Figure 44 (a), the coatings could not be detected by SEM. Similarly Figure 44 (c) and (d) show no presence of any passivation layers on the surface of the particles.

6 DISCUSSION

6.1 Introduction

This chapter discusses the results from chapter 4 and 5 to provide an understanding of the feasibility of ARD mitigation by passivation of pyrrhotite during flotation. Section 6.2 starts by evaluating the two depression mechanisms and the pyrrhotite rejection efficiency by reviewing the flotation results, the reactivity of the ore and mineralogical analysis of the feed, concentrate and tailings. Subsequently, section 6.3 gives an interpretation of the static and biokinetic ARD characterisation tests. Section 6.4 discusses the ability of the two depression mechanisms to promote the passivation of pyrrhotite based on the evidence from the results. The chapter concludes with section 6.5 which discusses the implications of the study based on the findings.

6.2 Pyrrhotite rejection

6.2.1 Rejection by oxygen

Oxidation of pyrrhotite promotes the formation of a hydrophilic oxyhydroxide layer (Pratt et al., 1994; Mycroft et al., 1995). The formation of this hydrophilic layer can enable the selective depression of metal sulfides by taking advantage of their different rates of oxidation. Legrand et al. (2005b) showed that as oxidation time increases xanthate adsorption on pentlandite is limited which decreases its recovery to the concentrate.

The pentlandite and pyrrhotite recovery graphs (Figure 33 and Figure 34) show that at 5 mins of oxidation the highest pentlandite recovery is obtained and the lowest pyrrhotite recovery is achieved. Thus 5 minutes of oxidation is sufficient to depress pyrrhotite and not limit the xanthate collector adsorption to pentlandite. A cumulative pentlandite recovery of 68 % is achieved and 65 % pyrrhotite rejection is achieved. Compared to no depressant conditions, there is a 15 % increase in the rejection of pyrrhotite when the slurry is oxidised before flotation. This shows that oxidation reduced the floatability of the pyrrhotite. However beyond 5 minutes of oxidation the rejection of pyrrhotite decreases whereas the recovery of pentlandite remains unchanged (± 1 % change). Therefore the selectivity ratio (see Table 14) decreased with further oxidation. The percentage rejection of pyrrhotite decreases possibly due to the increase of floatability which may result from formation of stable Fe (OH) S₂ species which increase hydrophobicity of pyrrhotite (Legrand et al., 2005a).

The reactivity numbers however do not show a significant change in the rate of decay of dissolved oxygen in the slurry when the pre-oxidation time is increased showing that the ore was insensitive to further oxidation. This may infer that 5 minutes of oxidation is sufficient to form a ferric oxyhydroxide layer which inhibits further oxidation of the mineral surface (see Figure 3 and Figure 14). Legrand et al. 2005a found that 5 minutes of oxidation was sufficient to form ferric oxyhydroxide layers which inhibited further oxidation. In comparison to other nickel sulfide ores (Figure 29) the ore from this study is very reactive as it contains mostly magnetic pyrrhotite. The insensitivity of the ore could also be due to possible oxidation between ore preparation and the time the ore was obtained from the mine. Although the SEM images did not detect the presence of oxidation products, the improvement of the recovery is evidence that pre-oxidation of the ore did improve rejection of pyrrhotite.

6.2.2 Rejection by TETA and SMBS

The mechanism by which TETA improves rejection of pyrrhotite has been studied by several authors (Yoon et al., 1995; Xu et al., 1997; Kelebek and Tukul, 1999). TETA has been shown to act as a chelating agent reducing activation of pyrrhotite by ions such as copper and nickel present in mine process water. TETA or DETA selectively remove nickel or copper ions from the surface of pyrrhotite leaving hydrophilic ferric species which promote depression of pyrrhotite (Xu et al., 1997).

When TETA alone was used the pentlandite and pyrrhotite recovery graphs show that at 125 g/t of TETA the best pentlandite recovery and pyrrhotite rejection were achieved, 75 % and 79 % respectively (Figure 34). With an increase in the TETA dosage both the recovery of pentlandite and pyrrhotite rejection decreased. The higher TETA concentrations may have inhibited mobile metal ion activity causing the flotation of pentlandite to slow down (Kelebek and Tukul, 1999).

When SMBS was used in conjunction with TETA a vast improvement in pyrrhotite rejection is observed, which is in agreement with findings in literature (Xu et al., 1997, Kelebek and Tukul, 1999). SMBS has been observed to lower the redox potential which destabilises the formation of xanthate species which increase hydrophobicity on pyrrhotite (Kelebek and Tukul, 1999). However when SMBS was introduced the recovery of pentlandite decreased slightly (Table 13) as compared to when TETA was used alone. Kelebek and Tukul, (1999) observed that the SMBS-TETA combination induces slow reaction kinetics and thus may decrease the flotation rate of pentlandite which explains the observed decrease of pentlandite recovery in these tests.

The reactivity results show the role of SMBS as a reducing agent, the dissolved oxygen content was greatly reduced when SMBS was added from 4 ppm to 0.8 ppm. The reactivity of the slurry greatly increased from 5 with no depressant to 14 when 1400 g/t of SMBS was added (Table 12). SMBS acts as a reductant, thereby enhancing the rate at which the sulfide surface is oxidised in the presence of oxygen. The pentlandite to pyrrhotite recovery ratios (Table 14) however remained relatively low (< 2.4), even at maximum depressant dosages (TETA: SMBS = 350: 1400 g/t).

6.2.3 Comparison of the two rejection methods

The two methods promote pyrrhotite rejection through different mechanisms. The combination of TETA and SMBS achieved the highest rejection of pyrrhotite (Table 13) and highest selectivity (Table 14). The focus of the project was however not to optimize either mechanism, the study aimed to compare and review the two rejection methods based on a typical plant practice. The xanthate collector dosage was maintained at 50 g/t, thus pentlandite recovery did not significantly change. However both methods showed an improvement in the selectivity ratio (Table 14) of pentlandite to pyrrhotite as compared to the no depressant tests.

Pre-oxidation however has not been implemented in nickel sulfide processing circuits, mostly chemical depressants are used. This study however shows the possibility of using pre-oxidation as an effective depressant mechanism. The complexity however with nickel sulfide ores is that disseminated and massive sulfide ores respond differently to different depressants and other factors such as weathering oxidation and stock piling make this method hard to control. As well as the presence of magnetic and non-magnetic pyrrhotite affects the reactivity of the ores (Becker et al., 2010a). Magnetic pyrrhotite is more reactive and thus will oxidize faster whereas pre-oxidation may not be a viable option with a non-magnetic pyrrhotite bearing ore. In Inco Clarabelle operations the nickel sulfide ore contains 20 % mixed magnetic and non-magnetic pyrrhotite and before flotation the ore is separated into two fractions containing magnetic and non-magnetic pyrrhotite (Lawson et al., 2005). The TETA/SBMS reagent combination is then used however it is seen to be only more effective when the magnetic fraction is first oxidized (Lawson et al., 2005). TETA and DETA have also been noted to further enhance the depression of nickeliferous pyrrhotite (Xu et al., 1997). Thus the efficiency of the rejection mechanism is highly dependent on the mineralogy of the ore.

Using depression by pre-oxidation may reduce reagent costs in the flotation processing circuit as oxygen is available onsite and it would be considered a 'green solution' by reducing impact on the environment by chemical reagent usage. Only 85 % rejection of pyrrhotite is achieved thus implementation of this method would have to depend on the iron ratio needed in smelting and the regulation of SO₂ emissions (Evans et al., 2005; Peek et al, 2010). In some Ni processing operations, pyrrhotite recovery is targeted such as Xstrata Strathcona Mill where 85 % rejection is required to enable recovery of fine grained

pentlandite locked in pyrrhotite during smelting (Peek et al., 2010). From the liberation data (Table 11) 16 % of the pentlandite is locked in binary with pyrrhotite, thus less than 100 % rejection would allow for regrinding to allow greater recovery of pentlandite. Rejection by TETA and SMBS on the other hand achieves 92 % rejection, however the drawback is that TETA is an expensive reagent. TETA costs approximately twice the amount of other flotation reagents such as xanthates (Alibaba, n.d).

6.3 ARD characterisation

ARD characterisation tests predict the acid producing potential of a sample based on a balance of the acid forming minerals and acid buffering minerals (Smart et al., 2002). The ore has 10 % Pyrrhotite in the feed mainly in form of the magnetic phase which is the more reactive phase. High rejection percentages were achieved by both depression methods resulting in the pre-oxidation test and TETA/SMBS test tailings having 9.60 % and 13.4 % pyrrhotite respectively. The tailings have approximately 1 % pyrite, thus pyrrhotite contributes largely to the acid producing potential of the tailings samples. In total the acid buffering mineral composition of the samples is 32 wt % for the feed, 32 wt % for pre-oxidation tailings and 47.3 % for the TETA/SMBS test tailings. The available buffering mineral content comprises mainly of pyroxenes (20 to 30 wt %) which are considered to be intermediate weathering however dissolution can take months to provide any buffering capacity (Miller et al., 2010). Thus main buffering minerals present are; calcite which readily dissolves, olivine which is fast weathering which makes up less than 8 wt % (see Table 17 section 5.2).

6.3.1 Acid base accounting

ABA tests were used to characterise the acid producing potential of the feed and tailings samples before and after further treatment. ABA chemical test results were compared with theoretical mineralogical calculations based on acid producing minerals and acid buffering minerals present in the samples. This comparison is important in understanding the results obtained from chemical test methodology. Values obtained from theoretical calculations should ideally give the maximum amount of acidity available and the ideal neutralizing

potential of a sample. The chemical tests however give much higher values than the theoretical mineralogical calculations, which show that chemical tests possibly overestimate the maximum potential acidity (MPA) and neutralizing potential of samples (ANC). Mineralogical calculations however have limitations, in that obtaining mineralogical data is costly and turn-around time maybe long.

6.3.2 Evaluation Net acid generation potential prediction

From the single addition NAG test a reduction of acid generating potential was observed as the tailings were further treated by both methods of treatment. However the sequential NAG tests, which give a cumulative amount of the acid which can potentially be produced, show that the samples are still acid forming. Figure 45 summarizes the classification of the samples and shows that the samples remained in the potentially acid forming zone based on classification guidelines from Stewart et al. (2006) (see section 2.6.3, Table 6).

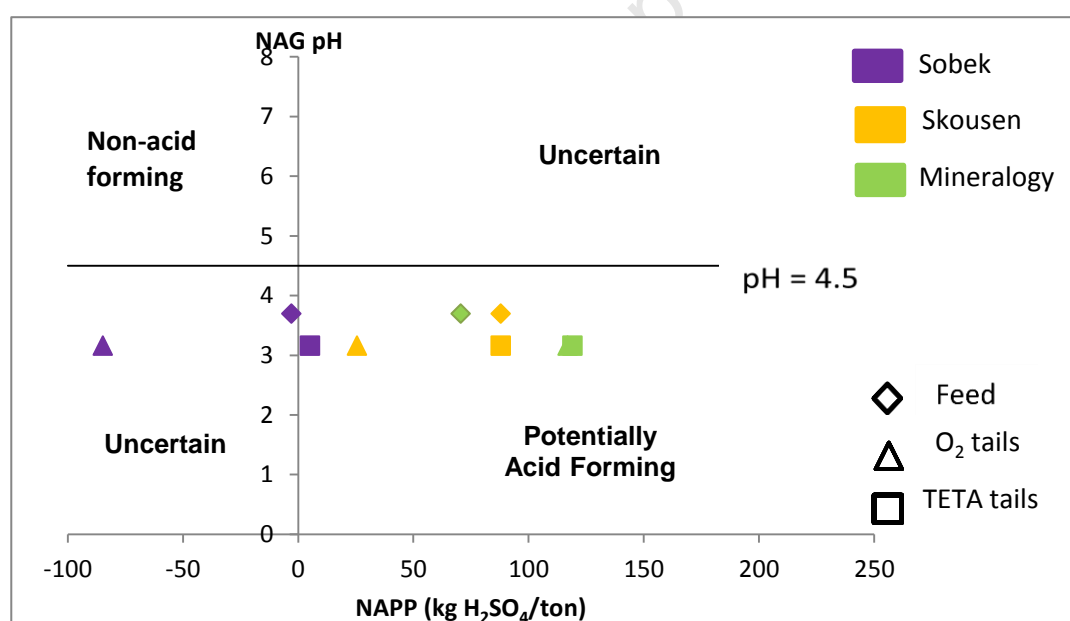


Figure 45: Classification plot comparing acid base accounting (NAPP) results with NAG pH

The net NAG potential predicted by sequential tests is still less than that predicted by $NAPP_{MN}$ and NAPP from chemical tests, which could either mean the NAPP values may be an overestimation or the net NAG is an underestimation. Despite the differences between NAG test results and ABA results, both the static test methods are in agreement that the samples are acid forming. These tests are however aggressive to samples with long periods

of boiling which increases oxidation rates but may not give a true reflection of sample acidity. Furthermore static tests have poor reproducibility and have uncertainty associated with the results. Thus biokinetic tests are always important in validating results from static tests.

6.3.3 Interpretation of Biokinetic test results

From the pH profiles it is evident under biotic conditions the rate of oxidation far exceeded the acid buffering mineral reactions such that the system stayed at a low pH through the 90 day period. Typically the microbial culture is at a very low pH of about 1.5, thus the pH of the culture was increased to pH 2 to attempt to provide a less aggressive acidic environment for the passivated tailings. Highly acidic conditions destabilize the ferric oxyhydroxide layer and fuel runaway ARD reactions (see equations 3 to 5 in section 2.4.1). This pH may have been still too low for the passivated tailings; it could have been pushed higher to prevent runaway reactions. The redox potential stayed high (at about 700 mv) for all the biotic tests indicating high microbial activity showing conversion of dissolved Fe (II) into Fe (III) which causes further oxidation thus generating more acidity. The ferric iron concentration increased in stage I showing the increase in the catalysis of Fe (II) to Fe (III). The Fe (III) concentration in stage II and III stays constant showing that possibly oxidation was largely by conversion of Fe (II) to Fe (III) rather than by Fe (III) oxidizing pyrrhotite. Treated and untreated samples exhibited the same trends thus showing that further treatment did not reduce the acid producing potential of the tailings.

However in the case of the abiotic test on the feed sample, the pH increased and stayed constant at around an average pH of 5.5. The redox potential stayed low showing no microbial activity as well as the Fe (III) concentration remained low, showing low oxidation rate in this system. There could be a number of explanations for this, possibly the neutralizing minerals provided enough buffering capacity in the absence of accelerated oxidation rates by microorganisms.

Or alternatively the feed sample may have oxidized between the time it was collected, to the time biokinetic tests were conducted resulting in a ferric oxyhydroxide layer retarding the oxidation rate. Cai et al. (2005) obtained a similar result where the abiotic sample showed a slight increase in pH and remained constant around pH 4.5. However on mine waste sites abiotic systems are rare (Gould and Kapoor, 2003), thus the biotic tests are a better

representation of the systems on mine waste sites. The feed sample subjected to a biotic system showed that the sample is highly acid forming which is more representative of what would occur on a mine waste site. Both the static chemical tests and the biokinetic test results were in agreement that even after further treatment the tailings remained highly acid producing. The biokinetic tests validated the findings of the sequential NAG tests, which showed that the samples remained acid forming even after further treatment.

6.4 Pyrrhotite passivation

6.4.1 Passivation by the ferric oxyhydroxide layer

From the ARD characterisation results further treatment of the tailings did not significantly reduce the acid producing potential of the samples. The single addition NAG results did however show a slight decrease in the NAG as the tailings were further oxidized. This could be evidence of the inhibition of oxidation as the ferric oxyhydroxide layer thickens. From literature a layer 5 Å layer has been observed to be sufficient to retard the oxidation rate of the pyrrhotite surface (Pratt et al., 1994, Mycroft et al., 1995). The recovery data from the flotation tests definitely show that the rejection of pyrrhotite changes with different pre-oxidation extents. This is proof of surface changes on the mineral surface, as flotation is surface chemistry driven. These conflicting results show that within the context of flotation the ferric oxyhydroxide layer was sufficient to affect pyrrhotite rejection but not enough to affect ARD potential measured by standard ARD tests. The sequential NAG test results show that even after further treatment of the samples, that any passivation layers formed on the sample were not significant enough to retard the rate of oxidation. Arguably the NAG test methodology could have affected any passivation layers that were possibly formed. With each NAG stage the sample is heated for more than two hours which could disintegrate any thin surface layers formed.

Theoretically once the ferric oxyhydroxide layer forms no additional treatment is not needed and further oxidation is simply supposed to thicken the coating until the sulfide mineral is replaced by goethite (Huminicki and Rimstidt, 2009). Although a layer of 5 Å has been observed in literature to inhibit further oxidation of pyrrhotite, under dynamic conditions in waste sites the layer may not be thick enough to withstand acidity already present on tailings dams. In acidic conditions the increase of Fe (III) ion concentration would result in an

increase in oxidation rate. This is shown by biokinetic tests; if the ferric oxyhydroxide layer was formed the acidity of the microbial inoculum may have simply accelerated the oxidation of the sample maintaining a low pH, both in the untreated and treated samples. SEM imaging was performed finally just as a confirmation of any presence of coating on the mineral surface. From the SEM images oxidation products are not visible on the mineral surface. However standard SEM imaging probably would have not been able to detect a layer as thin as 5 Å. Although coatings are not visible using SEM, this technique has limitations and employing other techniques such as transmission electron microscopy analysis (TEM), which can show nm resolution, would be better to observe alterations of the mineral surface.

6.4.2 Passivation by TETA

Further treatment by TETA decreased the single addition NAG potential of the tailings and there was an improvement to the NAG potential compared to treatment by further oxidation. It is important to note that the error obtained for the NAG tests on the TETA tailings was much higher (an 18 % error). Even though an initial reduction of acid producing potential after one stage test NAG was observed on tailings further treated, the tailings were still classified as acid producing.

The initial decrease in NAG could have been due to the possible adsorption of TETA on the pyrrhotite surface; the amine could have retarded initial oxidation but attachment may have been insufficient to reduce overall acid producing potential. Studies have shown that nickel and copper ions are more abundant on the pyrrhotite which reports to the concentrate than the rejected pyrrhotite (Yoon et al, 1995). Xu et al. (1997) showed that between pH 6 to 9, when DETA is added to a suspension of pyrrhotite containing nickel ions, after the nickel ions are removed by DETA, it can then adsorb onto the pyrrhotite surface by electrostatic attraction. So even though passivation by TETA has only been conducted on dry pyrrhotite samples by previous authors, Xu et al. (1997) shows the possibility of adsorption within a suspension. Thus this may explain the observed initial reduction of acid producing potential as the tailings were further dosed with TETA. However if there were still nickel ions in solution, the TETA complex with nickel would be favoured over adsorption on pyrrhotite surface as shown by Xu et al. (1997). Thus TETA may not have sufficiently adsorbed onto the surface to cause an appreciable reduction of ARD potential.

Similarly as with treatment with further oxidation, the sequential NAG test results show that any passivation layers possibly formed on treated samples were not significant enough to retard the rate of oxidation. Again it could be argued that the NAG test methodology could have destroyed any passivation layers that may have been formed. Furthermore from the SEM images taken, no coatings were visible on the sample surfaces. However the single addition NAG tests give an initial indication that there was definitely a change to the sample that affected the initial acid generation potential of the sample. On other hand the biokinetic tests show that if any TETA adsorption took place it was not significant enough to effect a change in the acid producing potential of the sample.

6.5 Implications of this study

The aim of this study was to attempt to depress pyrrhotite and simultaneously promote its passivation during flotation, without compromising pentlandite recovery, to ultimately mitigate ARD from pyrrhotite rich tailings. Both depression methods used in this study have been reported to be able to passivate pyrrhotite and inhibit further oxidation of the mineral by surface coating. The motivation behind this study was the potential to manipulate these depressant mechanisms to possibly combine flotation and passivation to produce benign pyrrhotite tailings. Current nickel processing flow sheets use chemical depressants such as the TETA/SMBS reagent combination. Depression by pre-oxidation has been explored but has however not been implemented. Thus this study also reviews the performance of both these depression methods.

The use of oxygen as a pyrrhotite depressant has been evaluated by other authors (e.g. Kelebek, 1993), but has not been implemented. The results of this study show that pre-oxidation can effectively reject pyrrhotite while maintaining pentlandite recovery. Although the use of TETA and SMBS achieved 92 % rejection of pyrrhotite, TETA is an expensive reagent and the use of oxygen as a depressant would provide a 'green solution'. TETA is a non-biodegradable solution and is known to be harmful to certain algae species however its long term effects have not been studied (UNEP, 1998) thus use of oxygen as a depressant would minimize environmental impacts. However the ore in this study is a magnetic ore and

it is therefore more reactive thus depression by oxidation may not be advisable for non-magnetic pyrrhotite which is less reactive. Variability of the reactivity of pyrrhotite bearing ores makes the effectivity of depression by oxidation uncertain. Ores would need to be characterized to assess the pyrrhotite phases present and their reactivity prior to determine if this method would be suitable.

This study shows the importance of mineralogical analysis during ARD characterisation. ARD reaction rates are very dependent on the mineralogy of the sample, therefore ARD prediction based on theoretical mineralogical calculations are very important in understanding chemical tests. Chemical ARD tests may overestimate or underestimate ARD potential therefore use of mineralogical calculations in conjunction with chemical tests can provide an insight into acid producing potential. This would be beneficial especially to samples which are classified as uncertain or non acid forming.

Overall results from this study show that passivation during flotation may not be feasible, seeing that the acid producing potential of the tailings was not significantly reduced. However passivation has been shown by other authors (Cai et al., 2005; Chen et al., 2006) to be effective on dry pyrrhotite samples. Thus the processing stage at which passivation may be used would need to be evaluated. Passivation could be potentially applied after the tails have been dewatered before they are disposed of in tailings dams. Passivation at the end of the mineral processing sheet would be rather be a waste management ARD treatment option, as opposed to a fully integrated preventive approach attempted by this study.

7 CONCLUSIONS AND RECOMMENDATIONS

Current ARD management technologies focus on end-of-pipe level treatments for flotation tailings. This project explores the concept of cleaner production which aims to identify options within a mineral beneficiation process flow sheet to minimise waste or produce benign waste. This study identified a possibility of simultaneously promoting pyrrhotite rejection and passivation during flotation while still maintaining pentlandite recovery. This project was limited to investigating two methods of depression and passivation, namely TETA and O₂ sparging (artificial oxidation). These two methods were chosen because of their current application in the depression and rejection of pyrrhotite, which means that limited costs would be incurred in their possible usage as passivating agents. The focus of the project was however not to optimize either mechanism, the study aimed to compare and review the two rejection methods based on current plant practices. The objective was to also compare the efficiency of these depression methods in promoting the passivation of pyrrhotite by conducting ARD characterisation tests on the treated and untreated tailings.

The outcomes of the study will be subsequently presented based on the key questions which had been set out. The integrated approach employed in this study by using knowledge across disciplines will be evaluated and finally recommendations will be given.

7.1 Research outcomes

The key questions which had been set out will now be reviewed;

- i. It is not plausible to simultaneously depress and passivate pyrrhotite. Both depression methods achieved high rejection of pyrrhotite, however further treatment did not manage to significantly reduce the acid producing potential of the tailings.
- ii. From reviewing the performance of both depression mechanisms, the TETA/SMBS reagent combination was more effective at pyrrhotite rejection; a 92 % rejection was achieved. Pre-oxidation did however achieve 85 % rejection of pyrrhotite and thus could be a viable alternative to chemical depressants worth exploring.

- iii. Further treatment by TETA resulted in a greater reduction of the acid producing potential of the tailings however the tailings were still classified as acid producing.

7.2 Integrated approach to ARD characterisation

The integrated approach used in this study has brought to light important aspects of ARD mitigation associated with pyrrhotite tailings. By exploring two viable pyrrhotite rejection methods and their potential to passivate the pyrrhotite surface, some observations have been made on the importance of the link between mineralogy, the mineral processing flow sheet and ARD characterisation. The diagram below shows the links between the different aspects of the study.

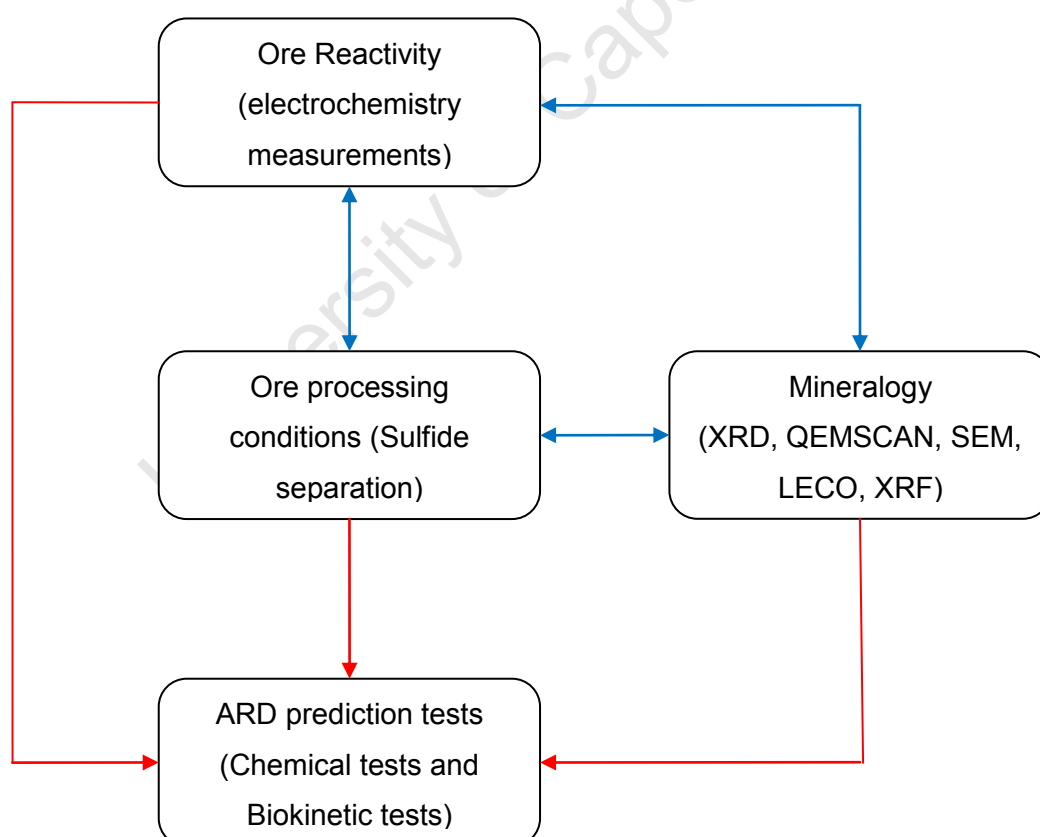


Figure 46: An integrated approach to ARD characterisation.

This methodology can be used to develop a generic approach to characterisation of the ARD potential of sulfide minerals as well as assessment and development of ARD mitigation options.

Influence of ore reactivity

Ore reactivity is affected by mineralogy, liberation, the type of pyrrhotite, sulfide grade and composition of the sample. Reactivity in turn affects the acid producing potential of a sample. Ore reactivity (oxygen uptake) measurements are especially important when comparisons of different ores are being done, as shown by Becker et al. (2010a). Different pyrrhotite crystallographic forms exhibit different reaction rates and therefore would vary in oxidation rates. This can inform downstream handling of pyrrhotite rich tailings. Even though the ore used in this study is a disseminated low grade pyrrhotite ore, the ARD characterisation results showed the high acid producing nature of the magnetic pyrrhotite bearing ore.

Ore processing (sulfide separation)

The separation stage of the mineral beneficiation flow sheet is important as it affects the minerals which report to waste streams as well as the concentrate. Production of benign tailings provides a means to avert ARD rather than manage drainage after it has been produced. Cleaner production offers mitigation options which do not involve major changes to the process flow sheet, which rather manipulate process operations to minimize waste or produce benign tailings. Cleaner production during flotation has been explored by other authors, e.g. Kazadi Mabamba et al. (2012) and Hesketh et al. (2010), by separating high sulfide and low sulfide (benign) streams. This method has been successful however flotation desulphurization still needs to be economically evaluated. In a continuous processing circuit new equipment would need to be added to allow for a desulphurization step. This study shows that passivation may not be plausible during flotation but promising results have been obtained by previous authors (Cai et al., 2005; Chen et al., 2006) when dry samples were coated by different surface coating agents. Thus the processing stage at which passivation can be applied would need to be reviewed e.g. passivation after thickening and dewatering.

Evaluation of ARD prediction methods

Mineralogical ARD prediction is important in understanding chemical tests. Mineralogical analysis before and after ARD characterisation tests is important. Mineralogy of ores affects

the reactivity of the ore and therefore will affect the acid producing potential of the samples. Parbhakar-Fox et al. (2011) have developed an acid rock drainage index (ARDI) based on intact rock texture. The ARDI incorporates chemical tests, geochemistry and mineralogy to provide a comprehensive rating for the acid producing potential of a sample. In this study only bulk mineralogy was looked at as opposed to Parbhakar-Fox et al. (2011) who looked at intact rock texture which would be the next step in using mineralogy to predict ARD formation. The link between mineralogy and ARD production is very important and essential for accurate ARD characterisation.

7.2.1 Concluding remarks

The main aim of this study was to determine if it is feasible to effectively reject pyrrhotite and promote its passivation during flotation while maintaining pentlandite recovery. Passivation efficiency was determined by ARD characterisation static chemical tests and biokinetic tests. The major findings of the study are summarized as follows;

- It is not feasible to simultaneously depress pyrrhotite and promote its passivation to sufficiently mitigate ARD during flotation.
- Both rejection methods were reviewed, the TETA and SMBS reagent combination achieved 92 % rejection of pyrrhotite. However, TETA is a very expensive reagent; it costs about twice the price of other flotation reagents. TETA alone however did achieve a better pentlandite recovery (75 % Pn recovery) as compared to when TETA/SMBS (55 % Pn recovery) was used.
- Depression by pre-oxidation achieved a maximum pyrrhotite rejection of 85 % and a pentlandite recovery of 68 %. This method has been investigated in the past but has never been implemented. Commercially it may be a feasible option for more reactive magnetic bearing nickel sulfide ores but consistent feed mineralogy would be required. Too much oxidation could result in a significant loss of pentlandite recovery.
- Further treatment of the pyrrhotite tailings however did initially show a decrease in the acid producing potential of the samples indicating possible passivation of the mineral surface. Further treatment by TETA resulted in a larger decrease in the initial net acid producing potential of the samples. However sequential NAG tests showed

that the initial reduction in NAG was insignificant and the samples remained acid forming.

- The chemical tests and biokinetic tests were in agreement that the samples remained acid forming. Vast differences in the results were however observed in the different chemical test methodologies showing the uncertainty associated with the tests. The test methodology still needs improvement to accurately predict ARD potential.
- Mineralogical based ARD predictions are important in gauging the accuracy of chemical tests and understanding the minerals which contribute to acid formation and neutralizing potential of a sample. Use of mineralogical analysis in conjunction with chemical tests can improve ARD potential prediction.

In conclusion even though simultaneous passivation and rejection during flotation was not achieved, the study provided some insight in the rejection of pyrrhotite. Rejection is an important stage in nickel processing; different methods have been explored in literature. Even though rejection by artificial oxidation has never been implemented this study shows a high percentage rejection can be achieved by this method. Furthermore, ARD chemical test methodology has been previously focused on pyrite, this study gave insight into combining chemical test and mineralogical analysis to predict ARD from pyrrhotite rich tailings.

7.3 Recommendations

Based on the findings of this study recommendations have been made where future work can be done;

- Rejection by pre-oxidation needs to be reviewed for its potential application in the depression of pyrrhotite bearing nickel sulfide ores. From this study high rejection of pyrrhotite was achieved on pyrrhotite bearing ore without compromising the recovery of pentlandite.

- Passivation by TETA has been shown by previous authors to be effective when dry pyrrhotite samples are coated. Therefore if this passivation method is to be further explored, the tailings would need to be dewatered to eliminate competition from TETA forming complexes with ions in process water with TETA adsorbing on the pyrrhotite surface.
- Usage of the ferric oxyhydroxide layer to retard oxidation rates of the pyrrhotite surface would need alkaline conditions to enhance and maintain the formation of the ferric oxyhydroxide layer. To investigate the feasibility of this method of passivation the use of leach columns may provide better conditions to promote the growth of the ferric oxyhydroxide layer as well as test its ability to provide long term inhibition of oxidation.
- Mineralogical ARD prediction needs to be used in conjunction with ARD chemical static tests and kinetic tests. Mineralogical analysis of feed and residues from ARD prediction tests can provide insight into the minerals that react during the tests. This can provide a more accurate prediction of ARD potential of a sample. The ARDI method developed by Parbhakar-Fox et al. (2011) would be the next step in integrating standard ARD tests with mineralogical analysis (such as intact rock texture).

BIBLIOGRAPHY

Akcil, A. and Koldas, S. 2006. Acid Mine Drainage (AMD): causes, treatment and case studies. *Journal of Cleaner Production*. 14(12-13):1139-1145.

Alibaba. n.d available: <http://www.alibaba.com/showroom/flotation-reagent.html> [2012, August 27]

Arnold, R.G. 1967. Range in composition and structure of 82 natural terrestrial pyrrhotites. *Canadian Mineralogist*. 9(1):31.

Arnold, R.G. 1966. Mixtures of hexagonal and monoclinic pyrrhotite and the measurement of the metal content of pyrrhotite by x-ray diffraction. *The American Mineralogist*. 51(7):1221.

Azarch, A. 2011. Acid Mine Drainage: A prolific threat to South Africa's environment and mining industry. Consultancy Africa Intelligence. 16 February [online]. Available: http://www.consultancyafrica.com/index.php?option=com_content&view=article&id=680:acid-mine-drainage-a-prolific-threat-to-south-africas-environment-and-mining-industry&catid=92:enviro-africa&Itemid=297 [2012, January 16]

Becker, M. 2009. The mineralogy and crystallography of pyrrhotite from selected nickel and PGE ore deposits and its effect on flotation performance, PhD thesis. University of Pretoria: Department of Materials Science and Metallurgical Engineering.

Becker, M., De Villiers, J. and Bradshaw, D. 2010a. The flotation of magnetic and non-magnetic pyrrhotite from selected nickel ore deposits. *Minerals Engineering*. 23(11-13):1045-1052.

Becker, M., De Villiers, J. and Bradshaw, D. 2010b. The mineralogy and crystallography of pyrrhotite from selected nickel and PGE deposits. *Economic Geology*. 105:1025 - 1037.

Belzile, N., Chen, Y., Cai, M. and Li, Y. 2004. A review on pyrrhotite oxidation. *Journal of Geochemical Exploration*. 84(2):65-76.

Belzile, N., Maki, S., Chen, Y. and Goldsack, D. 1997. Inhibition of pyrite oxidation by surface treatment. *Science of the Total Environment*. 196(2):177-186.

Benzaazoua, M., Bussière, B., Kongolo, M., McLaughlin, J. and Marion, P. 2000. Environmental desulphurization of four Canadian mine tailings using froth flotation. *International Journal of Mineral Processing*. 60(1):57-74.

Blowes, D.W. Ptacek, C.J., Jambor, J.L. and Weisener, C.G. (2005). The Geochemistry of Acid Mine Drainage, 149-204. In *Environmental Geochemistry* (ed. Lollar, B.S.) Vol 9 *Treatise on Geochemistry* (eds. Holland, H.D. and Turekian, K.K.), Elsevier-Pergamon, Oxford.

- Bradford, L., McInnes, C., Stange, W., de Beer, C., David, D. and Jardin, A. 1998. The development of the proposed milling circuit for the Nkomati main concentrator plant. *Minerals Engineering*. 11(12):1103-1117.
- Broadhurst, J.L. 2007. Generalised strategy for predicting environmental characteristics of solid mineral wastes- A focus on Copper, PhD Thesis. University of Cape Town.
- Bryan, C.G. 2006. A study of the microbiological populations of mine wastes, PhD thesis. School of Biological Sciences, University of Wales.
- Cai, M., Dang, Z., Chen, Y. and Belzile, N. 2005. The passivation of pyrrhotite by surface coating. *Chemosphere*. 61(5):659-667.
- Carpenter, R. and Desborough, G.A. 1964. Range in solid solution and structure of naturally occurring troilite and pyrrhotite. *The American Mineralogist*. 49:1350.
- Chen, Y., Li, Y., Cai, M., Belzile, N. and Dang, Z. 2006. Preventing oxidation of iron sulfide minerals by polyethylene polyamines. *Minerals Engineering*. 19(1):19-27.
- Craig, J.R. and Vaughan, D.J. 1981. Electrolyte polishing and Etching techniques. In *Ore Microscopy and Ore Petrography*. New York, U.S.A: John Wiley and Sons. 31-33.
- Crawford, G.A. 1995. Environmental improvements by the mining industry in the Sudbury Basin of Canada. *Journal of Geochemical Exploration*. 52(1):267.
- Cruz, R., González, I. and Monroy, M. 2005. Electrochemical characterisation of pyrrhotite reactivity under simulated weathering conditions. *Applied Geochemistry*. 20(1):109-121.
- de Villiers, J.P.R., Liles, D., Becker, M., 2009. The crystal structure of a naturally occurring 5C pyrrhotite from Sudbury, its chemistry and vacancy distribution. *The American Mineralogist*. 94, 1405–1410.
- Duncan, D. and Bruynesteyn, A. 1979. Determination of Acid Production potential of Waste Materials. *Metallurgy society, AIME*. paper A-79-29.
- Ekmekçi, Z., Becker, M., Tekes, E.B. and Bradshaw, D. 2010. The relationship between the electrochemical, mineralogical and flotation characteristics of pyrrhotite samples from different Ni Ores. *Journal of Electroanalytical Chemistry*. 647(2):133-143.
- Evans, C.L., Wightman, E.M., Manlapig, E.V. and Coulter, B.L. 2011. Application of process mineralogy as a tool in sustainable processing. *Minerals Engineering*. 24(12):1242-1248.
- Fuerstenau, M.C., Jameson, G.J. & Yoon, R.-. Eds. 2007. *Froth flotation; A century of innovation*. Illustrated ed. Colorado, USA: Society for Mining, Metallurgy and Exploration, Inc (SME).
- Gauert, C.D.K., De Waal, S.A. and Wallmach, T. 1995. Geology of the ultrabasic to basic Uitkomst complex, eastern Transvaal, South Africa: An overview. *Journal of African Earth Sciences*. 21(No. 4):553-570.
- Gould, W.D. and Kapoor, A. 2003. The Microbiology of Acid Mine Drainage. In *Environmental Aspects of Mine Wastes*. J.L. Jambor, D.W. Blowes & A.I.M. Ritchie, Eds. Short Course series Vol.31 ed. Mineralogical Association of Canada. 203-226.

- Gunsinger, M.R., Ptacek, C.J., Blowes, D.W. and Jambor, J.L. 2006. Evaluation of long-term sulfide oxidation processes within pyrrhotite-rich tailings, Lynn Lake, Manitoba. *Journal of Contaminant Hydrology*. 83(3-4):149-170.
- Hallberg, K.B. 2010. New perspectives in acid mine drainage microbiology. *Hydrometallurgy*. 104(3-4):448-453.
- Hamilton, I. 1984. A voltammetric study of the surface oxidation of sulfide minerals. *Proceedings - electrochemical society*. 84-10(Proc. Int. Symp. Electrochem. Miner. Met. Process., 1984):259.
- Harrison, S.T.L., Broadhurst, J.L., van Hille, R.P., Oyekola, R.P., Hesketh, A.H. and Opitz, A.K.B. 2010. *A systematic approach to sulphidic waste rock and tailings management to minimise AMD formation*. Water Research Commission of South Africa (WRC), K5/1831/3, Pretoria.
- Hesketh, A.H., Broadhurst, J.L. and Harrison, S.T.L. 2010a. Mitigating the generation of acid mine drainage from copper sulfide tailings impoundments in perpetuity: A case study for an integrated management strategy. *Minerals Engineering*. 23(3):225-229.
- Hesketh, A.H., Broadhurst, J.L., Bryan, C.G., van Hille, R.P. and Harrison, S.T.L. 2010b. Biokinetic test for the characterisation of AMD generation potential of sulfide mineral wastes. *Hydrometallurgy*. 104(3-4):459-464.
- Hesketh, A.H. 2010c. An integrated approach to AMD mitigation through sulfide removal from tailings, MSc thesis. University of Cape Town.
- Huminicki, D.M.C. and Rimstidt, J.D. 2009. Iron oxyhydroxide coating of pyrite for acid mine drainage control. *Applied Geochemistry*. 24(9):1626-1634.
- INAP 2009. *The International Network for Acid Prevention, Global Acid Rock Drainage Guide (GARD guide)*. [Online]. Available: <http://www.gardguide.com> [2011, 4/7].
- Janzen, M.P., Nicholson, R.V. and Scharer, J.M. 2000. Pyrrhotite reaction kinetics: reaction rates for oxidation by oxygen, ferric iron, and for nonoxidative dissolution. *Geochimica et Cosmochimica Acta*. 64(9):1511-1522.
- John, D.A. and Leventhal, J.S. 1995. *Bioavailability of metals*, in duBray, E.A., ed., *Preliminary compilation of descriptive geo-environmental mineral deposit models*. U.S Geological survey Open file report 95-831, pp 10 -18.
- Johnson, D.B. and Hallberg, K.B. 2003. The microbiology of acidic mine waters. *Research in Microbiology*. 154(7):466-473.
- Johnson, D.B. and Hallberg, K.B. 2005. Acid mine drainage remediation options: a review. *Science of the Total Environment*. 338(1-2):3-14.
- Kazadi Mbamba, C., Harrison, S.T.L., Franzidis, J. and Broadhurst, J.L. 2012. Mitigating acid rock drainage risks while recovering low-sulfur coal from ultrafine colliery wastes using froth flotation. *Minerals Engineering*. 29:13 -21.

- Keays, R.R. and Lightfoot, P.C. 2004. Formation of Ni-Cu-platinum group element sulfide mineralization in the Sudbury impact melt sheet. *Mineralogy and Petrology*. 82(3-4):217.
- Kelebek, S. 1993. The effect of oxidation on the flotation behavior of nickel-copper ores. *Publications of the Australasian Institute of Mining and Metallurgy*. 3(XVIII):999.
- Kelebek, S. 1995. Selective depression of pyrrhotite using sulfur dioxide-diethylenetriamine reagent combination. *Proceedings of the international mineral processing congress, 19th, San Francisco, 1995*. 3:181.
- Kelebek, S. 2007. Oxidation of complex Ni-Cu sulfide ores and its implication for flotation practice. *Canadian Metallurgical Quarterly*. 46(3):279.
- Kelebek, S. and Tukul, C. 1999. The effect of sodium metabisulfite and triethylenetetramine system on pentlandite-pyrrhotite separation. *International Journal of Mineral Processing*. 57(2):135-152.
- Kelebek, S., Wells, P. and Fekete S.O. 1995. *Selective flotation process for the separation of sulphide minerals*. Toronto, Canada: US005411148A.
- Kelly, D. and Vaughan, D.J. 1983. Pyrrhotite-pentlandite ore textures: a mechanistic approach. *Mineralogical Magazine*. 47(345):453.
- Kerr, A. 2002. An overview of recent developments in flotation technology and plant practice for Nickel ores. *Mineral processing plant design, practice and control proceedings*. 1:1142-1157.
- Khan, A. and Kelebek, S. 2004. Electrochemical Aspects of Pyrrhotite and Pentlandite in Relation to their Flotation with Xanthate. Part-I: Cyclic Voltammetry and Rest Potential Measurements. *Journal of Applied Electrochemistry*. 34(8):849-856.
- Kim, D. 1998. Studies of the pyrrhotite depression mechanism with diethylenetriamine. *Bulletin of the Korean Chemical Society*. 19(8):840-846.
- Kirk-Othmer 1984. In *Encyclopedia of Chemical Technology*. 3rd ed. 645-661.
- Knipe, S.W., Mycroft, J.R., Pratt, A.R., Nesbitt, H.W. and Bancroft, G.M. 1995. X-ray photoelectron spectroscopic study of water adsorption on iron sulphide minerals. *Geochimica et Cosmochimica Acta*. 59(6):1079-1090.
- Komadel, P. and Stucki, J.W. 1988. Quantitative assay of minerals for Fe²⁺ and Fe³⁺ using 1,10-Phenanthroline: III A rapid photochemical model. *Clays and Clay minerals*. 36(4):379-381.
- Kwong, Y.T.J. 1993. *Prediction and prevention of acid rock drainage from a geological and mineralogical perspective*. National Hydrology Research Institute Ottawa, Canada: MEND project 1.32.1.
- Lan, Y., Huang, X. and Deng, B. 2002. Suppression of Pyrite oxidation by Iron 8-Hydroxyquinoline. *Archives of Environmental Contamination and Toxicology*. 43:168-174.

- Lapakko, K. 2002. *Metal Mine Rock and Waste Characterisation tools; An overview*. Minnesota, U.S.A: Mining, Minerals and Sustainable Development Programme (MMSD), No. 67.
- Lawrence, R.W. and Wang, Y. 1996. *Determination of Neutralization Potential for Acid Rock Drainage Prediction*. Ottawa, Canada: MEND project 1.16.3.
- Lawrence, R.W. and Scheske, M. 1997. A method to calculate the neutralisation potential of mining wastes. *Environmental Geology*. 32(2):100-106.
- Lawson, V., Kerr, A.N., Shields, Y., Wells, P.F., Xu, M. and Dai, Z. 2005. Improving pentlandite pyrrhotite separation at INCO's Clarabelle Mill. *Publications of the Australasian Institute of Mining and Metallurgy*. 5(Centenary):875.
- Legrand, D.L., Bancroft, G.M. and Nesbitt, H.W. 2005a. Oxidation/alteration of pentlandite and pyrrhotite surfaces at pH 9.3: Part 1. Assignment of XPS spectra and chemical trends. *The American Mineralogist*. 90(7):1042.
- Legrand, D.L., Bancroft, G.M. and Nesbitt, H.W. 2005b. Oxidation of pentlandite and pyrrhotite surfaces at pH 9.3: Part 2. Effect of xanthates and dissolved oxygen. *The American Mineralogist*. 90(7):1055.
- Lehmann, M.N., Kaur, P., Penniford, R.M. and Dunn, J.G. 2000. A comparative study of the dissolution of hexagonal and monoclinic pyrrhotites in cyanide solution. *Hydrometallurgy*. 55(3):255-273.
- Lei, L. and Watkins, R. 2005. Acid drainage reassessment of mining tailings, Black Swan Nickel Mine, Kalgoorlie, Western Australia. *Applied Geochemistry*. 20(3):661-667.
- Lianxing, G. and Vokes, F.M. 1996. Intergrowths of hexagonal and monoclinic pyrrhotites in some sulfide ores from Norway. *Mineralogical Magazine*. 60(399):303.
- Lightfoot, P.C., Keays, R.R. and Doherty, W. 2001. Chemical evolution and origin of nickel sulfide mineralization in the Sudbury Igneous Complex, Ontario, Canada. *Economic Geology*. 96(8):1855.
- Lottermoser, B.G. 2007. *Mine Wastes: characterisation, treatment and environmental impacts*. 2nd ed. Berlin, Germany: Springer.
- Malysiak, V., O'Connor, C.T., Ralston, J., Gerson, A.R., Coetzer, L.P. and Bradshaw, D.J. 2002. Pentlandite–feldspar interaction and its effect on separation by flotation. *International Journal of Mineral Processing*. 66(1-4):89-106.
- Mbonambi, M.J., Becker, M., Franzidis, J., Bryson, M. and Bradshaw, D.J. 2010. Improving pentlandite selectivity over pyrrhotite using reagents. *INTERNATIONAL MINERAL PROCESSING CONGRESS (IMPC)*. 6-10, September 2010. Brisbane, Australia: IMPC. 2169 - 2176.
- Mikhlin, Y.L., Kuklinskiy, A.V., Pavlenko, N.I., Varnek, V.A., Asanov, I.P., Okotrub, A.V., Selyutin, G.E. and Solovyev, L.A. 2002. Spectroscopic and XRD studies of the air degradation of acid-reacted pyrrhotites. *Geochimica et Cosmochimica Acta*. 66(23):4057-4067.

- Miller, J.D., Li, J., Davidtz, J.C. and Vos, F. 2005. A review of pyrrhotite flotation chemistry in the processing of PGM ores. *Minerals Engineering*. 18(8):855-865.
- MMSD 2002. *Mining, Minerals and Sustainable development; Breaking New Ground*. London, UK: International Institute for Environment (IIED) and World Business Council for Sustainable Development (WBCSD), Earthscan publications Ltd.
- Moncur, M.C., Jambor, J.L., Ptacek, C.J. and Blowes, D.W. 2009. Mine drainage from the weathering of sulfide minerals and magnetite. *Applied Geochemistry*. 24(12):2362-2373.
- Moncur, M.C., Ptacek, C.J., Blowes, D.W. and Jambor, J.L. 2005. Release, transport and attenuation of metals from an old tailings impoundment. *Applied Geochemistry*. 20(3):639-659.
- Morimoto, N., Gyobu, A., Mukaiyama, H. and Izawa, E. 1975a. Crystallography and stability of pyrrhotites. *Economic Geology and the Bulletin of the Society of Economic Geologists*. 70(4):824.
- Morimoto, N., Gyobu, A., Tsukuma, K. and Koto, K. 1975b. Superstructure and nonstoichiometry of intermediate pyrrhotite. *The American Mineralogist*. 60(3-4):240.
- Morimoto, N., Nakazawa, H., Nishiguchi, K. and Tokonami, M. 1970. Pyrrhotites: stoichiometric compounds with composition $\text{Fe}_{1-x}\text{Sn}_x$ (x .geq. 8). *Science*. 168(3934):964.
- Mycroft, J.R., Nesbitt, H.W. and Pratt, A.R. 1995. X-ray photoelectron and Auger electron spectroscopy of air-oxidized pyrrhotite: Distribution of oxidized species with depth. *Geochimica et Cosmochimica Acta*. 59(4):721-733.
- Naldrett, A.J. 2004. *Magmatic sulfide deposits; Geology, Geochemistry and exploration*. Berlin Heidelberg, Germany: Springer.
- Paktunc, A.D. 1999a. Characterisation of mine wastes for prediction of acid mine drainage. *Azcue JM (ed). Environmental Impacts of Mining Activities. Springer-Verlag, Berlin Heidelberg, New York*. :19-40.
- Paktunc, A.D. 1999b. Mineralogical constraints on the determination of neutralization potential and prediction of acid mine drainage. *Environmental Geology*. 39(2):103-112.
- Parbhakar-Fox, A.K., Edraki, M., Walters, S. and Bradshaw, D. 2011. Development of a textural index for the prediction of acid rock drainage. *Minerals Engineering*. Article in press.
- Peek, E., Barnes, A. and Tuzun, A. 2011. Nickeliferous pyrrhotite – “Waste or resource?”. *Minerals Engineering*. 24(7):625-637.
- Pillay, K., Becker, M., Chetty, D. and Thiele, H. 2011. The effect of gangue mineralogy on the density separation of low grade nickel ore. *6th South African Base Metals Conference 2011*. South Africa: The South African Institute of Mining and Metallurgy (SAIMM). 493 -510.
- Plumlee, G.S. & Logsdon, M.J. Eds. 1999. *The Environmental Geochemistry of Mineral Deposits, Part A: Processes, techniques, and health issues*. vol 6A ed.: Society of Economic Geologists Inc., Reviews in Economic Geology.

- Pratt, A.R., Muir, I.J. and Nesbitt, H.W. 1994. X-ray photoelectron and Auger electron spectroscopic studies of pyrrhotite and mechanism of air oxidation. *Geochimica et Cosmochimica Acta*. 58(2):827-841.
- Prestidge, C.A., Ralston, J. and Smart, R.S.C. 1993. The competitive adsorption of cyanide and ethyl xanthate on pyrite and pyrrhotite surfaces. *International Journal of Mineral Processing*. 38:205-233.
- Ritchie, A.I.M. 1994. The waste rock environment. In *Environmental Geochemistry of Mine Wastes*. J.L. Jambor, D.W. Blowes & M.J. Logsdon, Eds. vol 22 (Short Course Handbook) ed. Mineralogical Association of Canada. 131- 161.
- Robertson, A.M. and Broughton, L.M. 1992. *Reliability of Acid Rock Drainage Testing*. July 30-31, Las Vegas, Nevada, U.S.A: Workshop on U.S. EPA Specifications for Tests to Predict Acid Generation from Non-Coal Mining Wastes.
- Romano, C.G., Ulrich Mayer, K., Jones, D.R., Ellerbroek, D.A. and Blowes, D.W. 2003. Effectiveness of various cover scenarios on the rate of sulfide oxidation of mine tailings. *Journal of Hydrology*. 271(1-4):171-187.
- Rumball, J.A. and Richmond, G.D. 1996. Measurement of oxidation in a base metal flotation circuit by selective leaching with EDTA. *International Journal of Mineral Processing*. 48(1-2):1-20.
- Sampson, M.I., Phillips, C.V. and Blake, R.C. 2000. Influence of the attachment of acidophilic bacteria during the oxidation of mineral sulfides. *Minerals Engineering*. 13(4):373-389.
- Schumann, R., Kawashima, N., Miller, S., Smart, R. and Stewart, W.A. 2009. Passivating Surface layer formation on Pyrite in Neutral rock drainage. *Securing the Future and 8th ICARD (The International Conference on Acid Rock Drainage)*, Skelleftea, Sweden. June 22-26 2009.
- Senior, G.D., Trahar, W.J. and Guy, P.J. 1995. The selective flotation of pentlandite from a nickel ore. *International Journal of Mineral Processing*. 43(3-4):209-234.
- Singer, P.C. and Stumm, W. 1970. Acidic mine drainage: rate-determining step. *Science*. 167(3921):1121.
- Skousen, J. 1997. Neutralization potential of overburden samples containing siderite. *Journal of Environmental Quality*. 26(3):673.
- Smart, R. et al., 2002. *AMIRA international, ARD test handbook, Project P387A Prediction and Kinetic control of Acid mine drainage*. Melbourne, Australia: Ian Wark Research Institute.
- Smart, R.S.C., Weber, P., Thomas, J.E. and Skinner, W.M. 2004. Improvements in acid rock drainage testing for short- and long-term neutralisation kinetics. *Proceedings of the 43rd Annual Conference of Metallurgists of CIM and Fifth International Symposium on Waste Processing and Recycling in Mineral and Metallurgical Industries V* pp. 525-540

- Sobek, A.A., Schuller, W.A., Freeman, J.R. and Smith, R.M. 1978. Field and laboratory methods applicable to overburden and mine soils. *U.S. Environmental Protection Agency*. (EPA 600/2-78-054):230.
- Steger, H. 1982. Oxidation of sulfide minerals. VII. Effect of temperature and relative humidity on the oxidation of pyrrhotite. *Chemical Geology*. 35(3-4):281.
- Stewart, W.A., Miller, S.D. and Smart, R. 2006. Advances in Acid Rock Drainage (ARD) characterisation of mine wastes. In *Proceedings of the 7th International Conference on Acid Rock Drainage (ICARD)*. St Louis, Missouri: .
- Stumm, W. and Morgan, J.J. 1996. *Aquatic Chemistry*. 3rd ed. New York: John Wiley & Sons.
- Thomas, J.E., Smart, R.S.C. and Skinner, W.M. 2000. Kinetic factors for oxidative and non-oxidative dissolution of iron sulfides. *Minerals Engineering*. 13(10-11):1149-1159.
- Tokonami, M., Nishiguchi, K. and Morimoto, N. 1972. Crystal structure of a monoclinic pyrrhotite (Fe₇S₈). *The American Mineralogist*. 57(7-8):1066.
- UNEP 1998. *Triethylene Tetramine Cas No: 112-24-3, The SIDS Initial Assessment Report for SIAM 8*. Paris, France: UNEP Publications.
- Wang, H., 2008. *A review of process-related characteristics of pyrrhotite*. Mineral Processing and Extractive Metallurgy Review. 29: 1-41.
- Weber, P.A., Thomas, J.E., Skinner, W.M. and Smart, R.S.C. 2004. Improved acid neutralisation capacity assessment of iron carbonates by titration and theoretical calculation. *Applied Geochemistry*. 19(5):687-694.
- Wells, P., Kelebek, S., Burrows, M.J. and Suarez, D.F. 1997. Pyrrhotite rejection at Falconbridge's Strathcona Mill. *Processing of complex ores: Mineral processing and the Environment, Proceedings of the UBC-McGill bi-annual International Symposium on Fundamentals of Mineral Processing, 2nd, Sudbury, Ont., aug.17-19, 1997*. 1997(51):51.
- Wiese, J., Harris, P. and Bradshaw, D.J. 2005. The influence of the reagent suite in the flotation of ores from the Merensky reef. *Minerals Engineering*. 18(2):189-198.
- Wills, B.A. and Napier-Munn, T. 2006. Froth flotation. In *Wills' Mineral Processing Technology: An introduction to the Practical Aspects of Ore Treatment and Mineral Recovery*. 7th ed. Elsevier Science and Technology Books. 267-352.
- Wolmarans, E. and Morgan, P. 2009. Milling circuit selection for Nkomati 375ktpm concentrator. *Base Metals Conference 2009*. The Southern African Institute of Mining and Metallurgy.
- Xu, Z., Rao, S.R., Finch, J.A., Kelebek, S. and Wells, P. 1997. Role of diethylene triamine (DETA) in pentlandite-pyrrhotite separation - part 1: complexation of metals with DETA. *Transactions. Section C, Mineral Processing Extractive Metallurgy*. 106(Jan):C15.

Yoon, R.-., Basilio, C.I., Marticorena, M.A., Kerr, A.N. and Stratton-Crawley, R. 1995. A study of the pyrrhotite depression mechanism by diethylenetriamine. *Minerals Engineering*. 8(7):807-816.

University of Cape Town

APPENDIX

APPENDIX A: Feed characterisation

APPENDIX B: Pyrrhotite reactivity data

APPENDIX C: Flotation

C.1: Milling conditions

C.2: Flotation procedures

C.3: Mass and water recovery data

C.4: Mineral recovery computation

C.5: Tailings mineral wt % composition

APPENDIX D: Static tests procedures

D.1: ANC test procedures

D.2: ANC and MPA mineralogy computation

D.3: NAG test procedure

APPENDIX E: Biokinetic test procedure

E.1: Adaptation of culture to pH 2

E.2: Biokinetic test procedure

APPENDIX A : Feed characterisation**Table A.1: Mineral wt % feed composition**

Mineral (wt%)	size fraction (um)						Combined
	-1000/+106	-106/+75	-75/+53	-53/+25	-25/+10	-10	
Pyrrhotite	0.09	0.46	0.84	2.84	3.46	3.17	10.86
Pentlandite	0.01	0.03	0.07	0.27	0.44	0.69	1.51
Chalcopyrite	0.01	0.03	0.05	0.19	0.28	0.39	0.95
Pyrite	0.03	0.09	0.17	0.45	0.47	1.69	2.90
Chromite	0.10	0.20	0.53	3.29	2.79	2.42	9.33
Magnetite	0.0	0.0	0.0	0.0	0.0	0.0	0.0
Chlorite	0.15	0.40	0.58	1.27	1.50	1.95	5.85
Other oxides	0.04	0.14	0.21	0.64	0.75	0.79	2.57
Amphibole	0.34	0.90	1.40	3.22	3.73	4.71	14.30
Biotite	0.13	0.32	0.41	0.72	0.55	0.43	2.56
Olivine	0.16	0.35	0.62	1.13	0.71	0.35	4.60
Serpentine	0.27	0.89	1.18	2.54	2.08	1.79	8.75
Talc	0.13	0.40	0.51	1.33	1.58	2.76	6.71
Plagioclase	0.13	0.33	0.59	1.26	1.07	0.87	4.25
Quartz	0.07	0.22	0.42	1.02	0.77	0.53	3.03
Pyroxene	0.0	0.0	0.0	0.0	0.0	0.0	0.0
Diopside	0.0	0.0	0.0	0.0	0.0	0.0	0.0
Enstatie	0.0	0.0	0.0	0.0	0.0	0.0	0.0
Orthopyroxene	0.36	0.52	0.82	1.23	0.81	0.43	4.17
Clinopyroxene	0.57	1.65	2.33	4.45	3.20	1.54	13.74
Tremolite	0.0	0.0	0.0	0.0	0.0	0.0	0.0
Epidote	0.03	0.08	0.12	0.28	0.25	0.19	0.94
Calcite	0.02	0.05	0.10	0.28	0.40	0.44	1.28
Other	0.09	0.21	0.41	0.73	0.48	0.71	2.63
Sum							100.0
BMS							16.2

Mineral grouping summary;

Alteration minerals	talc, serpentine, chlorite
Pyroxenes	orthopyroxene, clinopyroxene, diopside, enstatie
Oxides	Fe oxides/hydroxides, chromite, magnetite
Amphibole	amphibole, tremolite
Other	Other, quartz

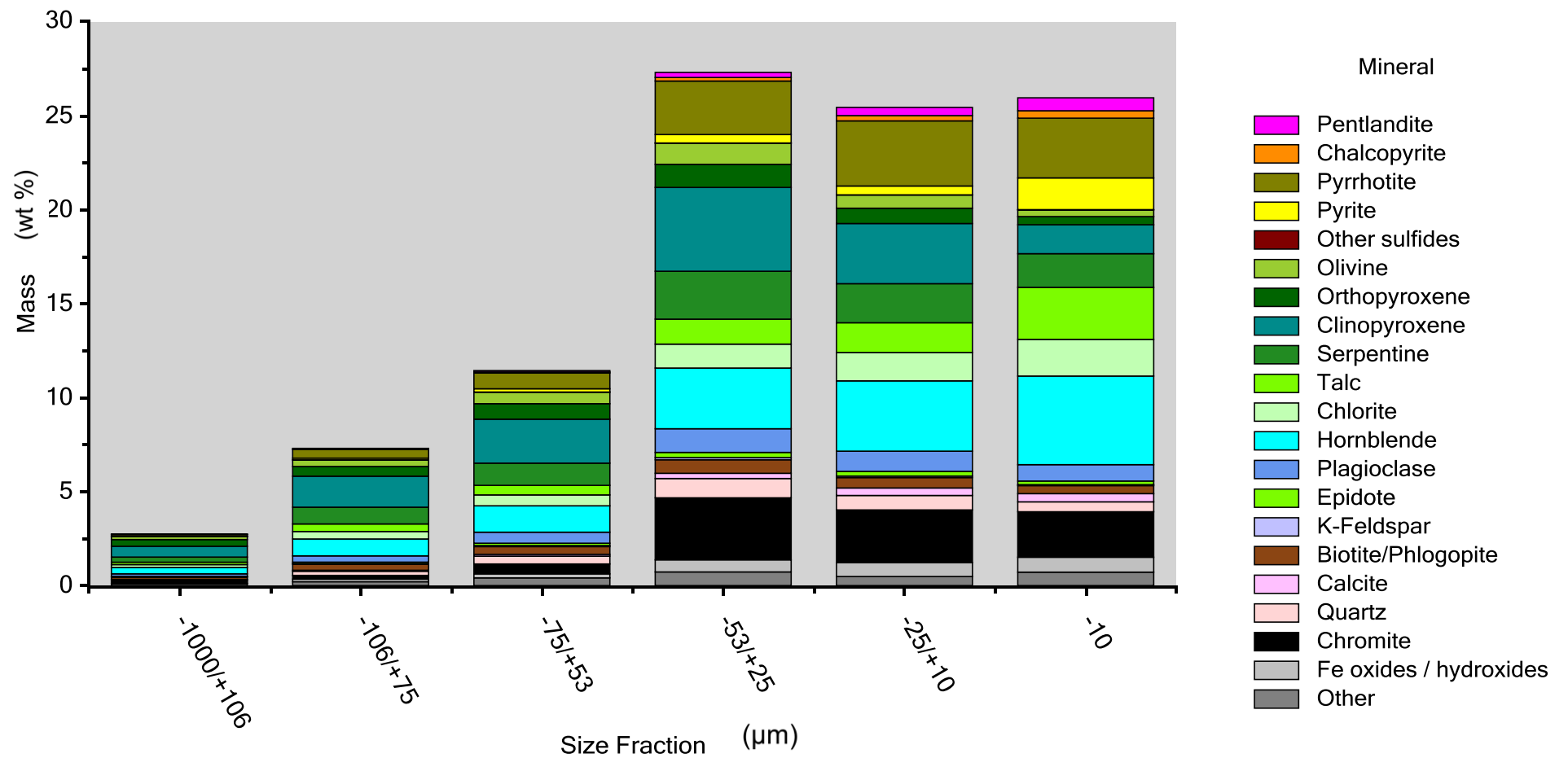


Figure A.1: Mineral wt % distribution in the feed

APPENDIX B : Pyrrhotite reactivity data

First order rate kinetics was fitted to model the rate of decay of dissolved oxygen slurry after sparging with a controlled amount of air. Figure B.1 shows an example of how the first order rate was fitted to the data.

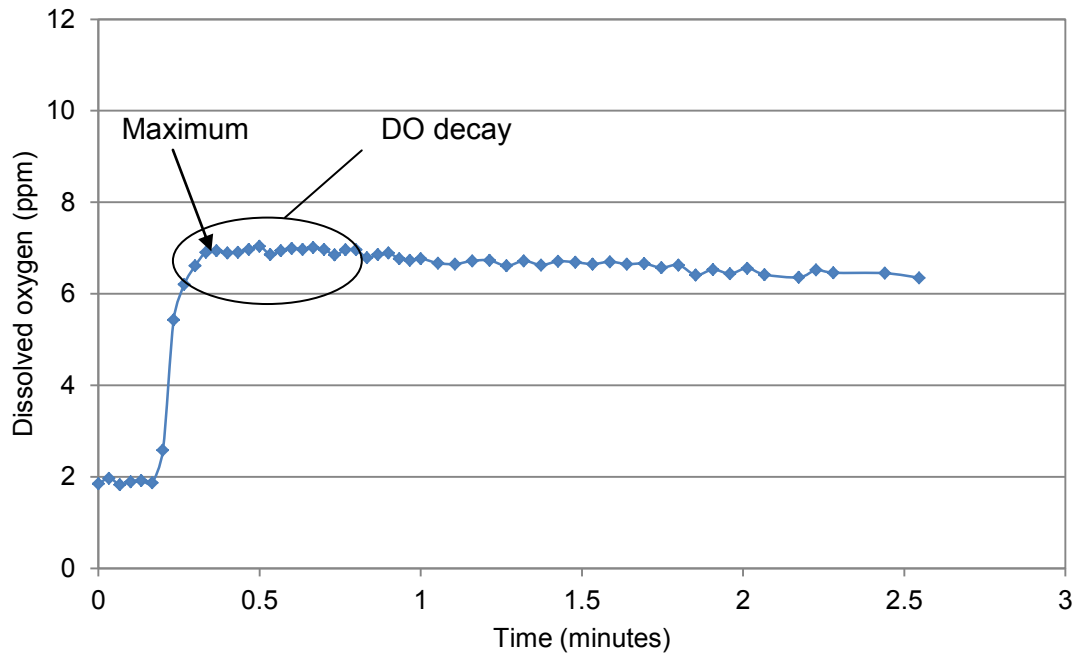


Figure B.1: Change in dissolved oxygen with time for no depressant conditions

Sample calculation using data from Figure B.1;

Figure B.2 isolates the region where the DO decays in figure B.1. An exponential model was fitted as per first order rate kinetics and the reactivity number (RN) was obtained.

$$\frac{dy}{dt} = k y \quad , \text{where } y = \text{DO}$$

Integrating $\int_{y_0}^y \frac{dy}{y} = \int_0^t k dt \rightarrow y = A e^{kt}$

From $y = A e^{kt}$ $RN = k * (-100)$, where -100 is the conversion factor

So from Figure B.2; $RN = -0.049 * -100 = 4.9$

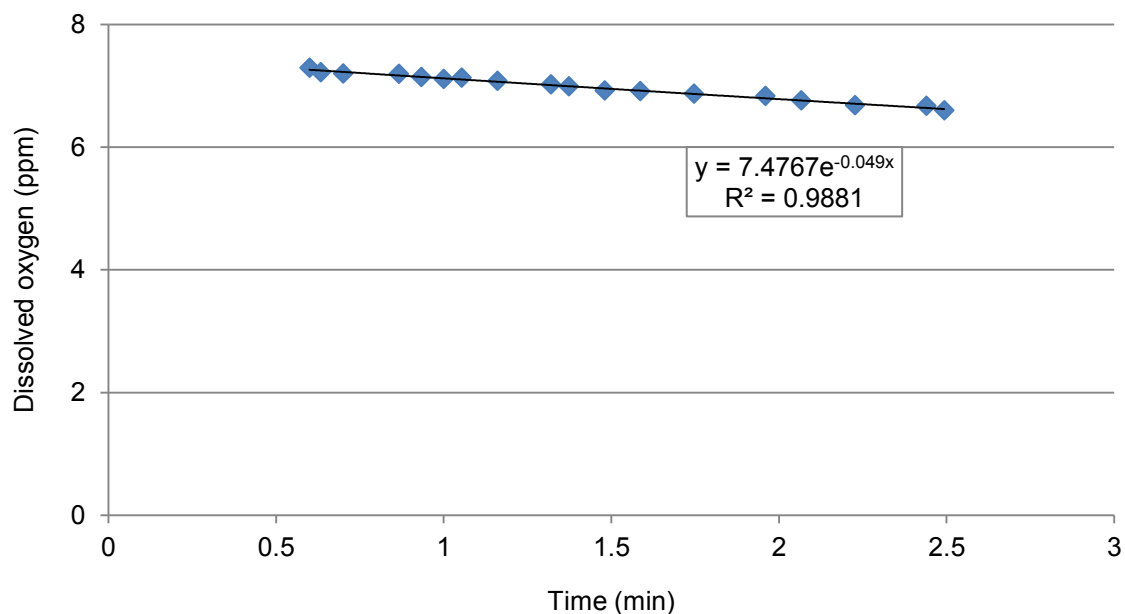


Figure B.2: First order rate kinetic model fitted to $\frac{dy}{dt}$

Table B.1: Comparison of reactivity numbers of case study and other nickel sulfide ores from Becker et al. (2010a)

	Measured RN	Po content (wt%)	RN _{norm}
Sudbury non magnetic	8	75.4	0.106
Sudbury magnetic	32	85.2	0.376
Phoenix magnetic	60	81.8	0.733
Nkomati MSB mixed	24	83.8	0.286
Case study	4.55	10.9	0.417

Tests were done in triplicate for reproducibility; however the error was computed over two runs. The following graphs show the data obtained at all the reagent conditions.

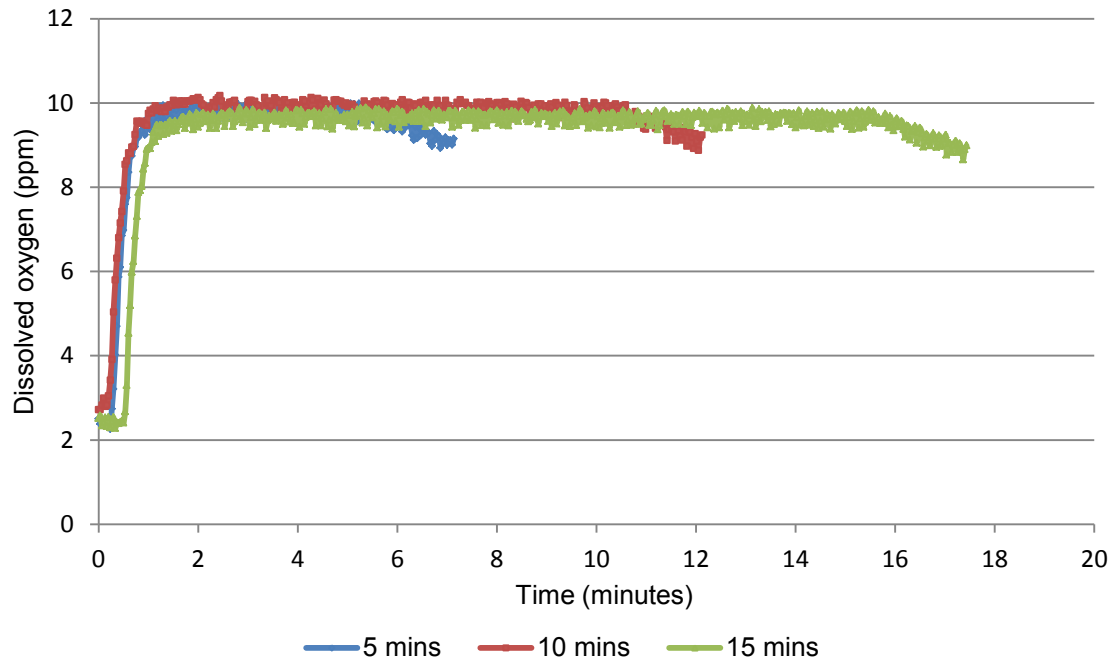


Figure B.3: Change in dissolved oxygen with time where oxygen was used as a depressant

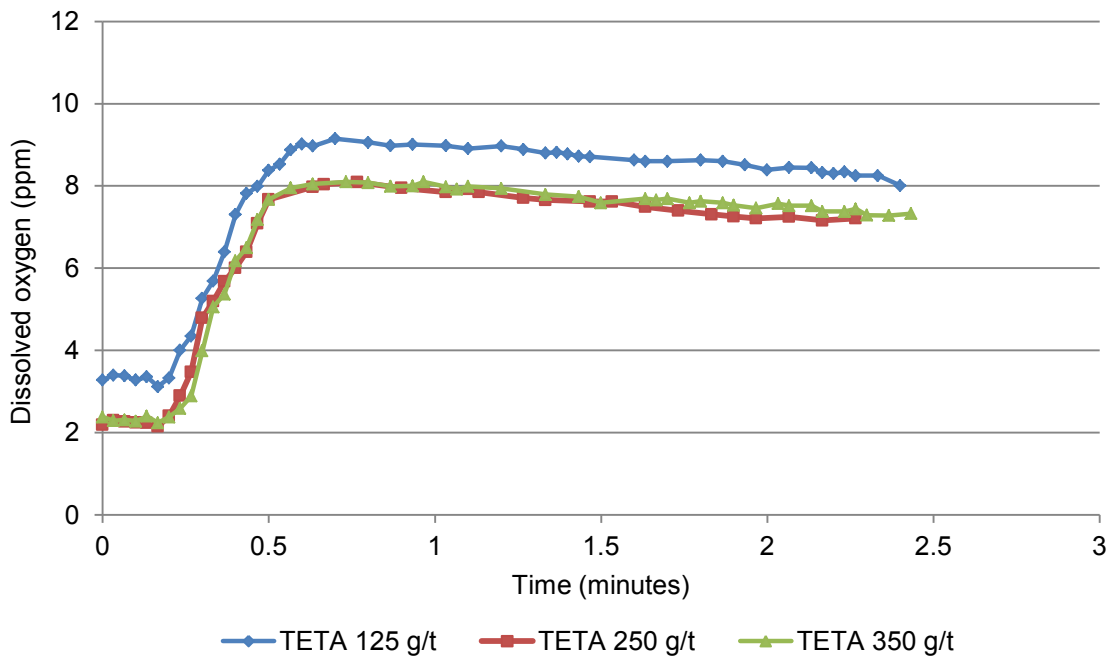


Figure B.4: Change in dissolved oxygen content with time where TETA only was used as a depressant.

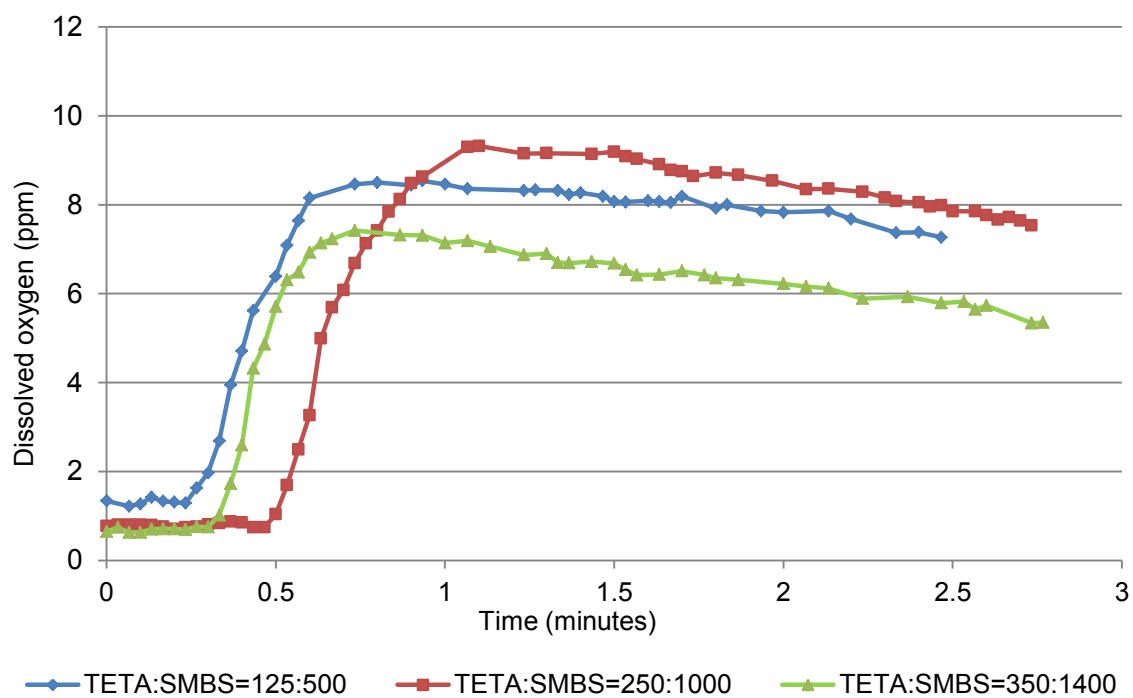


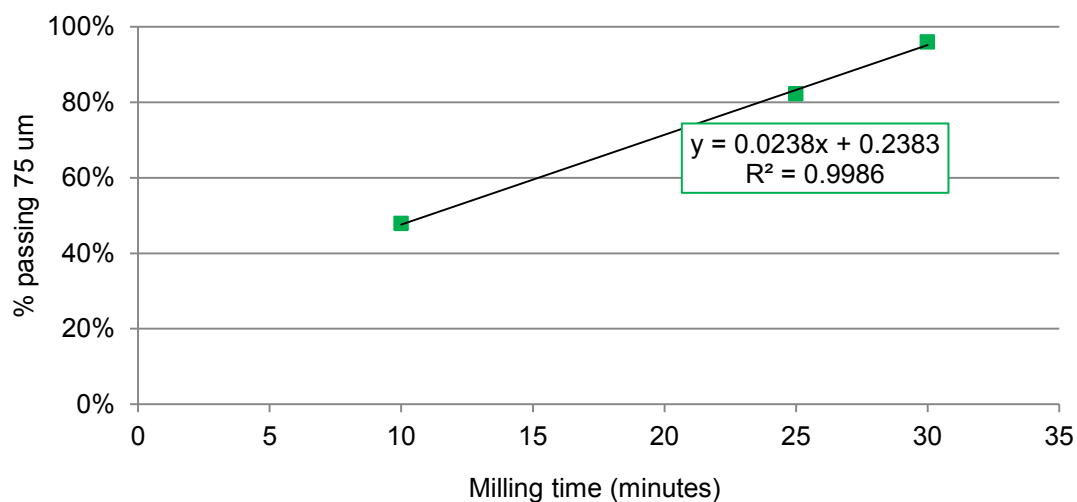
Figure B.5: Change in dissolved oxygen content with time where TETA and SMBS were used as a depressant.

APPENDIX C : Flotation

C.1 Milling conditions

Table C.1: Milling conditions

Grinding Conditions		
Mill Type (Rod or Ball)	Rod	
Mill Shape (Conical or Cylindrical)	Cylindrical	
Mill Diameter	200	mm
Mill Speed (Actual in Test)	90	rpm
% of Critical Speed	89%	%
Mill Ore Feed Size (F_{80})	2480	μm
Mill Ore Product Target Size (P_{80})	75	μm
Grinding time to reach target P_{80}	24.5	min
Mass Solids to Mill	1000	g
Volume water to Mill	500	ml
% Solids in Mill	66.7	%
Water Source for Grind Test	Synthetic water	

Figure C.1: Milling curve fitted with a linear correlation to obtain milling time for $p_{80} - 75 \mu\text{m}$

C.2 Flotation procedures

Table C.2.1: Flotation cell conditions

Test Cell Name	Modified Leeds Cell	
Test Cell Effective Flotation Volume	3000	ml
Shaft Speed	1200	rpm
Air Flow Rate	7	L/min
Test Start Pulp Temperature	Ambient	°C
Height of Froth Maintained in Test	30	mm

Table C.2.2: flotation procedure for no depressant conditions

No depressant	
action	time (mins)
lime addition 400 g/t	0
SIBX 50 g/t	5
<i>Start PDA DO sampling</i>	<i>6 min 30 s</i>
<i>Start 10 second sparge</i>	<i>6 min 40 s</i>
<i>Stop air sparge</i>	<i>6 min 50 s</i>
<i>Stop PDA sampling</i>	<i>8 min 50 s</i>
Dow 200 frother 35 g/t	7
air on	9
C1	11
C2	15
C3	21
C4	29

Table C.2.3: Flotation procedure for oxygen as a depressant for 5 minutes pre-oxidation

5 minutes depressant	
action	time (mins)
lime addition 400 g/t	0
SIBX 50 g/t (6 min 50 s start PDA)	5
sparge 5 minutes	7
stop sparge	12
Dow 200 frother 35 g/t (stop PDA sampling)	14
air on	16
C1	18
C2	22
C3	28
C4	36

Table C.2.4: Flotation procedure for oxygen as a depressant for 10 minutes pre-oxidation

10 minutes depressant	
action	time (mins)
lime addition 400 g/t	0
SIBX 50 g/t (6 min 50 s start PDA)	5
sparge 10 minutes	7
stop sparge	17
Dow 200 frother 35 g/t + stop	
sampling	19
air on	21
C1	23
C2	27
C3	33
C4	41

Table C.2.5: Flotation procedure for oxygen as a depressant for 15 minutes pre-oxidation

15 minutes depressant	
action	time (mins)
lime addition 400 g/t	0
SIBX (6 min 50 s start PDA)	5
sparge 15 minutes	7
stop sparge	22
dow 200 frother 35 g/t + stop	
sampling	24
air on	26
C1	28
C2	32
C3	38
C4	46

Table C.2.5: Flotation procedure where TETA alone was used as a depressant

TETA	
action	time (mins)
lime addition 400 g/t	0
SIBX 50 g/t	5
<i>Start PDA DO sampling</i>	<i>6 min 30 s</i>
<i>Start 10 second sparge</i>	<i>6 min 40 s</i>
<i>Stop air sparge</i>	<i>6 min 50 s</i>
TETA addition	7
<i>Stop PDA sampling</i>	<i>8 min 50 s</i>
Dow 200 frother 35 g/t	9
air on	11
C1	13
C2	17
C3	23
C4	31

Table C.2.6: Flotation procedure where TETA and SMBS were used together

TETA + SMBS	
action	time (mins)
lime addition	0
SMBS (ratio TETA: SMBS = 1: 4)	2
SIBX	5
<i>Start PDA DO sampling</i>	<i>6 min 30 s</i>
<i>Start 10 second sparge</i>	<i>6 min 40 s</i>
<i>Stop air sparge</i>	<i>6 min 50 s</i>
TETA addition	7
<i>Stop PDA sampling</i>	<i>8 min 50 s</i>
Dow 200 frother 35 g/t	9
air on	11
C1	13
C2	17
C3	23
C4	31

C.3 Mass and water recovery results

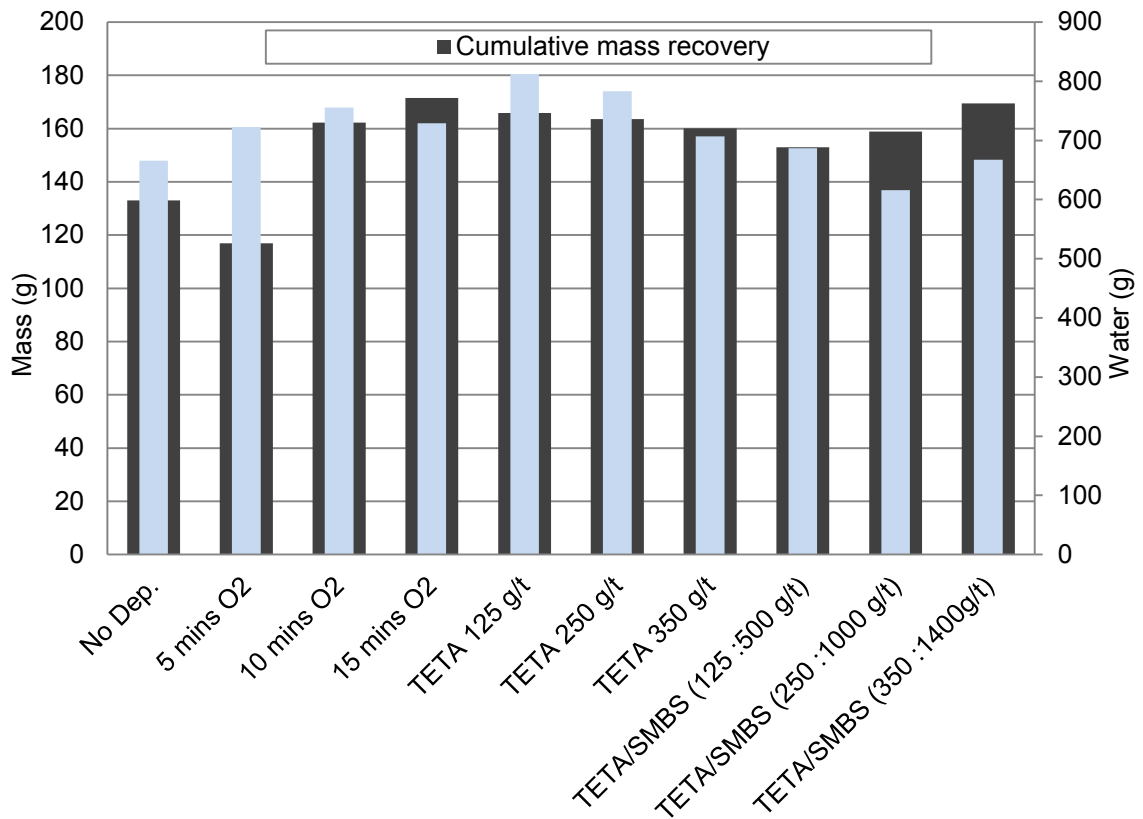


Figure C.3.1: Cumulative mass and water recovery data for the flotation tests

C.4 Mineral recovery computation

To obtain pentlandite recovery the following equation was used;

$$Recovery = \frac{\text{mass of pentlandite in sample}}{\text{mass of pentlandite in the feed}} \times 100$$

$$\text{mass of pentlandite in sample} = C_{Pn} \times \text{mass of sample}$$

$$C_{Pn} = \frac{C_{Ni}}{Mr_{Pn}}$$

Where C_{Pn} is the concentration of pentlandite in the sample, C_{Ni} is the concentration of nickel in the sample and M_r is the molar mass of pentlandite ($Fe_{4.5}Ni_{4.5}S_8$)

Similarly for pyrrhotite;

$$Recovery = \frac{\text{mass of pyrrhotite in sample}}{\text{mass of pyrrhotite in the feed}} \times 100$$

$$\text{mass of pyrrhotite in sample} = C_{Po} \times \text{mass of sample}$$

$$C_{Po} = \frac{\text{Mass of feed} \times S_T}{100 - \left[\frac{\text{Mass of feed}}{100} \times \frac{C_{Cp} \times S_{Cp}}{100} + \frac{\text{Mass of feed}}{100} \times \frac{C_{Pn} \times S_{Pn}}{100} \right]} \times \frac{Mr_{Po}}{Mr_S \times 1.13}$$

Where C_{Po} is the concentration of pyrrhotite in the sample,

C_{Cp} is the concentration of chalcopyrite, where;

$$C_{Cp} = \frac{C_{Cu}}{Mr_{Cu}}$$

S_i is the concentration of sulfur in sample/mineral (Cp = chalcopyrite, T = total sulfur in feed sample, Pn = pentlandite)

1.13 is the stoichiometric ratio of sulfur assuming pyrrhotite has the formula $FeS_{1.13}$

C.5 Tailings mineral wt % composition

Mineral	Mineral wt% composition in tailings sample		
	O ₂ tails	TETA tails	TETA + SMBS
Pyrrhotite	9.60	12.13	13.40
Pentlandite	0.31	0.30	0.19
Chalcopyrite	0.11	0.30	0.17
Pyrite	0.87	1.10	1.62
Chromite	10.55	8.77	7.66
Magnetite	0.00	0.00	0.00
Chlorite	6.53	0.00	0.00
Other oxides	3.24	0.00	0.00
Amphibole	14.60	0.00	0.00
Mica	2.69	9.70	10.07
Olivine	3.63	7.44	7.88
Serpentine	9.24	7.79	7.86
Talc	4.20	3.96	4.02
Plagioclase	4.37	0.00	0.00
Quartz	2.57	3.97	3.71
Pyroxene	0.38	0.00	0.00
Diopside	0.00	22.90	23.23
Enstatite	0.00	17.25	16.17
Orthopyroxene	3.48	0.00	0.00
Clinopyroxene	19.17	0.00	0.00
Tremolite	0.00	4.39	4.02
Epidote	1.35	0.00	0.00
Calcite	1.36	0.00	0.00
Other	1.70	0.00	0.00
Sum	100.0	100.0	100.0
BMS	10.9	13.8	15.4

APPENDIX D : Static test procedures

D.1 Acid Neutralizing Capacity (ANC) test procedures

The ANC is calculated by:

$$ANC = \frac{[Vol_{HCl} \times M_a] - Vol_{NaOH} \times C}{W} \times 49$$

Where M_a is the molarity of HCl (M), M_b is the molarity of NaOH (M), W is weight of sample (g) and $C = (M_a \times Vol_{HCl} \text{ in blank}) / (Vol_{NaOH} \text{ titrated in blank})$ to take into account the differences in stoichiometry in the acid and base solutions.

D.1.1 Fizz rating test

The reaction of carbonates within the sample is noted by an audible/visible fizz. This rating enables the selection of the HCl concentration required to react with the calcium carbonate and the volume of NaOH concentration for use in ANC tests. The procedure of the fizz test is as follows;

1. 0.5 g of the sample is placed on a watch glass
2. One to two drops of 25 % HCl are added to the sample
3. The intensity of the fizzing is rated according criteria in table.

Table D.1.1 Fizz rating criteria

Reaction	Fizz Rating	HCl molarity (M)	HCl volume (ml)	NaOH molarity (M)
None	0	0.5	4	0.1
Slight	1	0.5	8	0.1
Moderate	2	0.5	20	0.5
Strong	3	0.5	40	0.5
Very strong	4	1.0	40	0.5
Carbonate	5	1.0	60	0.5

*The sample was rated as moderate

D.1.2 Standard Sobek ANC test*Acid Digestion method for standard Sobek ANC test*

1. Weigh duplicate samples of 2 g into 250 ml Erlenmeyer flasks.
2. Carefully add HCl according to fizz rating
3. Add 20 ml of deionised water to flush the sample to the bottom
4. Heat the combined solid samples and HCl solution at 90 °C for 1 to 2 hours and then cool at room temperature for 1 hour.

NB: The reaction is complete when no gas evolution is visible and the particles settle evenly over the bottom of the flask.

5. Make up the volume to 125 ml with deionised water
6. Measure the pH of the mixture. If the pH is between, 0.8 to 1.5 proceed with the titration, if not adjust the fizz rating.

If pH > 1.5: additional HCl needs to be added so that total amount is equal to next highest fizz rating or fizz test is to be re-done on a fresh sub sample.

If pH < 0.8: too much acid may have been added unless the test is being run at fizz rating of 5. In such instances it is recommended to use the next lowest fizz rating.

7. Filter mixture and perform back titration on the liquor (filtrate)

Back titration for Standard Sobek test

1. Using a burette, back titrate liquor to pH 7.0
2. Leave solution for 24 hours
3. Check pH and back titrate with NaOH to pH 7.
4. Repeat steps 3 to 4 over 72 hours.

D.1.3 Skousen Test procedure

1. Weigh duplicate samples of 2 g into 250 ml Erlenmeyer flasks.
2. Carefully add HCl according to fizz rating
3. Top up solution with 100 ml of deionised water
4. Boil the solution for 5 min allow to cool and filter

Back titration for Skousen test

1. Confirm liquor pH is between 0.8 and 1.5, according to fizz rating
2. Using a burette, back titrate liquor to pH 4.5, recording NaOH addition.
3. Add 5 ml 30% H_2O_2 and boil for another 5min
4. Back titrate to pH 7
5. Leave solution for 24 hours
6. Check pH and back titrate to pH 7.
7. Add a further 5 ml H_2O_2 , boil for 5 min.
8. Repeat steps v. to viii. over 72 hours.

D.2 ANC and MPA mineralogy computation

The ANC was calculated using equation 13 from section 2.7.1 (Paktunc, 1999b)

$$ANC_{MN} = \sum_{i=1}^k \frac{w_a * 10 * X_i * c_i * n_s}{n_i * w_i}$$

Minerals used to compute the ANC were calcite (dissolving) and olivine (fast weathering).
Where;

w_a = molecular weight of acid H_2SO_4 ,

10 = conversion factor to $kg.t^{-1}$

X_i = amount of mineral i in wt%

c_i = number of non-oxidizable cations in one formula unit of neutralised mineral i

n_s = moles of sulfuric acid formed by the oxidation of one mole of sulfide mineral s

n_i = moles of mineral required to consume n_s

w_i = molecular weight the neutralising mineral

For example for the feed ANC_{MN} ;

	Feed	X_i	C_i	n_s	n_i	w_i	NP ($kg H_2SO_4/ton$)
$CaCO_3$	Calcite	1.28	1	1	1	100	12.9
$MgSiO_4$	Olivine	4.6	1	1	0.5	116.31	77.5
							90.5

The MPA mineralogy was calculated using equation 15 from section 2.7.1 (Paktunc, 1999b)

$$MPA_{MN} = \sum_{s=1}^m \frac{w_a * 10 * X_s * n_s}{w_s}$$

Where;

w_a = molecular weight of acid H_2SO_4 , w_s = molecular weight the sulfide mineral

10 = conversion factor to $kg.t^{-1}$

X_s = amount of sulfide mineral s in wt%

n_s = moles of sulfuric acid formed by the oxidation of one mole of sulfide mineral s

For example for the feed MPA_{MN} :

	Feed	X_s	n_s	w_a	w_s	MPA (kg H_2SO_4 /ton)
$FeS_{1.13}$	Pyrrhotite	10.9	1	87.9	98	113.7
FeS_2	Pyrite	2.9	2	120	98	47.3
						161

D.3 Net acid generation (NAG) test methods

Note: H_2O_2 must be at room temperature. Ensure that pH of H_2O_2 is > pH 4.5. Adjust with NaOH if necessary. Pyrite oxidation is an exothermic reaction, and solutions can “boil over”. Caution must be taken.

Single addition NAG test

1. Weigh 1.25 g sample into 250 ml Erlenmeyer flask.
2. Add 125 ml 15% H_2O_2 , cover, and allow to react for 24 hrs in a fume hood.
3. Measure pre-boil pH.
4. Heat solution until effervescence stops or for a minimum of 2 hours.
5. Allow to cool, make up volume to 125 ml with de-ionised water.
6. Record after-boil pH.
7. Filter, retaining solids residue and liquor.
8. Back titrate with NaOH recording volume added at pH 4.5 and pH 7.

NAG is calculated by:

$$NAG = \frac{49 \times V \times M}{W}$$

Where V = vol. NaOH (ml); M = molarity of NaOH and W = weight of sample (g).

Sequential NAG test

1. Carry out single addition NAG test as stage 1 of sequential NAG
2. Repeat steps 2 to 8 of single addition test on solid residue.
3. Repeat until no effervescent reaction is seen and after-boil NAG pH is $> \text{pH } 4.5$.

University of Cape Town

APPENDIX E : Biokinetic test procedure**E.1 pH adaptation of culture (to pH 2)**

Mixed culture comprising *Acidithiobacillus ferrooxidans* (DSM 584), *Leptospirillum ferriphilum* (ATCC 49881), *Acidithiobacillus caldus* (DSM 8584) and *Sulfobacillus benefaciens* (DSM 19468) was obtained which was at an pH of 1.7. The following steps were followed to raise the pH of the culture to pH 2.3;

1. An autotrophic basal salts (ABS) solution at a pH of 2.0 was prepared
2. Ferrous medium at a concentration of 5 g/l and a pH of 2.0 was prepared
3. 3 wt % solids of pyrite was added
4. Culture monitored over 1 to 2 weeks; measuring pH and monitoring the cell counts

E.2 Test procedure

All shake flask tests were conducted in triplicate.

1. Add 150ml autotrophic basal salts (ABS) solution at pH 4 to 250 ml Erlenmeyer flask.
2. Fit a cotton wool bung, cover with foil and autoclave to sterilise ABS solution.
3. After cooling, weigh in 7.5 g tailings sample to each flask.
4. Inoculate with 7.5 ml mixed culture of iron and sulfur oxidising microorganisms.
5. Measure Redox potential and pH
6. Weigh each flask and place in shaking incubator at 150 rpm at 37°C.
7. Before sampling, weigh flask. Top up with de-ionised water to account for water loss by evaporation.
8. Record pH, redox, ferrous and total iron concentrations every 2-4 days.

Redox potential was measured using a Crison ELP 21 Eh meter against a silver/silver chloride reference electrode (+199 mV vs. SHE). The pH was measured using a Metrohm 713 pH meter. Ferrous assay is conducted following the 1-10 phenanthroline method (Komadel and Stucki 1988).